



# Guidelines for Performing a Comprehensive Transesophageal Echocardiographic Examination in Children and All Patients with Congenital Heart Disease: Recommendations from the American Society of Echocardiography

Michael D. Puchalski, (Chair), MD, FASE, George K. Lui, MD, FASE, Wanda C. Miller-Hance, MD, FASE, Michael M. Brook, MD, FASE, Luciana T. Young, MD, FASE, Aarti Bhat, MD, FASE, David A. Roberson, MD, FASE, Laura Mercer-Rosa, MD, MSCE, Owen I. Miller, BMed (Hons), FRACP, David A. Parra, MD, FASE, Thomas Burch, MD, Hollie D. Carron, AAS, RDCS, ACS, FASE, and Pierre C. Wong, MD, *Salt Lake City, Utah; Stanford, San Francisco and Los Angeles, California; Houston, Texas; Seattle, Washington; Chicago, Illinois; Philadelphia, Pennsylvania; London, United Kingdom; Nashville, Tennessee; Boston, Massachusetts; and Kansas City, Missouri*

This document is endorsed by the following American Society of Echocardiography International Alliance Partners: Argentina Society of Cardiology, Asian-Pacific Association of Echocardiography, British Society of Echocardiography, Department of Cardiovascular Imaging of the Brazilian Society of Cardiology, Echocardiography Section of the Cuban Society of Cardiology, Indian Academy of Echocardiography, Indian Association of Cardiovascular Thoracic Anaesthesiologists, Indonesian Society of Echocardiography, Italian Association of Cardiothoracic Anesthesiologists, Japanese Society of Echocardiography, Korean Society of Echocardiography, National Society of Echocardiography of Mexico, Saudi Arabian Society of Echocardiography.

**Keywords:** Transesophageal echocardiography, TEE, Congenital heart disease, CHD, Echocardiography

From the University of Utah, Primary Children's Hospital, Salt Lake City, Utah (M.D.P.); Stanford University School of Medicine, Stanford, California (G.K.L.); Baylor College of Medicine and Texas Children's Hospital, Houston, Texas (W.C.M.-H.); University of California, San Francisco, California (M.M.B.); Seattle Children's Hospital and University of Washington, Seattle, Washington (L.T.Y. and A.B.); Advocate Children's Hospital, Chicago, Illinois (D.A.R.); University of Pennsylvania Perelman School of Medicine, The Children's Hospital of Philadelphia, Philadelphia, Pennsylvania (L.M.-R.); Evelina London Children's Hospital, London, United Kingdom (O.I.M.); Vanderbilt Medical Center, Nashville, Tennessee (D.A.P.); Tufts Medical Center, Boston, Massachusetts (T.B.); Children's Mercy Hospital, Kansas City, Missouri (H.D.C.); Children's Hospital, Los Angeles, California (P.C.W.).

The following authors reported no actual or potential conflicts of interest in relation to this document: Michael D. Puchalski, MD, FASE, George K. Lui, MD, FASE, Hollie D. Carron, AAS, RDCS, ACS, FASE, Laura Mercer-Rosa, MD, MSCE, Owen I. Miller, BMed (Hons), FRACP, Wanda C. Miller-Hance, MD, FASE, David Parra, MD, FASE, Luciana T. Young, MD, FASE.

The following authors reported relationships with one or more commercial interests: Michael Brook, MD, FASE receives research funding from Siemens. Thomas Burch, MD is owner and manager of PTEmasters, LLC, a board review website for the PTEeXAM. David A. Roberson, MD, FASE serves on the speakers bureau for Philips Ultrasound. Pierre C. Wong, MD, serves on the speakers bureau for Astra Zeneca.

**NOTICE AND DISCLAIMER:** This report is made available by ASE as a courtesy reference source for members. This report contains recommendations only and should not be used as the sole basis to make medical practice decisions or for disciplinary action against any employee. The statements and recommendations contained in this report are primarily based on the opinions of experts, rather than on scientifically-verified data. ASE makes no express or implied warranties regarding the completeness or accuracy of the information in this report, including

the warranty of merchantability or fitness for a particular purpose. In no event shall ASE be liable to you, your patients, or any other third parties for any decision made or action taken by you or such other parties in reliance on this information. Nor does your use of this information constitute the offering of medical advice by ASE or create any physician-patient relationship between ASE and your patients or anyone else.

**Reviewers:** This document was reviewed by members of the 2017–2018 ASE Guidelines and Standards Committee, ASE Board of Directors, and ASE Executive Committee. Reviewers included Alicia Armour, BS, MA, RDCS, FASE, Federico M. Asch, MD, FASE, Scott D. Choyce, RDCS, RVT, RDMS, FASE, Frederick C. Cobey, MD, FASE, Gregory J. Ensing, MD, FASE, Craig Fleishman, MD, FASE, Mark K. Friedberg, MD, FASE, Neal Gerstein, MD, FASE, Yvonne E. Gilliland, MD, FASE, Robi Goswami, MD, FASE, Lanqi Hua, RDCS (AE/PE/FE), FASE, Pei-Ni Jone, MD, FASE, James N. Kirkpatrick, MD, FASE, Stephen H. Little, MD, FASE, Rick Meese, ACS, RDCS, RCS, RCIS, FASE, Andy Pellett, PhD, RCS, RDCS, FASE, Dermot Phelan, MD, PhD, FASE, and David H. Wiener, MD, FASE.

#### **Attention ASE Members:**

Visit [www.aseuniversity.org](http://www.aseuniversity.org) to earn free continuing medical education credit through an online activity related to this article. Certificates are available for immediate access upon successful completion of the activity. Nonmembers will need to join the ASE to access this great member benefit!

Reprint requests: American Society of Echocardiography, Meridian Corporate Center, 2530 Meridian Parkway, Suite 450, Durham, NC 27713 (E-mail: [ase@asecho.org](mailto:ase@asecho.org)).

0894-7317/\$36.00

Copyright 2018 by the American Society of Echocardiography.

<https://doi.org/10.1016/j.echo.2018.08.016>

**Abbreviations**

<b>2D</b> = Two-Dimensional
<b>3D</b> = Three-Dimensional
<b>ACHD</b> = Adult Congenital Heart Disease
<b>ASE/SCA</b> = American Society of Echocardiography/ Society of Cardiovascular Anesthesiologists
<b>AoV</b> = Aortic Valve
<b>Asc Ao</b> = Ascending Aorta
<b>CA</b> = Coronary Artery
<b>CHD</b> = Congenital Heart Disease
<b>DTG</b> = Deep Transgastric
<b>IVC</b> = Inferior Vena Cava
<b>LA</b> = Left Atrium
<b>LAX</b> = Long Axis
<b>LV</b> = Left Ventricle
<b>LVOT</b> = Left Ventricular Outflow Tract
<b>ME</b> = Midesophageal
<b>MV</b> = Mitral Valve
<b>PA</b> = Pulmonary Artery
<b>PV</b> = Pulmonary Valve
<b>RA</b> = Right Atrium
<b>RV</b> = Right Ventricle
<b>RVOT</b> = Right Ventricular Outflow Tract
<b>SAX</b> = Short Axis
<b>SVC</b> = Superior Vena Cava
<b>TG</b> = Transgastric
<b>TTE</b> = Transthoracic Echocardiography
<b>TEE</b> = Transesophageal Echocardiography
<b>TV</b> = Tricuspid Valve
<b>UE</b> = Upper Esophageal

**INTRODUCTION**

Since its introduction nearly four decades ago, transesophageal echocardiography (TEE) has witnessed a remarkable evolution. The important strides made in improving TEE technology – including development of multiplane phased array transducers, matrix array transducers for three-dimensional (3D) imaging, and extensive improvements in echocardiographic imaging platform technology – have catalyzed the establishment of TEE as a critically important cardiovascular imaging modality.<sup>1-15</sup> The esophageal position of the ultrasonic transducer provides superior cardiac imaging and allows monitoring of the heart before, during, and after cardiac or non-cardiac procedures without interruption.

TEE in the pediatric population became widespread after the introduction of commercially available miniaturized probes in the late 1980s.<sup>1-3</sup> Since then, the safety and invaluable clinical utility of this technique for many types of pediatric and adult congenital cardiac surgery and cardiac interventional procedures has become well established.<sup>4-15</sup> The increasing applications of TEE coupled with newer technology led the American Society of Echocardiography and the Society of Cardiovascular Anesthesiologists (ASE/SCA) to publish the most recent recommendations for a comprehensive TEE evaluation in 2013 geared primarily to adult patients with structurally normal hearts.<sup>16</sup>

Similarly, pediatric TEE has incorporated the use of 3D

technology and exploited the advances in probe and software technology, leading to the need for a position document to update the current state-of-the-art for pediatric and congenital cardiology.<sup>12,17-32</sup> The current document was written to provide guidelines for the use of TEE, and recommendations for standardized TEE views and techniques that can be used in the assessment of children or any patient with congenital heart disease (CHD).

**Table 1** Indications for TEE in the patient with CHD**Diagnostic Indications**

- Patient with suspected CHD and non-diagnostic TTE
- Presence of patent foramen ovale (PFO) with and without agitated saline contrast and direction of shunting as possible etiology for stroke
- Evaluation for cardiovascular source of embolus with no identified non-cardiac source
- Evaluation of intra- or extra-cardiac baffles following the Fontan, Senning, or Mustard procedure
- Suspected acute aortic pathology including but not limited to dissection/transection (e.g., Marfan syndrome, bicuspid aortic valve, coarctation of the aorta)
- Intra-cardiac evaluation for vegetation or suspected abscess
- Evaluation for intra-cardiac thrombus prior to cardioversion for atrial flutter/fibrillation and/or radiofrequency ablation
- Pericardial effusion or cardiac function evaluation and monitoring postoperative patient with open sternum or poor acoustic windows
- Evaluating status of prosthetic valve in the setting of inadequate TTE images
- Re-evaluation of prior TEE finding for interval change (e.g., resolution of thrombus after anticoagulation, resolution of vegetation after antibiotic therapy)

**Perioperative Indications**

- Immediate preoperative definition of cardiac anatomy and function
- Postoperative surgical results and function
- Intraoperative monitoring of ventricular volume and function
- Monitoring of intra-cardiac/intravascular air and adequacy of cardiac de-airing

**TEE-guided Interventions**

- Guidance for placement of occlusion device (e.g., septal defect, Fontan or intra-atrial baffle fenestration)
- Guidance for blade or balloon atrial septostomy
- Guidance for creation/stenting of interventricular communication
- Guidance during percutaneous valve interventions
- Guidance during radiofrequency ablation procedure
- Assessment of results of minimally invasive surgical incision or video-assisted cardiac procedure
- Guidance during placement of catheter-based cardiac assist device (e.g., Impella ® heart pump)

Modified from Ayres *et al.*<sup>31</sup>

**GENERAL GUIDELINES****Indications and Contraindications for TEE**

**Indications in the Pediatric Patient.** TEE in children is commonly used for the assessment of anatomy and function during cardiac surgery, typically for CHD (Table 1).<sup>11,31</sup> However, due to certain inherent limitations in the imaging of key cardiac structures (discussed below), it should not serve as the sole or primary diagnostic modality for assessment of pediatric heart disease. Instead, the task force recommends preoperative transthoracic echocardiography (TTE) for all children undergoing cardiac surgery as it may provide information unobtainable with intraoperative TEE alone. Intraoperative TEE performed immediately prior to the surgical intervention allows the operative team to review the preoperative diagnostic findings, identify any new findings, and assist in the assessment of hemodynamics and myocardial function prior to onset of the operative procedure. TEE may facilitate catheter placement, real-time monitoring of volume status and myocardial

function in order to inform selection of anesthetic agents, inotropic support, and management decisions.<sup>33-36</sup> In the intraoperative setting, TEE can be used to assess cannula position and venous drainage during cardiopulmonary bypass, facilitate intra-cardiac de-airing, and characterize rhythm disturbances. An important role of the post-intervention TEE is to evaluate the adequacy of the surgical repair and assess ventricular function. However, it should be recognized that the postoperative TEE findings could be influenced by a number of factors such as anesthetic depth, hemodynamic state, and vasoactive drug administration. Decisions to return to bypass, therefore, should consider not only the TEE findings, but also clinical information, hemodynamics, and the risk versus benefit of a re-intervention.

TEE serves an important role in the cardiac catheterization laboratory.<sup>37-39</sup> During placement of septal closure devices, TEE provides precise identification of the location, geometry, and number of defects, allowing the interventionalist to develop clear strategies for closure.<sup>40-42</sup> TEE use during catheter-based procedures limits fluoroscopy time, decreases contrast load, and improves the overall safety of the interventions.<sup>38,39,43,44</sup>

Outside of the procedural setting, TEE is used to provide diagnostic images when the patient has poor acoustic windows, if TTE is non-diagnostic, or in cases where TEE imaging has proven superior, such as evaluation for atrial thrombi prior to cardioversion, assessment for intra-cardiac shunting in patients with a cerebrovascular accident, visualization of the Fontan pathway, assessment of prosthetic valve function and associated pathology, and evaluation of endocarditis on both native and prosthetic valves.<sup>33-35,45-48</sup>

Intraoperative TEE use is increasing for monitoring myocardial function and ventricular loading conditions in patients with CHD and other acquired pathologies undergoing high-risk non-cardiac procedures, as well as for the visualization of landmark structures during minimally invasive surgery.<sup>36,49-54</sup> In the intensive care unit, TEE provides diagnostic information in the postoperative patient with suboptimal transthoracic windows or an open sternum, and in the management of patients undergoing mechanical circulatory support.<sup>46,55-57</sup>

### Indications in the Adult with Congenital Heart Disease (ACHD)

TEE is indicated in the ACHD patient for many of the same reasons as noted above: inadequate TTE images, guidance of cardiac interventions in the operating room or catheterization laboratory, assessment of intra-cardiac thrombus (particularly prior to elective cardioversion or radiofrequency ablation), and for diagnosis of infective endocarditis with moderate to high pretest probability.<sup>16</sup> TEE is often superior to TTE for assessment of interatrial shunts, anomalous pulmonary venous return, atrioventricular valves (AV), complex atrial baffle procedures, the Fontan pathway, prosthetic heart valves and conduits, and coronary artery anomalies.

TEE may be very useful in the assessment of all ACHD patients who are undergoing cardiac surgery for the first time and during reoperations for management of residual hemodynamic lesions as well as in the setting of non-cardiac surgery.<sup>58</sup> In these settings, TEE can provide complete morphologic and functional assessment of simple to complex CHD.<sup>9</sup>

### Contraindications in the Pediatric Patient

Probe placement and esophageal instrumentation are semi-invasive and carry potential risks. The patient's history should be reviewed for relative and absolute contraindications (Table 2). If the contraindication is relative, potential benefits should outweigh the associated risks. For example, special consideration must be given to the patient

**Table 2** Contraindications to TEE

Absolute	Relative
Unrepaired tracheoesophageal fistula	History of esophageal or gastric surgery
Esophageal obstruction or stricture	History of esophageal cancer
Perforated hollow viscus	Esophageal varices or diverticulum
Active gastric or esophageal bleeding	Recent gastrointestinal bleed
Poor airway control	Active esophagitis or peptic ulcer disease
Severe respiratory depression	Vascular ring, aortic arch anomaly with or without airway compromise
Uncooperative, unседated patient	Oropharyngeal pathology
	Severe coagulopathy
	Significant thrombocytopenia
	Cervical spine injury or anomaly
	Post-gastrostomy or fundoplication limit imaging to esophageal windows

Modified from Ayres *et al.*<sup>31</sup>

who has undergone esophageal surgery since it is unclear whether/when probe placement is safe. The risk/benefit ratio of TEE after gastrostomy tube/button placement (with or without associated Nissen fundoplication) might require limiting or avoiding imaging from the stomach (transgastric or deep transgastric imaging). Care must be taken in children with Down syndrome secondary to a relatively large tongue, narrow hypopharyngeal structures, and/or cervical spine instability.<sup>59</sup> In the pediatric patient with a vascular ring, TEE is relatively contraindicated because the esophagus and trachea are confined to a restricted space and a rigid TEE probe in the esophagus can produce significant airway compromise.

### Contraindications in the ACHD Patient

Absolute and relative contraindications to TEE in the adult are outlined in the 2013 ASE/SCA Comprehensive TEE Guidelines.<sup>16</sup> The same considerations described above for the child with Down syndrome or with a vascular ring apply to the ACHD population.

### Key Points

1. Indications for TEE in children and all patients with CHD include pre and postoperative evaluation of cardiac anatomy and function, guidance of transcatheter interventions, non-diagnostic TTE, intra-cardiac thrombus, prosthetic valve function, and diagnosis of infective endocarditis.<sup>1</sup>
2. The benefits of the procedure should outweigh the risks when patients with relative contraindications are evaluated for TEE. Relative contraindications primarily relate to the potential of esophageal trauma or airway compromise (Table 2).

### Training and Certification

**Cognitive Skills, Technical Skills, and Training Guidelines.** TEE imaging is considered an advanced skill, thus, it is expected that the pediatric or ACHD echocardiographer performing the study should have expertise in the TTE diagnosis of structural and acquired heart disease. Core pediatric echocardiography skills that include medical knowledge

**Table 3** Guidelines for training and maintenance of competence

Component	Objective	Duration	Number of cases
Echocardiography	Prior experience in performing/interpreting TTE	6 mo or equivalent	Minimum of 450 cases across all age groups
Esophageal intubation (if part of practice)	TEE probe insertion	Variable	25 cases (50% under 2 years of age)
TEE exam	Perform and interpret with supervision	Variable	50 cases
Ongoing TEE experience	Maintenance and competency	Annual	25-50 cases per year or achievement of laboratory-established outcome variables

Modified from Ayres *et al.*<sup>31</sup>

and patient care or procedural skills as outlined in the Task Force addressing Pediatric Cardiology Fellowship Training in Noninvasive Cardiac Imaging are recommended for pediatric cardiologists planning to perform TEE independently (Table 3).<sup>31,60</sup> This does not preclude a categorical fellow from starting to learn TEE skills during his/her fellowship, including but not limited to time on a simulator which can optimize the ability to rapidly and fluidly obtain images. Evaluation of the anatomic and hemodynamic complexity of pediatric and ACHD patients demands an in-depth knowledge of all congenital and acquired pediatric cardiovascular pathologies, along with associated palliative and corrective surgical and transcatheter procedures. In addition, a rich experience in two-dimensional (2D) ± 3D echocardiography, as well as pulsed-wave, continuous-wave, and color flow Doppler imaging techniques, is necessary.<sup>9</sup>

Performance of TEE requires understanding of oropharyngeal anatomy, endoscopic techniques, and the indications, contraindications, and risks involved in the procedure, particularly if one is responsible for probe insertion. In small children, proper probe selection and supervision of intubation for the novice echocardiographer can mitigate risk.<sup>61,62</sup> The individual responsible for probe placement should be skilled in esophageal intubation. Suggested training guidelines for those expected to be involved in probe insertion in children include the performance of at least 25 esophageal intubations with direct supervision by an experienced pediatric echocardiographer, gastrointestinal endoscopist, or anesthesiologist, optimally in an active, accredited, and high-volume pediatric heart center, before unsupervised probe placement in this population is considered. This supervised experience should also include children and adults in a variety of clinical settings, including but not limited to operating rooms, catheterization laboratories, hybrid rooms, intensive care units, and sedation suites. The echocardiographer must develop skills in image acquisition and optimization, probe manipulation, and interpretation of the data. The findings should be rapidly and effectively communicated to the surgical and/or interventional team(s) as appropriate.<sup>63</sup>

Supervised performance and interpretation of at least 50 TEE examinations in pediatric and ACHD patients prior to independent TEE imaging is recommended.<sup>64</sup> For ACHD imaging by practitioners involved primarily in adult TEE, the minimum requirements for training and maintenance of competence are outlined in the 2013 ASE/SCA Comprehensive TEE Guidelines but ideally this imaging should be performed by physicians with experience and/or training in ACHD.<sup>16</sup> In addition to cardiologists, some cardiac anesthesiologists who care for children have received appropriate training and experience in pediatric TEE and provide interpretation in the operating room. In these cases, a second provider trained in TEE or congenital cardiovascular anesthesiology should be available to mitigate distraction from performing peri-procedural TEE monitoring. While some international societies support non-physician led TEE in adult patients, in the setting of congenital heart disease it is

appropriate that the procedure is performed under direct medical supervision.

**Recommendations for Physicians Not Formally Trained in TEE Performance in Pediatric and ACHD Patients.** Physicians interested in performing TEE without a formal pediatric cardiology fellowship will benefit from intensive training in an accredited congenital/pediatric echocardiography laboratory with emphasis on TEE imaging.<sup>31</sup> These guidelines aim to promote safety and quality by clarifying the necessary skills and the extent of supervised training and experience needed to perform TEE. There is no intent to exclude physicians from performing TEE, but rather to promote a standard of safety and effective performance of the exam in complex and often frail pediatric and ACHD populations.

**Maintenance of Skills.** Maintenance of skills should be achievable with 25-50 annual TEE examinations in pediatric and/or ACHD patients. In large programs where duties are shared among many TEE-competent physicians, it is conceivable that this metric may not be met for each trained physician. In these cases, alternative evaluations of maintenance of proficiency are often based on outcomes variables established by the laboratory director. Ongoing quality improvement is recommended, focusing upon updating laboratory guidelines and assessing outcomes as well as an annual review of the physician's TEE performance and accuracy of interpretation. The Intersocietal Accreditation Commission (IAC) – an independent body that provides accreditation to pediatric echocardiography laboratories based upon published, accepted standards – regularly updates its guidelines for accreditation in pediatric echocardiography, including pediatric TEE (<http://www.intersocietal.org/>).

**Certification.** There is currently no certification pathway specifically designed for the physician performing TEE for the pediatric or ACHD patient.

### Key Points

1. Physicians wishing to perform TEE in children and all patients with CHD should:
  - a. Receive supervised training and interpretation by a practitioner with significant TEE experience. That person can be a pediatric echocardiographer, congenital cardiovascular anesthesiologist, or echocardiographer with experience and/or training in ACHD.
  - b. Undergo supervised performance and interpretation of at least 50 TEE examinations in pediatric and/or ACHD patients prior to independent TEE imaging.
2. There is currently no certification pathway specifically designed for the physician performing TEE for the pediatric or ACHD patient.

## Patient Selection and Complications

The overall clinical experience with TEE demonstrates a favorable safety profile, with a 1-3% complication rate in the pediatric age group.<sup>11,61,65-69</sup> Most problems are seen in neonates and small infants and are associated with respiratory compromise or vascular compression.<sup>70-75</sup> Mild sinus slowing and even bradycardia for age have been reported from vagal stimulation during probe insertion as well as alterations of cardiac rhythm.<sup>61,76</sup> When intraoperative TEE imaging is performed, the imaging probe ideally should be inserted before placement of sterile drapes. The preoperative study should be completed prior to skin incision in order to minimize electrocautery artifacts. At most centers, the tip of the probe is maintained in the stomach during the bypass phase in an effort to limit esophageal morbidity given that the widest diameter of the probe is at its tip. Hardware availability or other reasons may preclude leaving the probe in situ throughout the bypass period. The probe might be removed after the preoperative study and reinserted prior to separation from bypass or used only for postoperative assessment. In these settings, potential additional risks should be recognized such as those associated with oropharyngeal/esophageal instrumentation in the fully anticoagulated patient, potential tracheal extubation or tube malposition, or bypass cannula dislodgement. Serious complications such as esophageal perforation, inadvertent gastric laceration during sternotomy, and subglottic stenosis have been rarely described.<sup>77,78</sup> The risks associated with bleeding related to TEE imaging in anticoagulated patients are largely unknown and the risk/benefit of TEE in this setting should be considered.

The incidence of oropharyngeal dysphagia after TEE has been estimated at 18% in children undergoing open heart procedures.<sup>79-81</sup> Risk factors included age < 3 years, preoperative endotracheal intubation, longer duration of endotracheal intubation, and interventions for left-sided obstructive lesions. The presence of dysphagia can affect postoperative recovery and contribute to major morbidity. Given the relatively large probe size in the neonate and small infant and the complexity and duration of many interventions, every effort should be made to modify these risk factors. Another clinical concern in children is that of upper airway obstruction requiring the need for tracheal reintubation in certain high-risk patients.<sup>82</sup> A significant increase in endotracheal tube cuff pressure is reported during TEE probe insertion; however, this increase is transient and returns to baseline values upon probe advancement into the stomach.<sup>83</sup> Although a high incidence (64%) of abnormal findings (erythema, edema, and hematoma; less frequently, mucosal erosion and petechiae) were found by flexible endoscopy after TEE for pediatric cardiac surgery, no long-term feeding or swallowing difficulties were identified.<sup>84</sup>

Special consideration should be given to critically ill infants with total anomalous pulmonary venous anomalies who might develop hypotension and hypoxemia from compression of the pulmonary venous confluence by the imaging probe.<sup>85,86</sup> Placement of the transducer after sternotomy is often uneventful, however, suggesting that if TEE is used in this setting, the probe should be inserted after the chest is open and close observation for hemodynamic compromise is warranted.

## Sedation and Anesthesia

**The Pediatric Patient.** Sedation and anesthesia for TEE in patients with CHD and children should be performed by experienced providers who understand the anatomy and pathophysiology of the specific lesions.<sup>87</sup> Esophageal intubation can be quite stimulating, therefore most children require deep sedation or general anesthesia, and an anesthesiologist or equivalent provider with expertise in caring for pediatric

patients is usually involved in selecting, administering, and monitoring these agents. Close communication between the anesthesiologist and the echocardiographer prior to and during the procedure is essential.

**The ACHD Patient.** TEE in the ACHD patient is routinely performed with conscious sedation as described in the 2013 ASE/SCA Comprehensive TEE Guidelines.<sup>16</sup> Serious complications are rare in this patient population; however, additional considerations may apply if there are associated hemodynamic disturbances, severe pulmonary hypertension, residual cyanosis, or single ventricle physiology.<sup>9</sup> In the adult with Fontan circulation, it is important to minimize changes in systemic venous volume since venodilation or dehydration can reduce the central venous pressure and decrease flow through the pulmonary circuit.<sup>88</sup> Intravenous hydration may be needed to offset the detrimental effects of fasting combined with the vasodilatory and/or myocardial depressant effects of sedatives. Hypoventilation with consequent hypoxia can increase pulmonary vascular resistance, resulting in an overall reduction in cardiac output in the Fontan patient, therefore supplemental oxygen and capnography for monitoring are strongly recommended.<sup>88</sup> Since any patient with a Fontan fenestration or residual shunt is at high risk for paradoxical embolism, meticulous care, including the use of IV filters, should be considered. Changes in afterload can exacerbate right-to-left shunts, increasing the risk of paradoxical emboli and decreasing arterial oxygen saturation.<sup>9</sup> Therefore, it may be prudent to ask for the assistance of the anesthesia team when performing TEE in the ACHD patient with Fontan physiology, unrepaired or palliated cyanotic cardiac lesions, pulmonary hypertension, or a history suggestive of moderate to severe obstructive sleep apnea.

## Key Points

1. TEE demonstrates a favorable safety profile and low complication rate in children and all patients with CHD.
2. Most complications are related to respiratory compromise or vascular compression. Rare serious complications include esophageal perforation, gastric laceration, and subglottic stenosis.
3. While general anesthesia is typically employed for the performance of TEE in children, TEE in the adult with CHD is routinely performed with conscious sedation. Anesthesia assistance should be considered in the adult with Fontan physiology, unrepaired or palliated cyanotic cardiac lesions or severe pulmonary hypertension.

## Probe Selection, Insertion Techniques, and Care

**Probe Selection.** Transducer technology for TEE imaging has evolved significantly and probes now have higher resolution, more options for image plane acquisition, and enhanced modes to better assess the cardiovascular system even in very small infants. Initial *monoplane* (single plane) TEE devices allowed only transverse or horizontal imaging planes.<sup>89</sup> The incorporation of a second scanning plane in *biplane* probes enabled the longitudinal or vertical imaging plane (90°), thereby providing for interrogation of structures with orthogonal views.<sup>90-94</sup> The development of *multiplane* (omniplane) probes permitted imaging in planes anywhere between 0°-180°.<sup>95-98</sup> Advances in 3D technology for TEE devices has evolved from off-line reconstruction of sequentially acquired 2D image planes, to real-time imaging using a specialized matrix-array probe. The probe renders a selected volume of the heart as a real-time 3D dataset able to display anatomy from any perspective, including the surgeon's view.<sup>99,100</sup>

TEE probe selection for infants and children relies primarily on two factors: the weight of the patient and the size of the probe. The *pediatric mini-multiplane* probe was the initial miniaturized device with multiplane capabilities available for use in neonates, infants and small children. Subsequently the *pediatric micro-multiplane probe* was developed for use in the tiniest babies, representing the smallest multiplane device available today.<sup>18,21,64</sup> Equipment manufacturers have suggested a patient weight limit for the use of these devices (over 3.0-3.5 kg for the mini-multiplane and over 2.5 kg for the micro-multiplane), however, in clinical practice both probes have been safely used quite extensively in patients well below these weight recommendations.<sup>19,101</sup> Both the micro- and the mini-multiplane probes have 2D and Doppler capabilities. The adult 2D multiplane TEE probe should be considered for a patient weight >25 kg, however, this device has also been applied to smaller children. The advantage of using an adult sized probe when possible is better image quality due to having a greater density of piezoelectric crystals, and the larger size may allow for improved contact with the esophagus. The risk/benefit ratio of oversizing the TEE probe should be considered on a case-by-case basis but may be safe when placed with minimal resistance. Current 3D TEE imaging probes have slightly larger dimensions than 2D multiplane adult TEE probes and should be considered for a patient weight >30 kg rendering them unsuitable for use in most young children.

Intra-cardiac echocardiography catheters (8-10 F) have been used for TEE in neonates and small infants and may provide clinically useful information in some cases.<sup>102-104</sup> Imaging is limited to a single longitudinal (90°) plane, and lack of formal regulatory approval for this specific application, coupled with the stiffness of the catheter, have prevented widespread use.

Intraoperative epicardial echocardiography may be used in patients in whom TEE imaging is not feasible due to patient size constraints, contraindications to esophageal instrumentation, or when TEE is not available. Epicardial imaging may also be indicated when the patient is not able to tolerate TEE imaging or when there are concerns for probe-related hemodynamic or respiratory compromise. In some instances, epicardial imaging can overcome limitations of TEE, such as interrogation of the branch PAs (in particular the left PA), and in patients undergoing interventions addressing muscular ventricular septal defects either by direct surgical closure or periventricular transcatheter interventions. While there is potential for hemodynamic alterations and rhythm abnormalities, infection risks, and a need for operator expertise while directly touching the heart, most experienced centers have used this approach safely.

**Probe Insertion Techniques.** The TEE probe should be inserted after adequate sedation/anesthesia and following an appropriate period of fasting. The technique for probe insertion may vary among institutions but can be facilitated by maintaining the patient's head, as well as the probe within the oropharyngeal cavity, in the neutral, midline position. In most cases, the unlocked, well-lubricated transducer is blindly but gently advanced into the esophagus. Slight ante-flexion of the probe tip, subluxation of the mandible, reverse cricoid maneuver, and/or device guidance with a gloved finger can facilitate probe insertion. Lifting the head may also help in older children. In some cases, direct laryngoscopy by an anesthesiologist may aid visualization and esophageal intubation if there is difficulty during blind probe-placement. Transducer insertion is an important skill in the practice of TEE. Although some effort might be expected, distinguishing normal from excessive resistance requires expertise and ongoing experience with the technique.

In children, positioning the head to the side has been reported to facilitate passage of the probe, as this maneuver reportedly results in closure of the ipsilateral pyriform sinus, a site where the probe may encounter obstruction.<sup>105</sup> In the intraoperative setting, once the TEE probe has been inserted, the patient's head can be repositioned to avoid interference with the surgical field during device manipulation. Factors that may render probe insertion difficult in infants weighing 4 kg or less include lower weight, abnormal craniofacial anatomy, prematurity, and a diagnosis of 22q11 deletion.<sup>106</sup> Occasionally an appropriate sized probe may experience difficulty in insertion if a cuffed endotracheal tube is used which can reduce the esophageal lumen. Communication with the anesthesiologist to temporarily deflate the cuff for insertion and confirmation of adequate ventilation should be considered. If there are respiratory or hemodynamic changes resulting in compromise, a smaller probe can be attempted or the exam should be aborted.

Preoperative evidence by TTE or other modality of an aberrant subclavian artery or unusual arch laterality should be communicated to the anesthesia team allowing for intraoperative arterial pressure monitoring to be established on the contralateral upper extremity before TEE probe insertion given that the arterial tracing may be lost or severely dampened from compression of the aberrant artery.

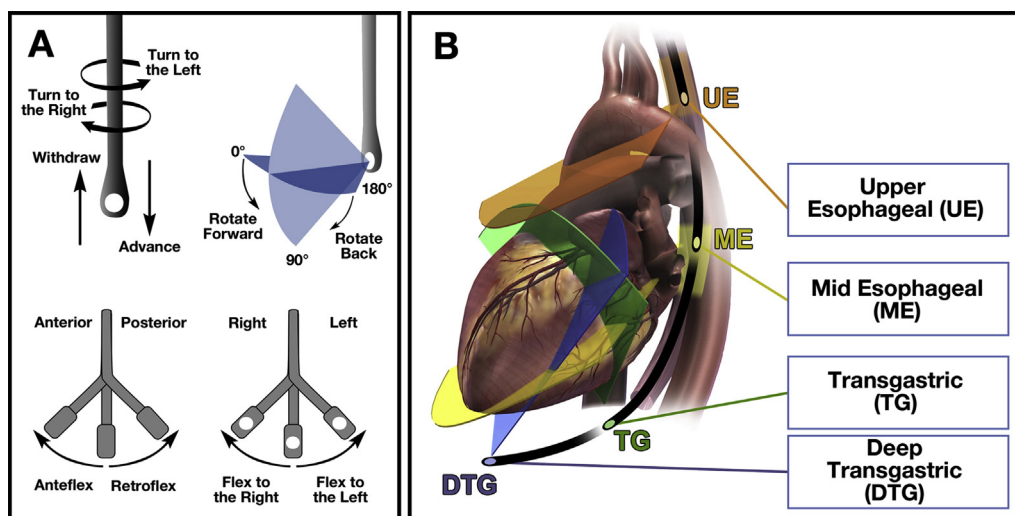
**Probe Care.** The Centers for Disease Control and Prevention (CDC) categorizes all medical devices according to their potential for patient infection.<sup>107</sup> Because TEE probes contact mucous membranes, they require high-level disinfection after each use. Current recommended practices have evolved to cover the handling, cleaning, disinfection, and storage of all TEE probes. Each institution should develop a standard practice and protocol for TEE probe care that incorporates regulatory guidelines and manufacturer's recommendations (Table 4). Care should be taken to protect the piezoelectric crystals from rough handling or physical trauma. The probe tip and shaft should be inspected for damage or cracks as part of routine maintenance, before probe insertion, and after probe withdrawal. Only the probe shaft and tip can be immersed. The handle, connector, and cable should be cleaned separately by wiping them down with the recommended disinfectant. Adequate rinsing is crucial for patient safety. Probes should be labeled with a disinfection date and reprocessed according to the institution's laboratory policy. As the recommendations evolve, the high-level disinfection process should be updated accordingly.

## Key Points

1. TEE probe selection is primarily based upon patient weight and probe size.
  - a. Pediatric 2D TEE probes are available as a micro-multiplane probe for patients > 2.5 kg, and a mini-multiplane probe for patients > 3.0-3.5 kg.
  - b. The adult 2D and 3D TEE probes are available for use in patients > 25 kg and >30 kg, respectively.
  - c. In clinical practice, each probe has been used safely below these weight recommendations
2. TEE probe insertion should be performed with adequate sedation/anesthesia, and after an appropriate period of fasting. Careful monitoring for complications is essential.
3. TEE probe rinsing and high-level disinfection should be performed after each use, according to manufacturer's instructions and institutional laboratory policy.

**Table 4** Steps involved in TEE probe care

Point of care wipe down	When the probe is removed from the patient, it should be immediately wiped down to remove all superficial material with an enzymatic product before it dries and adheres to the probe.
Transported in container	The probe should then be placed in a container that protects the integrity of the fragile terminal tip of the probe as well as preventing the contamination from secretions on the probe. This will allow for safe transportation to the location of cleaning and disinfection.
Cleaning	A cycle of rinsing the initial enzymatic cleaner off the probe should be followed by another enzymatic cleaning and prolonged rinse.
Manual drying	Use lint-free drying cloth to prevent dilution of disinfectant.
Electrical leakage testing	Promotes patient safety and now required for IAC accreditation
Disinfection	Manual or automated high-level disinfection with documentation. Manual processing requires strict adherence to soaking and rinsing times to prevent probe damage and chemical burns.
Rinsing	Follow instructions of the disinfectant manufacturer and Joint Commission recommendations for water quality.
Probe drying	Probes should hang in a vertical cabinet to dry, with probe not touching anything.
Storage	Store probes in a well-ventilated dust-free cabinet with probe tip protectors covering the piezoelectric crystal. (A positive-pressure HEPA-filtered cabinet is optimal.)
Transport	Transport the probe to needed location in a clean, protective container.



**Figure 1** Terminology used to describe manipulation of the transesophageal echocardiographic probe during image acquisition. **(A)** Terminology used for the manipulation of the transesophageal echocardiographic probe. **(B)** Four standard transducer positions within the esophagus and stomach and the associated imaging planes. Reprinted with permission from Hahn *et al.*<sup>16</sup>

**Instrument Manipulation and Probe Controls**

The TEE probe can be manipulated in several directions for image acquisition of cardiovascular structures (Figure 1). The terminology used to describe TEE probe manipulation assumes the patient is lying in the supine position and the imaging plane is directed anteriorly through the heart from the esophagus. The established nomenclature in reference to the heart considers the following positions: superior (toward the head), inferior (toward the feet), posterior (toward the spine), and anterior (toward the sternum). The terms right and left in reference to the patient denote his/her right and left sides, respectively.

The probe shaft can be advanced (pushed in) or withdrawn (pulled out), and rotated to the right (clockwise) or to the left (counterclockwise). The controls on the probe handle allow for movement (flexion) of the probe tip. In the adult multiplane probe, one control (the larger wheel) allows for anteflexion (flexion anteriorly) or retroflexion (flexion posteriorly) and the other control (smaller wheel) provides for right or left flexion. Pediatric TEE probes can be anteflexed and retroflexed but generally lack the right-left flexion control, limiting the available imaging planes. In small infants, minimal adjustments in probe

position allow navigation across multiple cross-sections. The multiplane probe tip allows the imaging plane angle to rotate between 0°-180° (forward rotation) and from 180° toward 0° (backward rotation).

**Role of the Sonographer**

ASE recognizes that sonographers are an integral part of the cardiac imaging team and support their active role during the performance of a TEE. However, that role should be limited to their scope of practice. Specifically, ASE supports sonographers using their expertise and skills to optimize images (i.e., adjust gain, contrast, and other machine settings) as well as crop and display 3D data sets during the TEE exam. ASE does not advocate for sonographers to perform TEE intubation or manipulation of the probe.<sup>108</sup>

**Comprehensive Imaging Examination**

The 2013 ASE/SCA Comprehensive TEE Guidelines provided a series of key 2D tomographic views written and oriented toward adults with structurally normal hearts. Proper performance of a pediatric or CHD

TEE examination was outside the scope of that document, requiring modifications to address several important and unique considerations, but whenever possible this document uses the same views and follows the same nomenclature for the sake of consistency, including the assumption that patients have levocardia with normal situs.

TEE imaging is performed from *four* primary positions within the gastrointestinal tract (Figure 1): midesophageal (ME), transgastric (TG), deep transgastric (DTG), and upper esophageal (UE). Images in the ME, TG, and UE positions will be displayed in the same manner as the 2103 guidelines with near field and far field referring to structures closer and further from the probe, respectively (Figure 2). In contrast however, we will present the DTG views inverted, with the apex of the heart at the bottom of the screen in an “anatomically correct” position.

The echocardiographic evaluation of children and all patients with CHD is based on structures rather than views. Given the wide diversity of CHD with innumerable anatomic variations, some TEE views need to be modified to discern the precise cardiac anatomy for any given patient. The 28 tomographic views described herein do not have to occur in order and should serve as a starting point, with the understanding that improvisation and nonstandard views (using various probe maneuvers such as left-right rotation, slow advancement/withdrawal, or slow rotation of the transducer angle) may be necessary for optimal visualization of the structure in question (Table 5). Similarly, single-beat loops of a tomographic view might be inadequate for imaging the anatomy, and longer video clips (sweeps) may be needed to capture essential information. For any valve or structural abnormality, 2D, color flow, and spectral Doppler imaging in SAX and multiple LAX views, as well as 3D structural and color Doppler imaging should be utilized when appropriate. Image resolution should be optimized by minimizing sector angle and increasing magnification to maximize frame rate. Likewise, Nyquist color scale, sector angle, and color depth should be adjusted to limit the amount of color speckle in the far field.

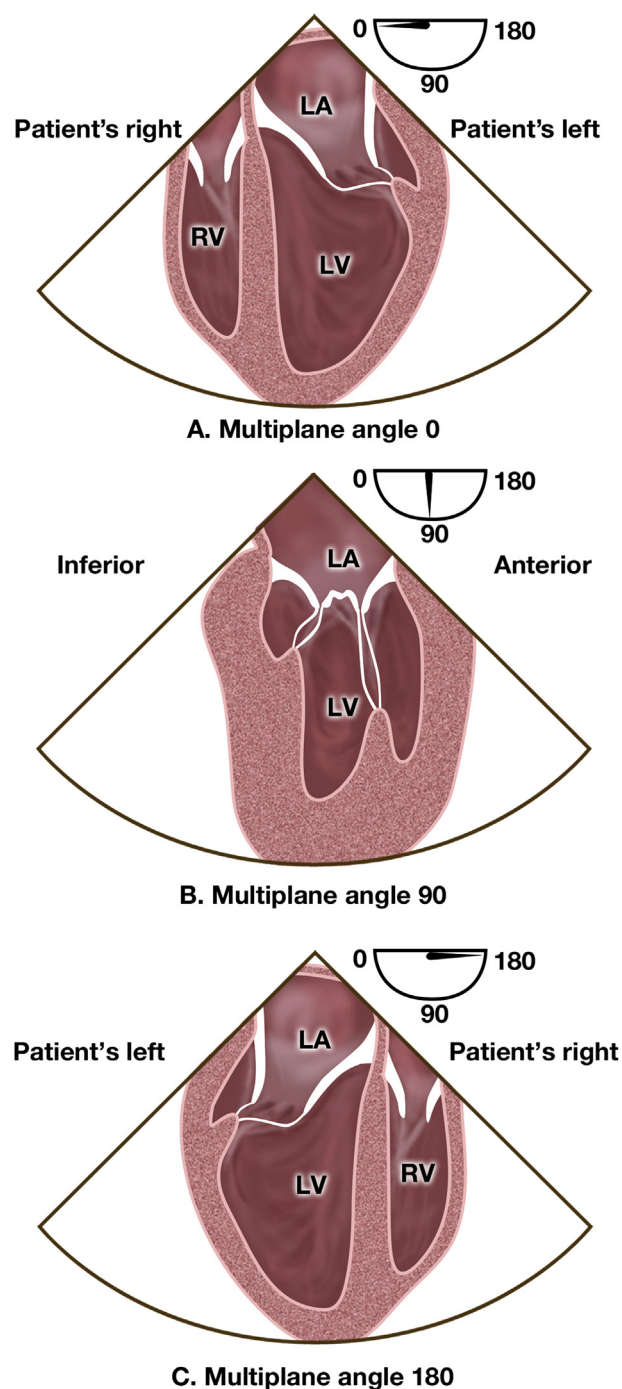
By utilizing the 28 views outlined in this document, a comprehensive TEE examination can be performed in virtually any pediatric patient with or without CHD, and in most ACHD patients. For each view, accompanying videos are available online at [www.onlinejase.com](http://www.onlinejase.com).

### 1. ME 4-Ch (Video 1)

The **ME Four-Chamber View** is obtained after initial probe insertion in the esophagus when all cardiac chambers—right atrium (RA), left atrium (LA), right ventricle (RV), and left ventricle (LV) – the interatrial (IAS) and interventricular (IVS) septa, and the mitral (MV) and tricuspid valves (TV) are visualized. All ME views obtained below start from this “home base.” This view simulates a transthoracic apical 4-Ch view and is one of the most useful for evaluating intracardiac anatomy and function. It is typically obtained with some degree of probe retroflexion and transducer angle rotation between 0-10°. With further probe retroflexion, the coronary sinus (CS) and entrance of the inferior vena cava (IVC) to the RA can be visualized. The ME 4-Ch view provides information regarding regional and global biventricular function, and atrioventricular (AV) valve stenosis and regurgitation.

### 2. ME 5-Ch (Video 2)

The **ME Five-Chamber View** is obtained by applying slight antelexion from the ME 4-Ch view to allow better visualization of the aortic valve (AoV) and left ventricular outflow tract (LVOT). Color flow and spectral Doppler can be utilized to evaluate MV, TV, and AoV stenosis and regurgitation.



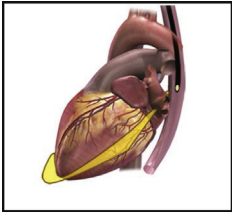
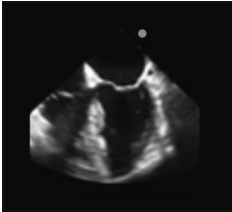
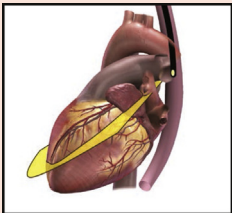

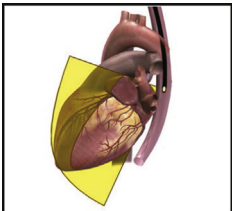

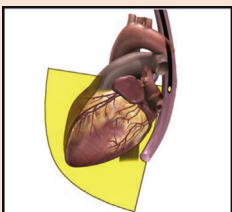
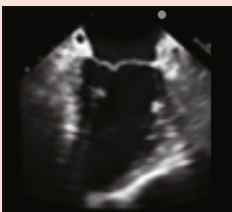
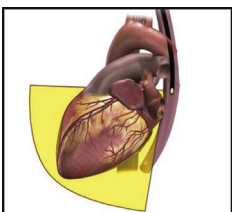

**Figure 2** Conventions of 2D transesophageal echocardiographic image display. The transducer location and the near field (*vertex*) of the image sector are at the top of the display screen and far field at the bottom. **(A)** Image orientation at transducer angle 0°. **(B)** Image orientation at transducer angle 90°. **(C)** Image orientation at transducer angle 180°. Of note, we present the DTG views inverted, with the apex of the heart at the bottom of the screen in an anatomically correct position. LA, Left atrium; LV, left ventricle; RV, right ventricle. Reprinted with permission from Hahn *et al.*<sup>16</sup>

### 3. ME Mitral (Video 3)

The **ME Mitral Commissural View** is obtained by starting from the ME 4-Ch view and rotating the transducer angle to

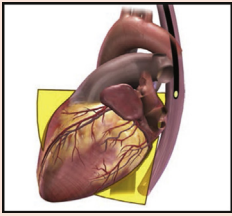
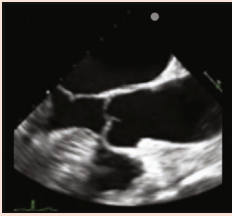
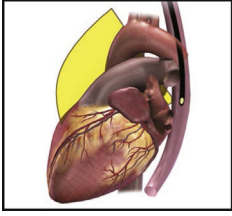

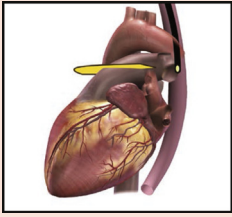
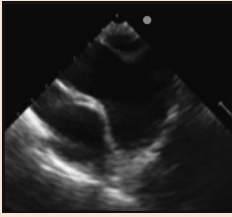
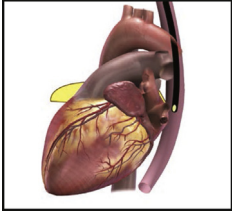

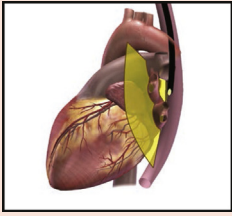
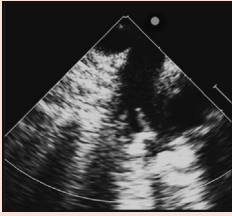


**Table 5** Comprehensive transesophageal echocardiographic examination. The table lists the suggested 28 views included in a comprehensive TEE exam. Each view is shown in its imaging plane, on a corresponding 3D model, with the 2D TEE image. The acquisition protocol and the structures imaged in each view are listed in the subsequent columns.

Imaging plane	3D model	2D TEE image	Acquisition protocol	Structures imaged
<b>Midesophageal views</b>				
1. ME 4-Ch			Transducer angle: ~0°–10° Level: ME	LA/RA IAS LV/RV/IVS MV (A <sub>3</sub> A <sub>2</sub> -P <sub>2</sub> P <sub>1</sub> ) TV CS
2. ME 5-Ch			Transducer angle: ~0°–10° Level: ME	AoV LVOT LA/RA LV/RV/IVS MV (A <sub>2</sub> A <sub>1</sub> -P <sub>1</sub> ) TV
3. ME Mitral			Transducer angle: ~50°–70° Level: ME	LA CS LV MV (P <sub>3</sub> -A <sub>3</sub> A <sub>2</sub> A <sub>1</sub> -P <sub>1</sub> ) Papillary muscles Chordae tendineae
4. ME 2-Ch			Transducer angle: ~80°–100° Level: ME	LA CS LAA LV MV (P <sub>3</sub> -A <sub>3</sub> A <sub>2</sub> A <sub>1</sub> ) Circumflex CA
5. ME LAX			Transducer angle: ~120°–140° Level: ME	LA LV LVOT RVOT MV (P <sub>2</sub> -A <sub>2</sub> ) AoV Proximal Asc Ao

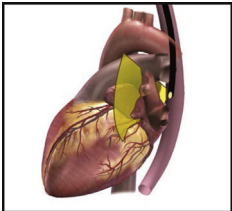
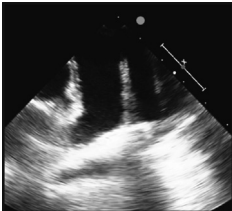
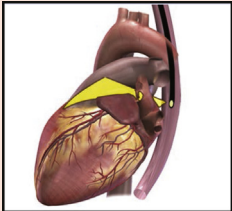
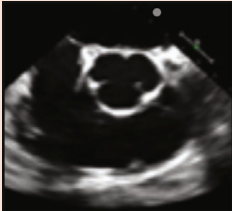
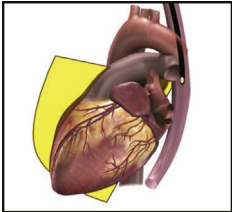
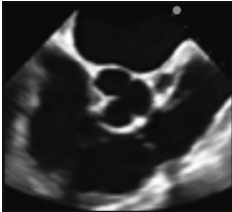
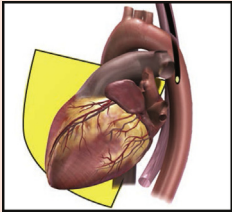
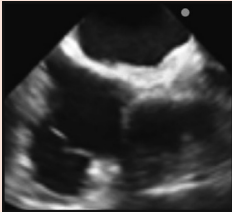
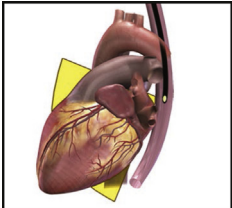

(Continued)

Table 5 (Continued)

Imaging plane	3D model	2D TEE image	Acquisition protocol	Structures imaged
6. ME AoV LAX			Transducer angle: $\sim 120^\circ$ – $140^\circ$ Level: ME	LA LVOT MV (P <sub>2</sub> -A <sub>2</sub> ) AoV Proximal Asc Ao LCA
7. ME Asc Ao LAX			Transducer angle: $\sim 90^\circ$ – $110^\circ$ Level: ME	Mid Asc Ao RPA
8. ME Asc Ao SAX			Transducer angle: $\sim 0^\circ$ – $30^\circ$ Level: ME	Mid Asc Ao MPA/Br PAs SVC
9. ME Rt Pulm veins			Transducer angle: $\sim 0^\circ$ Level: ME	Mid Asc Ao SVC RUPV RLPV
10. ME Lt Pulm veins			Transducer angle: $\sim 90^\circ$ – $110^\circ$ Level: ME	LUPV LLPV LPA


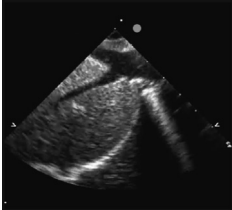
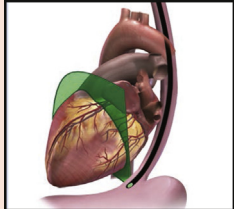
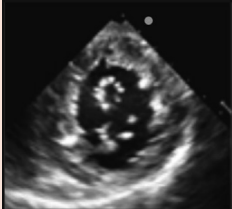
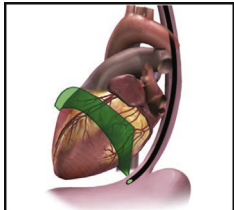
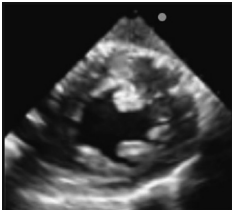
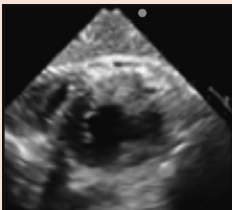
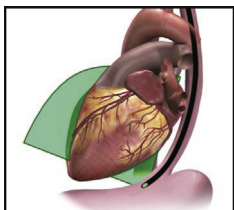
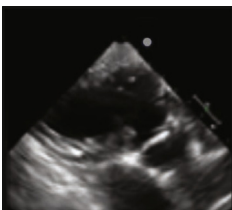
(Continued)

**Table 5** (Continued)

Imaging plane	3D model	2D TEE image	Acquisition protocol	Structures imaged
11. ME LAA			Transducer Angle: ~90°–110° Level: ME	LAA LUPV
12. ME AoV SAX			Transducer angle: ~25°–45° Level: ME	AoV PV LA/RA Superior IAS RVOT LCA/RCA
13. ME RV In-Out			Transducer angle: ~50°–70° Level: ME	AoV PV LA/RA Superior IAS TV RVOT IVS: membranous, outlet
14. ME Mod Bicaval TV			Transducer angle: ~50°–70° Level: ME	LA/RA Mid IAS TV SVC IVC CS
15. ME Bicaval			Transducer angle: ~90°–110° Level: ME	LA RA/RAA IAS SVC IVC

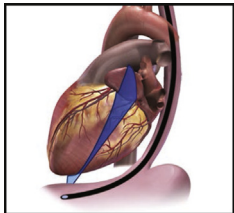
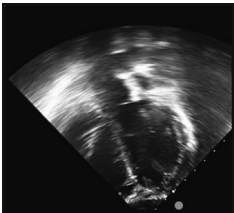
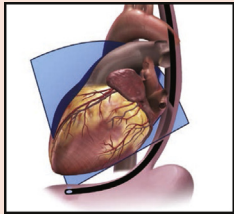
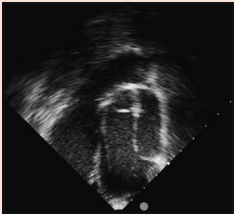
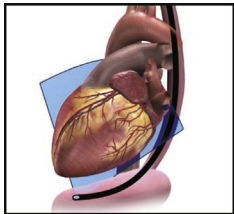
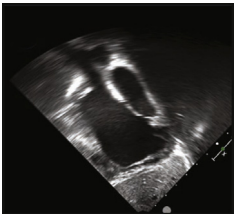
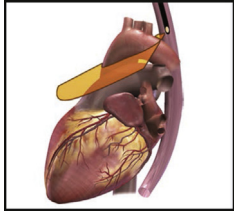

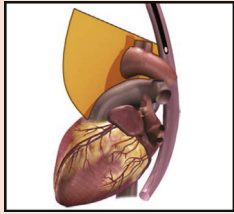
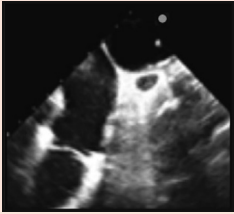
(Continued)

Table 5 (Continued)

Imaging plane	3D model	2D TEE image	Acquisition protocol	Structures imaged
<b>Transgastric views</b>				
16. TG IVC/Hep veins			Transducer angle: $\sim 80^\circ$ – $100^\circ$ Level: TG	IVC Hepatic veins
17. TG Basal SAX			Transducer angle: $\sim 0^\circ$ – $20^\circ$ Level: TG	LV (base) RV (base) MV TV IVS: muscular
18. TG Mid Pap SAX			Transducer angle: $\sim 0^\circ$ – $20^\circ$ Level: TG	LV (mid) Papillary muscles RV (mid) IVS: muscular
19. TG Apical SAX			Transducer angle: $\sim 0^\circ$ – $20^\circ$ Level: TG	LV (apex) RV (apex) IVS: apical muscular
20. TG LAX			Transducer angle: $\sim 120^\circ$ – $140^\circ$ Level: TG	LV LVOT AoV Ao root MV

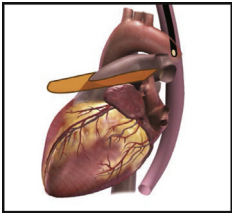
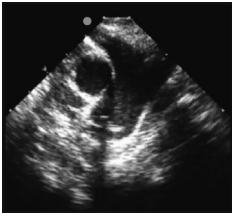
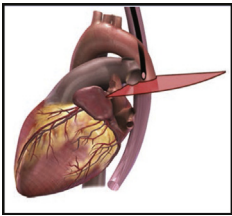
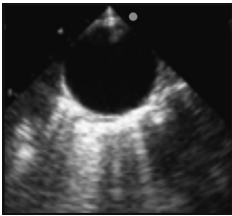
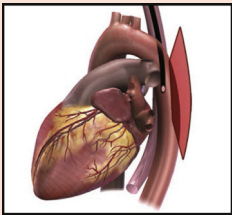
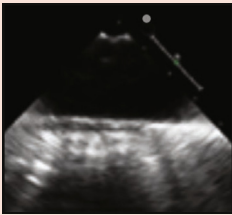
(Continued)

**Table 5** (Continued)

Imaging plane	3D model	2D TEE image	Acquisition protocol	Structures imaged
<b>Deep transgastric views</b>				
21. DTG 5-Ch			Transducer angle: $\sim 0^\circ$ – $20^\circ$ Level: DTG	LV/RV LVOT AoV Ao root MV IVS
22. DTG RVOT			Transducer angle: $\sim 50^\circ$ – $90^\circ$ Level: DTG	LV/RV RVOT PV LVOT AoV MV IVS
23. DTG Atr Sept			Transducer angle: $\sim 80^\circ$ – $90^\circ$ Level: DTG	RA/RAA LA RPA IAS SVC IVC
<b>Upper esophageal views</b>				
24. UE Ao Arch LAX			Transducer angle: $\sim 0^\circ$ – $10^\circ$ Level: UE	Ao arch Innominate vein
25. UE Ao Arch SAX			Transducer angle: $\sim 70^\circ$ – $90^\circ$ Level: UE	Ao arch Innominate vein MPA Br PAs PV

(Continued)

Table 5 (Continued)

Imaging plane	3D model	2D TEE image	Acquisition protocol	Structures imaged
26. UE PA			Transducer angle: $\sim 0^\circ$ – $20^\circ$ Level: UE	MPA LPA RPA Mid Asc Ao
Aortic views				
27. Desc Ao SAX			Transducer angle: $\sim 0^\circ$ – $10^\circ$ Level: UE to TG	Desc Ao
28. Desc Ao LAX			Transducer angle: $\sim 90^\circ$ – $100^\circ$ Level: UE to TG	Desc Ao

CS, Coronary sinus; IAS, interatrial septum; IVS, interventricular septum; LAA, left atrial appendage; LCA, left coronary artery; LLPV, left lower pulmonary vein; LUPV, left upper pulmonary vein; RAA, right atrial appendage; RCA, right coronary artery; RLPV, right lower pulmonary vein; RUPV, right upper pulmonary vein.

50–70°. As the name implies, the ME Mitral view is used primarily to evaluate the MV. This imaging plane crosses both the anterolateral and posteromedial commissures. The sections of MV on the image display (from left to right) are P<sub>3</sub>-A<sub>3</sub>A<sub>2</sub>A<sub>1</sub>-P<sub>1</sub>. Turning the probe leftward (counterclockwise) allows imaging of the posterior leaflet scallops (P<sub>3</sub>P<sub>2</sub>P<sub>1</sub>) and rightward (clockwise) allows imaging of the anterior leaflet segments (A<sub>3</sub>A<sub>2</sub>A<sub>1</sub>). This view is also useful for evaluating the anterolateral and posteromedial papillary muscles and their corresponding tensor apparatus as well as regional LV function and MV stenosis or regurgitation.

#### 4. ME 2-Ch (Video 4)

The **ME Two-Chamber View** (orthogonal to ME 4-Ch view) is obtained by maintaining the same neutral position and rotating the transducer angle to 80–100° to allow visualization of the LA, left atrial appendage (LAA), MV (P<sub>3</sub>-A<sub>3</sub>A<sub>2</sub>A<sub>1</sub>), and LV. The CS is seen in cross section just above the posterior MV annulus and basal inferior LV segment. From this view, clockwise rotation of the probe demonstrates the ME Bicaval view (View #15 below); rotation counterclockwise visualizes the LAA and also the left circumflex coronary artery (CA)

can be seen coursing along the AV groove. Color flow Doppler as well as spectral Doppler of the MV can aid in identification of valvular stenosis or regurgitation.

#### 5. ME LAX (Video 5)

The **ME Long Axis View** can be obtained from the ME 4-Ch or 2-Ch views by continuing forward rotation of the transducer angle to approximately 120–140° to visualize the LA, MV (P<sub>2</sub>-A<sub>2</sub>), LV, LVOT, AoV, and proximal ascending aorta. A portion of the right ventricular outflow tract (RVOT) can also be noted anterior to the LVOT. This view allows assessment of the MV and AoV as well as subvalvular and supra-valvular anatomy. The size and function of the mitral and aortic valves and assessment of the LV inferolateral and anteroseptal walls can be evaluated with 2D, color flow, and spectral Doppler imaging.

#### 6. ME AoV LAX (Video 6)

The **ME Aortic Valve LAX View** is obtained from the ME LAX view by slight withdrawal of the probe, while maintaining a transducer angle of 120–140°. Transducer image depth is also reduced to focus primarily on the LVOT, AoV, and proximal aorta, including the sinuses of Valsalva, to allow accurate measurements with 2D, color, and spectral Doppler imaging.

especially when used in conjunction with the orthogonal ME AoV SAX view (see View #12 below). Color flow Doppler can provide a significant amount of information on LVOT and AoV pathology. The anterior (far field) AoV cusp is the right coronary cusp, and the right coronary ostium can often be seen arising from the sinus. The posterior (near field cusp) is either the left or noncoronary cusp, depending upon transducer rotation. When the probe is rotated counterclockwise, the origin of the left main CA can often be seen, and with further leftward rotation, sometimes the bifurcation into left anterior descending and circumflex CAs can be visualized.

7. ME Asc Ao LAX (Video 7)

The **ME ascending aorta LAX View** is obtained from the ME AoV LAX view (View #6 above) by withdrawal of the TEE probe, and rotation of the transducer angle to between 90° and 110°. The right pulmonary artery (PA) is seen in cross-section posterior to the ascending aorta (in the near field). Pathology involving the ascending aorta, such as supravalvular aortic stenosis and hypoplasia or aneurysmal dilation, can be identified. Aortic flow is typically perpendicular to the angle of insonation, hence spectral Doppler evaluation of the aorta will be limited but color Doppler can be useful. When the image plane is centered on the right PA, turning the probe counterclockwise can provide LAX imaging of the pulmonary valve (PV) and main PA. Probe antelexion enables optimal color and spectral Doppler interrogation (pulsed- and continuous-wave) of the RVOT, PV, and main PA.

8. ME Asc Ao SAX (Video 8)

From the ME ascending aorta LAX view (View #7 above), backward rotation of the transducer angle to 0°-30° results in the **ME Ascending Aorta SAX View**. Structures imaged from this view include the ascending aorta and superior vena cava (SVC) in cross section, main PA, and proximal branch PAs. Color flow and spectral Doppler evaluation of the PA may be useful.

9. ME Rt Pulm Veins (Video 9)

The **ME Right Pulmonary Veins View** can be obtained from the ME 4-Ch view, using a transducer angle of 0° and rotating clockwise. The right upper (superior) and lower (inferior) pulmonary veins take slightly different angles: the right upper pulmonary vein (RUPV) is more parallel to the angle of insonation, and with slight probe advancement, the right lower pulmonary vein (RLPV) can be visualized in a more perpendicular orientation. In addition, a transducer angle of 30°-50° may allow visualization of the veins simultaneously. Color flow Doppler (sometimes with decreasing the Nyquist limit) can display flow in both pulmonary veins, but a more favorable angle of insonation of the RUPV makes spectral Doppler of this pulmonary vein preferable. In addition to the right pulmonary veins, the superior vena cava (SVC) and ascending aorta can be visualized in cross-section.

10. ME Lt Pulm Veins (Video 10)

The **ME Left Pulmonary Veins View** displays the left pulmonary veins from a sagittal plane, orthogonal to that described for the ME Rt Pulm Veins view (View #9 above). From the ME neutral position behind the LA, forward rotation of the transducer angle to 90°-110° and turning counterclockwise, one can visualize separately the left upper (LUPV) and left lower (LLPV) pulmonary veins as they converge and enter the LA. The left PA can also be seen just superior to the LUPV. If the

probe is turned clockwise, the IAS, SVC, IVC (View #15 below), and finally the right pulmonary veins become visible. Of note, the left pulmonary veins can also be imaged using a transducer angle of about 0° with rotation of the probe counterclockwise to visualize the LAA and veins adjacent and lateral to it by advancing and withdrawing the probe.

11. ME LAA (Video 11)

The **ME Left Atrial Appendage View** can be obtained from the ME Lt Pulm Veins view (View #10 above) using the same transducer angle of 90°-110° and turning the probe slightly clockwise with some probe advancement and/or antelexion as necessary. Given the highly variable anatomy of the LAA, a complete assessment of this structure typically requires using multiple views, including backward rotation of the transducer from 90° to 0° (while imaging the appendage) and/or simultaneous multiplane imaging. Color flow and spectral Doppler can also be used to assess flow in the LUPV as well as into and out of the LAA.

12. ME AoV SAX (Video 12)

From the ME 5-Ch view, the AoV is located in the center of the display and the probe is withdrawn slightly and antelexed while maintaining a transducer angle between 25°-45° to obtain the **ME Aortic Valve SAX View**. For a trileaflet valve, the left coronary cusp will be posterior (near field) and to the patient's left, the right coronary cusp anterior (far field) and adjacent to the RVOT, and the noncoronary cusp rightward and adjacent to the IAS. The morphology and function of the AoV can be displayed both by 2D imaging and color flow Doppler, allowing for precise localization of stenotic and/or regurgitant jets. Slight withdrawal of the probe can reveal the anterior origin of the right CA and posterior origin of the left CA from their respective sinuses. A change in transducer angle to between 0°-40° can often be useful to see the origins (0°-20° for right CA, 30°-40° for left CA). The superior portions of the left and right atria and the anterior portion (aortic rim) of the IAS, as well as the RVOT and PV in the far field can be seen. Color flow and spectral Doppler can aid in evaluation of these areas. Of note, the orthogonal view obtained during simultaneous biplane imaging is the ME AoV LAX view (View #6 above).

13. ME RV In-Out (Video 13)

The **ME RV Inflow-Outflow View** can be obtained from the ME AoV SAX view or ME 5-Ch view by rotating to 50°-70° and applying some antelexion until the TV, RV, RVOT, PV, and proximal main PA are displayed simultaneously. This view is the equivalent of an inverted transthoracic parasternal SAX view, so the LA, RA, and IAS can also be seen. RV size and function, TV and PV morphology and function, distinguishing membranous from outlet IVS (and visualizing VSDs in these areas), and RVOT stenosis can be evaluated, especially in conotruncal abnormalities (see below). Color flow and spectral Doppler should be utilized to evaluate flow across the TV and PV, and identify any possible VSDs.

14. ME Mod Bicaval TV (Video 14)

From the ME RV In-Out View, the **ME Modified Bicaval TV View** can be obtained by maintaining a transducer angle of 50°-70° and turning the probe clockwise until the TV is centered in the view. The LA, RA, IAS, IVC, SVC, and sometimes the right atrial appendage (RAA) can be seen. Detailed evaluation of the TV by both 2D and Doppler imaging should be performed.

## 15. ME Bicaval (Video 15)

The **ME Bicaval View** is obtained by rotating the transducer angle forward to 90°-110° from the neutral ME position and turning the probe clockwise until both SVC and IVC are visualized along with the LA, RA, RAA (far field), and IAS (which is positioned perpendicular to the insonation beam). Atrial septal defects (ASD) and aneurysms can be seen with 2D, color, and spectral Doppler imaging of the atrial septum. Color flow Doppler is also useful to visualize IVC and SVC inflow. The orthogonal view (seen by simultaneous biplane imaging) is the ME 4-Ch view and further turning the probe clockwise can visualize the right pulmonary veins (orthogonal to View # 9, ME Rt Pulm Veins).

## 16. TG IVC/Hep Veins (Video 16)

The **TG IVC/Hepatic Veins View** is obtained by straightening and advancing the TEE probe from the ME views into the stomach and adjusting the transducer angle to 80°-110°. The probe is then turned clockwise and anteflexed slightly to maintain contact with the stomach wall. The IVC is seen in LAX and, with a small amount of probe withdrawal and left/right probe rotation, the hepatic veins can be visualized entering the IVC. With slow probe withdrawal to the ME position, the IVC/RA junction is visualized. Color flow Doppler can be used to evaluate flow patterns in the veins; spectral Doppler can be performed to evaluate hepatic venous flow for assessment of right-sided diastolic function, as well as any higher-velocity flow such as anomalous pulmonary venous drainage. The orthogonal view, using a transducer angle of 0°-20° and slight right/left probe rotation, demonstrates the IVC in SAX as it courses through the liver, receives hepatic veins, and returns to the RA.

## 17. TG Basal SAX (Video 17)

The **TG Basal SAX View** is obtained by adjusting the transducer angle to 0°-20° from the TG IVC/Hep Veins view to allow the left and right ventricles to be seen in SAX with the typical "fish mouth" appearance of the MV. The anterior leaflet is on the left of the display and the posterior leaflet is on the right. MV morphology and function can be assessed by 2D imaging and color flow Doppler as well as a global assessment of right and left ventricular function and wall motion, and presence of mid muscular VSDs. Advancing and turning the probe clockwise, while applying slight anteflexion, can display the TV in a SAX view to allow similar interrogation as the MV.

## 18. TG Mid Pap SAX (Video 18)

From the TG Basal SAX position, the anteflexed TEE probe can be advanced further into the stomach with the same transducer angle (0°-20°) to obtain the **TG Mid Papillary SAX View**. The LV papillary musculature, the muscular IVS, and the RV papillary musculature (by turning the probe clockwise) can be evaluated. This view is principally utilized to evaluate LV size and function (global and segmental).

## 19. TG Apical SAX (Video 19)

From the TG Mid Pap SAX View (View #18), the TEE probe continues to be advanced while maintaining contact with the gastric wall to obtain the **TG Apical SAX View**. Evaluation of the apical segments of both ventricles and also visualization of apical muscular VSDs is possible by rotating clockwise.

## 20. TG LAX (Video 20)

The **TG LAX View** is obtained by rotating the transducer angle to 120°-140° from the neutral position. This view allows visualization of the subvalvular MV apparatus (including the chordae tendineae), MV, LVOT, AoV, LV inferolateral and anteroseptal walls, and proximal aortic root. Color flow Doppler should be used to evaluate flow across the MV and LVOT/AoV.

## 21. DTG 5-Ch (Video 21)

The DTG views require advancement of the TEE probe further into the stomach, often with significant anteflexion to direct the ultrasound plane posteriorly. The **DTG Five-Chamber View** is obtained using a transducer angle of 0°-20° to visualize the MV, RV, LV, IVS, LVOT, AoV, and aortic root. The inlet, membranous, and trabecular portions of the IVS can be evaluated by color flow Doppler to search for possible VSDs. The MV and LVOT should be interrogated with color and spectral Doppler. When DTG views are not available, the TG LAX view (View #20) serves as a suitable alternative for spectral Doppler evaluation of the LVOT and AoV.

## 22. DTG RVOT (Video 22)

From the DTG 5-Ch View, the probe is withdrawn slightly and the transducer angle rotated forward to 50°-90° to obtain the **DTG RV Outflow Tract View**. Some probe rotation clockwise might also be needed to display the RVOT and PV. The MV inflow and AoV outflow can be visualized, as well as the trabecular and outflow portions of the IVS for any shunting suggestive of a VSD. Color and spectral Doppler can be used to evaluate the RVOT, MV, and LVOT with forward rotation to 80°-90° and the TEE probe rotated slightly counterclockwise. This view is very useful for evaluation of conotruncal malformations (see below).

## 23. DTG Atr Sept (Video 23)

From the DTG RVOT View, the transducer angle is rotated forward to 80°-90° and the TEE probe rotated clockwise until the SVC, RA, RAA, LA, and IAS are seen, producing the **DTG Atrial Septal View**. This view simulates a transthoracic subcostal bicaval image, providing excellent visualization of the atrial septal morphology and length. Color Doppler is useful for evaluation of interatrial shunting, and SVC flow can be visualized and evaluated by color and spectral Doppler. To visualize the IVC entrance to the RA, the probe is advanced slightly and the transducer angle rotated forward to 100°-120°. If the transducer angle is instead rotated back to 0°-10°, the IAS can be seen in an orthogonal plane, as can the RA, entrance of the right and left pulmonary veins into the LA, and both ventricles and atrioventricular valves.

## 24. UE Ao Arch LAX (Video 24)

Withdrawal of the probe to the UE position (transducer angle 0°-10°) can be used to obtain the **UE Aortic Arch LAX View**. Color and spectral Doppler will demonstrate pulsatile antegrade flow in the Ao and with further slight withdrawal, the innominate vein can be seen crossing anterior to the Ao arch. Because the left mainstem bronchus typically crosses between the esophagus and the Ao, a portion of proximal Ao arch and distal ascending Ao might not be visualized. If no innominate vein is seen, the probe should be rotated counterclockwise to determine whether a left SVC is present in SAX.

## 25. UE Ao Arch SAX (Video 25)

From the UE Ao Arch LAX view, the transducer angle is rotated forward to 70°-90° to obtain the **UE Aortic Arch SAX View**. The Ao arch is seen in SAX, and the main PA and PV can frequently be seen in LAX in the far field. The innominate vein is also seen in cross section just superior and anterior to the Ao arch. Color and spectral Doppler of the PV and main PA is very effective here, and a patent ductus arteriosus can also be seen in this view, entering the PA. With the main PA centered in the image, counterclockwise and clockwise rotation of the probe provides visualization of the left and right



pulmonary arteries, respectively. The head and neck arteries (right brachiocephalic, left common carotid, left subclavian) can sometimes be seen arising from the Ao arch.

26. UE PA (Video 26)

From the UE Ao Arch LAX View (View #24), the probe is advanced slowly (transducer angle 0°-10°) and rotated slightly clockwise to obtain the **UE Pulmonary Artery View** that demonstrates the junction between main PA and right and left pulmonary arteries. From this position, clockwise probe rotation displays the right PA behind the ascending Ao and right SVC (both seen in SAX). Counterclockwise rotation along with slight probe advancement can visualize the proximal to mid left PA. Color and spectral Doppler should be used to determine the presence of stenosis across both branch PAs. A patent ductus arteriosus can be seen by color flow Doppler with counterclockwise probe rotation and advancing/withdrawing the probe. Spectral Doppler can also be performed to assess the gradient between Ao and main PA through the patent ductus arteriosus.

27 and 28. Desc Ao SAX (Video 27) and Desc Ao LAX (Video 28)

From the UE Ao Arch LAX view (transducer angle 0°-10°), the probe is rotated counterclockwise and slowly advanced to follow the Ao arch as it becomes the **Descending Aorta SAX View**. Rotating the transducer angle to 90°-100° produces the **Descending Aorta LAX View**. While keeping the Ao in the center of the image, the probe can be advanced slowly with either view in order to evaluate the entirety of the descending thoracic Ao. The lack of internal anatomic landmarks can make it difficult to describe the precise location of the probe and any detected pathology, so one solution is to rotate the probe clockwise to identify the cardiac anatomy at that level, thereby providing a point of reference. Color and spectral Doppler can be used to evaluate the pulsatility of aortic flow. Intercostal arteries can sometimes be seen arising posteriorly from the descending Ao, with pulsatile flow directed away.

### Transesophageal 3D Examination Protocol

Since the publication of the last pediatric and congenital TEE guidelines document in this journal,<sup>31</sup> there have been major advancements in 3D echocardiography, including a) high quality real-time imaging, b) adult-size 3D TEE transducers, c) efficient cropping tools, and d) quantitative 3D software programs.<sup>16,109-115</sup> In pediatric and congenital cardiology, the most useful applications of 3D TEE are during catheter-based therapies and CHD surgeries. In the recent 3D echocardiography in CHD guidelines document,<sup>116</sup> specific recommendations for the particular anomalies and procedures in which 3D TEE is recommended (and also some in which 3D TEE has been used effectively) are presented in Table 6.

Three-dimensional echocardiography generally requires increased technical training and expertise as compared to conventional 2D imaging regarding specific optimization and acquisition protocols for various displays that best highlight CHD. These most commonly include options of “live” narrow angle, wide angle or zoom imaging, full volume, and live multiplane.<sup>16,110-113</sup> These methods must be mastered in order to effectively perform 3D TEE in the time-constrained settings of the cardiac catheterization laboratory and operating room. 3D TEE imaging protocols should be routinely utilized in conjunction with other echocardiographic modalities as part of the regular workflow of either a detailed segmental study or a more focused TEE examination. It is important that image orientation for viewing the 3D dataset be practical and foster clear communica-

**Table 6** Reported clinical use of 3D TEE in congenital heart disease

3D TEE has been recommended for:
ASD device closure guidance
VSD device closure guidance
Visualization of catheters, delivery systems, and devices
Measurement of defects visualized in <i>en face</i> views
Analysis of the anatomy and function of atrioventricular valves
Visualization of the aortic valve and left ventricular outflow tract
3D TEE has been used effectively during:
Fontan fenestration closure
Ruptured sinus of Valsalva aneurysm device closure
Coronary artery fistula device closure
Prosthetic valve paravalvular leak device closure
Atrial switch baffle leak device closure and baffle obstruction stenting
Atrial septum trans-septal puncture during various procedures
Biventricular pacemaker synchrony assessment and lead placement guidance

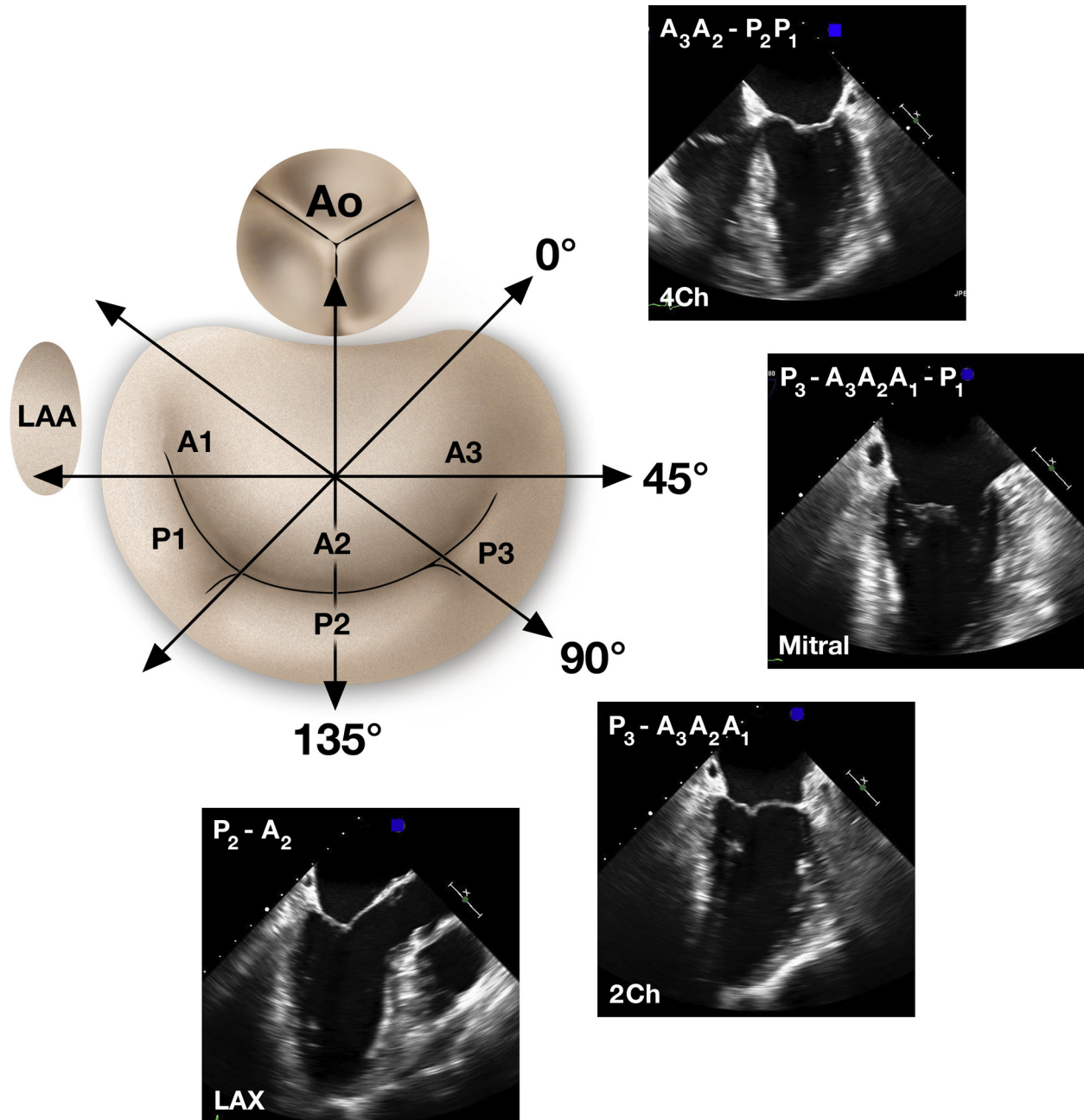
tion among cardiovascular care providers.<sup>29,113</sup> Where applicable, recommendations regarding the use of 3D TEE to analyze specific anomalies, procedures, and quantitative parameters have been added to the respective sections of this document.

### Key Points

1. We recommend a series of 28 tomographic views be used to perform a comprehensive TEE examination in children and all patients with CHD.
2. The views are obtained from four primary positions within the esophagus/stomach: midesophageal (ME), transgastric (TG), deep transgastric (DTG), and upper esophageal (UE). All views are presented with the standard “apex up” orientation except for the DTG views, which are inverted to an “apex down” position to present an “anatomically correct” display.
3. The views serve as a starting point for CHD evaluation, and can be altered as needed. The exam should be structure-based, not view-based, and include a minimum of 2D imaging, color flow and spectral Doppler, obtained from multiple views.
4. 3D TEE imaging can be performed in conjunction with 2D TEE in patients > 30 kg, and involves the use of specific 3D techniques including adjustable sector, full volume, and live multiplane methods. Table 6 lists a number of clinical uses for 3D TEE in CHD.

### SPECIFIC STRUCTURAL IMAGING

The following section describes the anatomy and imaging of specific structures and congenital anomalies. Clear and precise visualization is essential for detecting and quantifying structural and functional abnormalities prior to and during any intervention and will be discussed in detail. The focus will be on differentiating features from normal valve anatomy and acquired pathology, which was extensively



**Figure 3** Schematic of the MV with leaflet scallops (or segments) labeled. Corresponding images from different standard imaging views are labeled with the respective scallops and segments. Although this labeling scheme is applicable in the majority of cases, the exact regions of the MV leaflets image vary on the basis of the relation of the heart to the esophagus as well as transesophageal echocardiographic probe position within the esophagus. Ao, Aorta; LAA, LA appendage; LAX, long-axis; Mitral, mitral commissural; 2Ch, two-chamber; 4Ch, four-chamber. Adapted from Hahn et al.<sup>16</sup>

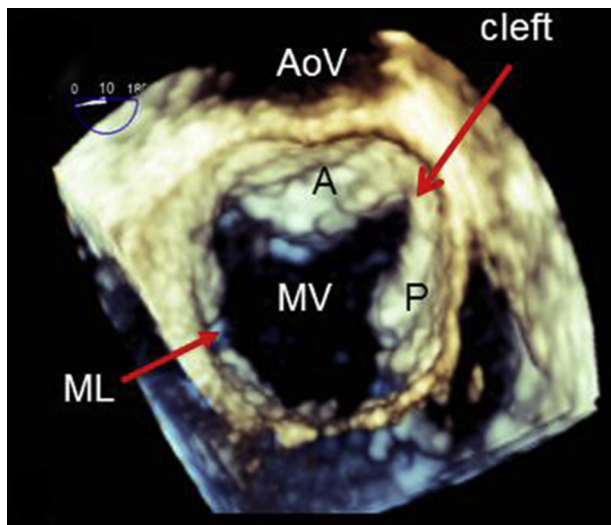
covered in the 2013 ASE/SCA Comprehensive TEE Guidelines, and an array of congenital cardiac abnormalities.<sup>30</sup>

### Mitral Valve

**Anatomy.** The basic components of the MV apparatus include the anterior and posterior valve leaflets, annulus, chordae tendineae, and papillary muscles. Several views are employed for examining the MV and have been shown to correlate well with surgical evaluation.<sup>117</sup> The ME views (4-Ch, 5-Ch, Mitral, 2-Ch, LAX, and AoV LAX) axially

transect the MV leaflets from 0 – 140°, and are helpful for delineating all scallops of both leaflets (Figure 3).<sup>16</sup> The TG and DTG views provide further characterization of valve and commissural anatomy and are especially valuable for demonstrating congenital abnormalities.

TEE imaging is useful for distinguishing primary etiologies of mitral valve dysfunction from secondary etiologies such as mitral regurgitation related to annular dilation. Primary causes of mitral valve dysfunction are associated with intrinsic valve pathology and may include 1) *congenital* abnormalities such as clefts (Figure 4), double orifice mitral valve, mitral arcade, or abnormal papillary musculature

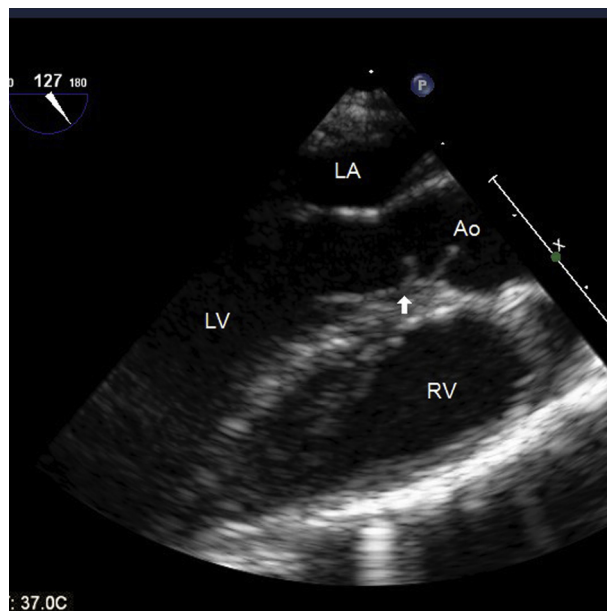


**Figure 4** TEE 3D midesophageal wide angle left atrial *en face* view of a left atrioventricular (mitral) valve cleft associated with an ostium primum atrial septal defect. A, Anterior/superior component of the anterior leaflet in a cleft left atrioventricular valve; AoV, aortic valve; ML, mural leaflet; MV, mitral valve; P, posterior/inferior component of the anterior leaflet in a cleft left atrioventricular valve.

(i.e. parachute mitral valve); 2) *myxomatous* changes resulting in prolapse, elongation of the chordae, or flail; 3) *infectious* damage from endocarditis; or 4) *inflammatory* effects related to rheumatologic or collagen vascular diseases.<sup>118,119</sup>

**Role of TEE in Mitral Valve Repair.** TEE imaging is reliable for assessing adequacy of mitral valve repair, and for determining the need for return to bypass.<sup>11,120</sup> Early identification of findings requiring modification of the repair may prevent need for a reoperation at a later date, and may decrease morbidity, mortality, and overall hospital costs over the long term.<sup>15</sup> The decision should take into account several factors, including hemodynamic status, as well as severity of the residual lesion.

Although there are no established echocardiographic measures to quantify severity of residual mitral dysfunction in the pediatric population, criteria do exist for grading residual mitral stenosis and regurgitation by Doppler.<sup>121</sup> With regard to mitral stenosis, the following measures have been used: *insignificant* = pulsed/CW Doppler mean gradient  $\leq 5$  mm Hg *potentially significant* = pulsed/CW Doppler mean gradient of 5-8 mm Hg; and *significant* = pulsed/CW Doppler mean gradient of  $> 8$  mm Hg. A mean mitral valve inflow gradient of more than 5 mm Hg has been suggested as a cut-off point for consideration of further repair or valve replacement.<sup>122</sup> In the presence of residual regurgitation, the mitral valve should be carefully examined for leaflet prolapse, abnormal leaflet excursion, or persistent annular dilatation. Dynamic systolic anterior leaflet motion can displace the coaptation point of the leaflets toward the left ventricular outflow tract resulting in a posteriorly directed jet of mitral regurgitation, which may be exacerbated by a hypovolemic, hypercontractile left ventricle upon separation from cardiopulmonary bypass.<sup>123</sup> Objective parameters such as width of the vena contracta should be taken into consideration and used to grade mitral regurgitation as follows: *insignificant* = absent or trivial regurgitation jet width ( $< 2$  mm) by color at the level of the valve leaflets; *potentially significant* = regurgitant jet width 2-4 mm by color Doppler at the level of the valve leaflets; and



**Figure 5** Midesophageal LAX view around  $125^\circ$  shows a sub-aortic fibromuscular ridge associated with subvalvar aortic stenosis. Ao, Aorta; LA, left atrium; LV, left ventricle; RV, right ventricle.

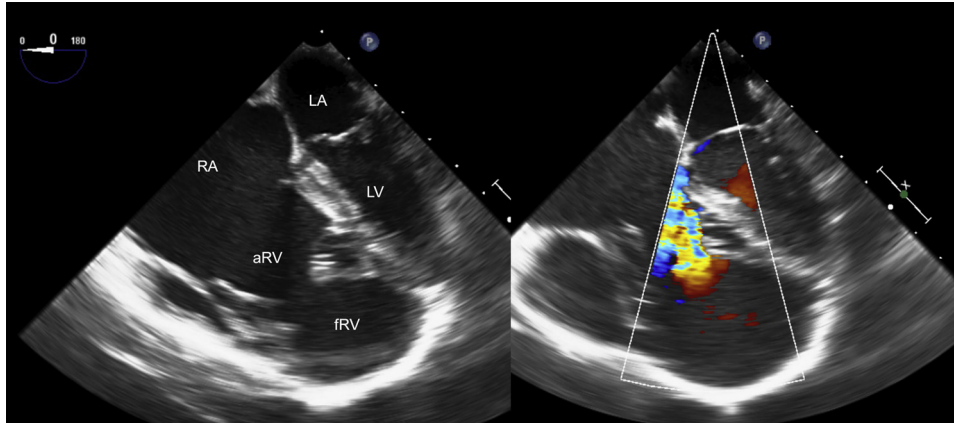
*significant* = regurgitant jet width  $> 4$  mm by color Doppler at the level of the valve leaflets.<sup>121</sup> Additionally, the ratio of the maximum regurgitant jet area by color Doppler to the left atrial area on 2D imaging can be used for quantifying MR, with mild defined by a ratio of  $\leq 30\%$ . Return to bypass for further correction or valve replacement should be considered for more than mild MR, as the risk for reoperation is increased. This is typically a joint decision made by the surgeon and the echocardiographer and may require a more comprehensive evaluation of the valve to make the right decision.<sup>124</sup>

**Use of 3D TEE in Mitral Valve Assessment.** The best 3D TEE view of the MV is obtained using the wide-angle live 3D modality from the ME position viewed from the LA aspect. Examples of this approach are presented in [Figure 4](#), [Videos 29 and 30](#). Live 3D with color flow Doppler mapping may be useful if the temporal resolution (volume rate) is adequate. Biplane 2D imaging and color flow Doppler mapping methods are useful and can be time saving because two views are obtained simultaneously.

## Aortic Valve and Aorta

**Anatomy of Aortic Valve.** The AoV complex includes the left ventricular outflow tract, aortic valve, and aortic root. The AoV complex should be carefully evaluated for potential subaortic, aortic, and supra-valvular obstruction in the ME LAX ([Figure 5](#)), ME AoV LAX ([Video 31](#)), and DTG 5-Ch views. Familiarity with all of these structures is important, as obstruction or dilatation at any level may ultimately affect AoV function. Measurement of the AoV annular diameter is performed at the hinge points of the valve leaflets, while the sinuses of Valsalva and sinotubular junction are measured from inner edge-to-inner edge at end-systole or at the maximal diameter in pediatrics.<sup>116</sup> However, in adult patients, the ASE guidelines recommend leading edge-to-leading edge at end-diastole or at the maximal diameter.<sup>125</sup>

**Role of TEE in Aortic Valve Repair and Left Ventricular Outflow Surgery.** A thorough understanding of the underlying mechanism of AoV dysfunction, including leaflet and root



**Figure 6** Midesophageal 4-Ch view of Ebstein's anomaly including apical displacement of the septal leaflet of the tricuspid valve, redundancy of the anterior leaflet, and atrialization of the right ventricle. On the right hand side, color Doppler shows regurgitation of the tricuspid valve starting in the body of the right ventricle due to the apical displacement. RA, Right atrium; aRV, atrialized right ventricle; fRV, functional right ventricle; LA, left atrium; LV, left ventricle.

morphology, is needed prior to any transcatheter or surgical intervention on the valve. In pediatric patients undergoing AoV repair, TEE imaging is used to identify markers for recurrent regurgitation necessitating early reoperation.<sup>126</sup> While shorter coaptation length and decreased coaptation height have been designated as predictors of need for early reoperation in adults, coaptation asymmetry, measured as an increased percentage difference in short-axis coaptation lengths, has been shown to be a strong predictor of early reoperation for residual aortic regurgitation in pediatric patients following valve repair.<sup>127</sup>

Quantification of valve stenosis and regurgitation should be performed according to previously published echocardiographic guidelines.<sup>118</sup> For AoV/LVOT stenosis, the TG LAX and DTG 5-Ch views provide excellent angles of insonation for both PW and CW Doppler evaluation of preoperative and postoperative gradients. A peak gradient  $>40$  mm Hg in the LVOT may be hemodynamically significant and require reintervention. However, in the setting of decreased ventricular function and low cardiac output immediately post-bypass, TEE may not accurately reflect the degree of residual obstruction in all cases.<sup>121</sup>

For aortic regurgitation, a regurgitant jet width  $>4$  mm by color Doppler at the level of the valve leaflets may represent a risk for hemodynamically significant aortic regurgitation postoperatively.<sup>127</sup> Additional reported risk factors for early reoperation include concomitant valve-sparing aortic root and/or ascending aortic replacement, and leaflet prolapse.<sup>128,129</sup>

**Use of 3D TEE in Aortic Valve Assessment.** Live narrow-angle 3D TEE in the ME AoV SAX view provides excellent views of the AoV. Examples of a normal and abnormal AoV are shown in [Video 32](#). Biplane 2D imaging and color flow Doppler mapping methods are useful if the frame rate is adequate and can be time saving because two views are obtained simultaneously. Imaging to guide device closure of a ruptured sinus of Valsalva aneurysm can also be helpful (3D [Video 33](#)).

**Anatomy of Thoracic Aorta.** Visualization of the mid ascending Ao, Ao arch, and descending Ao is best achieved from the ME, UE, and aortic views. Doppler interrogation of flow in the descending Ao may confirm severe aortic regurgitation if other views are limited.<sup>16,130,131</sup> In patients undergoing arch repair (i.e., coarctation or interrupted aortic arch), color and spectral Doppler interrogation

of flow in the descending Ao can be helpful in identifying residual arch obstruction. Imaging in the setting of aortic dissection is addressed in detail in other guidelines.<sup>132,133</sup>

### Tricuspid Valve

**Anatomy.** The tricuspid valve is anatomically and functionally complex, comprising three leaflets attached to a fibrous annulus, chordal apparatus, and papillary muscles. The ME 4-Ch view demonstrates the anterior and septal leaflets, as well as abnormalities such as tethering, flail segments, involvement of the septal leaflet in tricuspid septal aneurysmal tissue in a membranous VSD, apical displacement and tethering of the septal leaflet in Ebstein anomaly ([Figure 6](#) and [Video 34](#)), and endocarditis related to these leaflets. Color Doppler in this view demonstrates the flow pattern across the TV, and is often well aligned with a central regurgitant jet, which is typically physiologic. Clockwise rotation and if possible rightward flexing of the probe from the Modified Bicaval TV view may best assess the posterior leaflet and its coaptation with the adjacent leaflets.

TV abnormalities may be anatomical, such as Ebstein anomaly, TV dysplasia, stenosis, pacemaker lead-induced non-coaptation, flail leaflet, straddling or over-riding valves in complex CHD; or functional, secondary to right-sided (pulmonary hypertension, RV dysfunction and dilatation), or left-sided (elevated LA filling pressures from various causes and abnormal septal contour) dysfunction.

**Role of TEE in TV Repair/Replacement.** It is not unusual for an intra-operative evaluation to underestimate the extent of tricuspid regurgitation (TR) in an intubated, anesthetized child with low preload due to overnight feeding restrictions. The ME 4-Ch, ME RV In-Out, and ME Mod Bicaval TV views show a larger TR jet compared to other views.<sup>134</sup> Incorporating multiple views at multiple time points in the post-bypass period (with variable systemic and pulmonary arterial pressure, improving contractility post-cardioplegia, and return of AV synchrony) can assist in surgical decision-making, such as the need to return to bypass to address residual lesions if TR is significant or indicates an elevated RV systolic pressure.<sup>120</sup>

Physiologic TR is common, always less than mild, and can be useful in predicting RV systolic pressures. These jets, which are typically small or intermittent, when combined with substantial through-plane motion, may be elusive in the rapidly changing post-bypass period. It may be helpful to annotate simultaneous central venous

pressure as well as systemic arterial pressure along with Doppler measurements of peak instantaneous pressure gradients. A Nyquist limit of 50 to 60 cm/s may be set to compare pre- and post-bypass images at the same technical settings, as TR may be underestimated at higher scale settings.<sup>135</sup> Accurate Doppler assessment of TR is important for a variety of reasons: high TR velocities after VSD repair raise concern for a sizeable residual defect, may indicate residual outflow obstruction after an RVOT repair, or need for initiation of inhaled nitric oxide in a patient with late presentation of an unrestricted left to right shunt; TR velocities discrepant from the systemic arterial pressures may alert toward residual arch obstruction when the RV is the systemic ventricle; and low TR velocities may indicate high filling pressures with decreased cardiac function.

Transvenous pacemaker leads can be imaged as they traverse the TV, sometimes causing regurgitation due to leaflet retraction, fibrosis of leaflet edges, leaflet tethering, or perforation. In this situation, analysis of the TV anatomy as well as lead position will aid in planning for valve repair. Lead- or central line-related endocarditis require detailed assessment of right sided structures.

**Use of 3D TEE in TV Assessment.** The best 3D TEE view of the TV is usually obtained using the wide-angle live 3D modality from the ME 4-Ch position viewed from the RA aspect and may better clarify dysfunction of specific leaflets. Live 3D with color flow Doppler mapping may be useful if the volume rate is adequate. Biplane 2D imaging and color Doppler flow mapping methods are useful and time-efficient. Normal TV, Ebstein anomaly, and Sapien valve replacement in the catheterization lab are presented in [Videos 35-37](#).

## Pulmonary Valve

**Anatomy.** The PV is the anterior, leftward, and cephalad of the two semilunar valves in the structurally normal heart. Its anterior location in the chest can make it difficult to assess by TTE and ironically, its distance from the TEE probe as well as proximity to the left upper lung lobe can also make it difficult to visualize in detail. The ME RV In-Out and DTG RVOT views profile the PV. Pulmonary stenosis may occur at the sub-valvular, valvular, or supra-valvular regions. Supravalvular narrowing can be seen in the MPA at the level of the systolic excursion of dysplastic leaflets or as a circumferential fibrotic waist in patients with supravalvular pulmonary stenosis (e.g., Williams syndrome). Stenosis within valved or non-valved conduits can be similarly assessed, though fibrosis and calcification of native valves or conduits can challenge image resolution. In these situations, color and spectral Doppler can be utilized to estimate location and severity of obstruction. Increased systolic flow velocity across the PV may be secondary to increased transpulmonary flow, but is usually less than 2 m/s in this situation. An increase in peak pulmonic velocity may be seen in large left-to-right shunts, and focused imaging of the PV to rule out dysplasia will prevent surgical intervention. Functional pulmonary regurgitation is common and is seen as a small, central jet from the PV. More significant jets are likely to be wider; a jet width in excess of 50-65% of the right ventricular outflow tract indicates severe regurgitation,<sup>136</sup> as does a more holodiastolic pattern of leakage.<sup>137</sup> Rapid flow deceleration, early termination of diastolic flow, and diastolic flow reversal in the branch PAs almost always indicates significant pulmonary regurgitation.

**Role of TEE in PV Repair/Replacement.** Determining the presence and severity of residual obstruction in subvalvular, valvular, or supravalvular regions may guide decisions regarding method of treatment (e.g., approach via TV, PV or right ventriculotomy/infundibulotomy in rare situations). Dynamic or fixed pulmonary stenosis at

different levels is an important cause for elevated RV systolic pressures and should be investigated. A quick and accurate assessment of residual RVOT obstruction can be obtained from the DTG RVOT view where the entire RVOT, PV, and supravalvular regions can be aligned and 'stepped-through' to determine the exact location and extent of obstruction. Similarly, patients undergoing replacement (either surgical or catheter based) in the setting of a dilated RV outflow tract may have a paravalvular leak, which should be carefully looked for because it may be easily addressed in most cases.

**Use of 3D TEE in Pulmonary Valve Assessment.** Due to the distance of the PV from the esophagus, 3D TEE imaging of the PV is often limited. Narrow-sector live 3D or full-volume 3D acquisitions with cropping may provide sufficient views in some cases.

## Key Points

1. Primary causes of MV dysfunction include congenital abnormalities, myxomatous changes, infectious damage from endocarditis, or inflammatory disorders. The ME views (4-Ch, 5-Ch, Mitral, 2-Ch, LAX, and AoV LAX) from 0 - 140° are most helpful to delineate MV anatomy and physiology but TG and DTG are especially valuable for congenital abnormalities. Color flow and spectral Doppler aid in return to bypass decisions following MV repair.
2. Assessment of the entire AoV complex includes the LVOT, AoV, aortic root and supravalvular region. Both ME SAX and LAX views provide complete evaluation of AoV and LV outflow tract morphology and function. TG LAX and DTG 5-Ch views are very useful for assessment of PW/CW Doppler gradients.
3. The ascending and descending thoracic aorta are best visualized systematically using a combination of ME and UE views, at different levels of the esophagus, with appropriate transducer rotation to visualize the various portions of the thoracic aorta.
4. Tricuspid valve abnormalities may be anatomical, such as Ebstein anomaly, TV dysplasia, stenosis, pacemaker lead-induced non-coaptation, flail leaflet, straddling or over-riding in some complex CHD; or functional, secondary to right or left-sided ventricular dysfunction. ME views provide assessment of TV morphology and function.
5. The pulmonary valve complex includes the sub-valvular, valvular and supra-valvular regions. ME, DTG, and UE Ao Arch SAX/PA views allow visualization of the PV complex. Color flow and spectral Doppler can be used to assess the degree of stenosis or regurgitation across this area. Due to the distance of the PV from the esophagus, 3D TEE is often limited.
6. 3D TEE provides further evaluation of valve size, pathology, mechanism and severity of valve dysfunction.

## Assessment of Ventricular Size and Function

The assessment of ventricular size and function is an important part of TEE in children and adults with CHD in the following settings: before and after congenital heart surgery, during percutaneous CHD interventions or electrophysiology studies, during some complex non-cardiac surgeries, and in the setting of a non-diagnostic TTE.<sup>138,139</sup> Additionally, the immediate postoperative setting in the intensive care unit is a challenging time for TTE, with open sternotomies and poor acoustic windows, and is another area where TEE can be beneficial in children, especially in

patients with transposition of the great arteries after arterial switch, immediately after heart transplantation, or following implantation of a ventricular assist device.<sup>140</sup>

**Left Ventricle.** Normal LV assessment is reviewed in the 2013 ASE/SCA Comprehensive TEE Guidelines.<sup>16</sup> Standard imaging planes for measurement of size have not been established in TEE but there is general agreement between TTE and TEE measurements in adults. Guidelines suggest using the TG Mid Pap SAX or the orthogonal TG LAX of the LV for measurement of ventricular size, as measurements in the ME views have reduced lateral resolution.<sup>16,141-143</sup> In children, the recommended approach is the Mid Pap SAX view, because the LAX view does not account for the lateral motion of the LV seen in many children and does not guarantee circular LV short-axis geometry throughout the cardiac cycle. Simultaneous multiplane imaging should be used to ensure that LV diameter measurements are made perpendicular to the chamber. The modified biplane Simpson's or area-length methods have been suggested to calculate LV volume in children.<sup>116</sup> The ME 4-Ch and 2-Ch views allow tracing of the LV endocardial borders and using the formula for calculating LV volume. Linear measurements may be made from M-mode tracings or 2-D images in TG views as there are normative pediatric data from TTE imaging.<sup>116,144</sup>

**LV Systolic Function.** Assessment of ventricular function requires reviewing multiple imaging planes in TEE. Qualitative assessment is generally reported as either normal or with variable degrees of dysfunction such as mild, moderate, or severe. Quantitative parameters for LV systolic function include linear shortening fraction (SF), fractional area change, and 2D volumetric ejection fraction.<sup>116</sup> SF can be assessed in TG SAX projections at the level of the MV leaflet tips in young patients or at the level of the papillary muscles in older patients and adults.<sup>116</sup> Ejection fraction (EF) can be obtained from ME 4- and 2-Ch views using the modified biplane Simpson's method. It is important to optimize ME views so that the LV is not foreshortened and endocardial borders are clear. Using fractional area change is fraught with error and difficult to reproduce so it should only be used as a qualitative measure.<sup>145</sup> Multiple orthogonal views should be employed to assess regional wall motion abnormalities. TG Basal SAX, Mid Pap SAX, and Apical SAX views best facilitate assessment of all 17 segments for radial function. Orthogonal views at TG LAX as well as ME 4-Ch, 2-Ch, and 5-Ch allow for confirmation and evaluation of longitudinal function.

**LV Diastolic Function.** LV diastolic filling assessment is generally performed with TTE. Similar measurements can be made in TEE views, including the ME 4-Ch, to assess MV inflow velocities, pulmonary vein velocities, and tissue Doppler velocities, but attention must be paid to differences in mitral inflow parameters and PW Doppler tissue velocities by age group.<sup>146,147</sup> In addition, these Doppler parameters are affected by loading conditions and heart rate, which may make assessment of diastolic function in the operating room with TEE challenging in individuals with CHD. A simplified algorithm for grading diastolic dysfunction using only E-wave velocity and lateral mitral annular early diastolic tissue velocity ( $e'$ ) was shown to predict adverse outcome in adults after coronary artery bypass graft surgery but there is no data in patients immediately after congenital heart surgery.<sup>148</sup> A transmitral E to  $e'$  ratio <10 is considered normal.<sup>146</sup>

**Right Ventricle.** The normal RV is crescent-shaped and composed of three portions: inflow, muscular, and outflow. The inlet portion contains the TV, whose septal leaflet is apically positioned relative to the MV hinge point. Coarse muscular trabeculations and a moderator band are exemplary of the body of the RV while the outlet

portion is composed of the infundibulum. The normal RV also has unique chordal insertions from the tricuspid valve onto the septum as opposed to the discrete papillary muscles in the normal LV.

Assessment of RV size and function is an integral part of TEE evaluation in patients with CHD. While acoustic windows in TTE are often challenging, TEE provides excellent visualization of the complex geometric shape of the RV. The ME 4-Ch, ME RV In-Out, TG Mid Pap SAX, TG Basal SAX, and DTG RVOT offer evaluation of RV inflow, basal, and outflow views. Quantification of RV function includes fractional area change (FAC), tricuspid annular plane systolic excursion (TAPSE), and Doppler measurements (MPI, RV dP/dt, and annular tissue Doppler velocity). While various quantitative methods exist for measuring RV function, in most cases function is assessed qualitatively including contraction of the free wall, longitudinal motion of base towards apex, and bulging of the ventricular septum into the RV cavity.<sup>149</sup> This is especially true in the case of congenitally corrected transposition of the great arteries (l-TGA) or complete transposition of the great arteries (d-TGA) after atrial switch, where the shape of the normal RV is altered significantly in the systemic position, so visual estimation of systolic function from the ME 4-Ch or TG SAX views are best used.

**Use of 3D TEE in Assessing Ventricular Volumes and Function.** Contrary to 2D echocardiographic methods, 3D echocardiography does not rely on geometrical assumptions to calculate LV volumes, and has been applied in patients with CHD and abnormally-shaped ventricles.<sup>150,151</sup> Measurement of LV and RV volume requires a full acquisition from the ME 4-Ch view and application of one of the semi-automated quantitative volumetric programs available on cart and on off-line workstations.

## Key Points

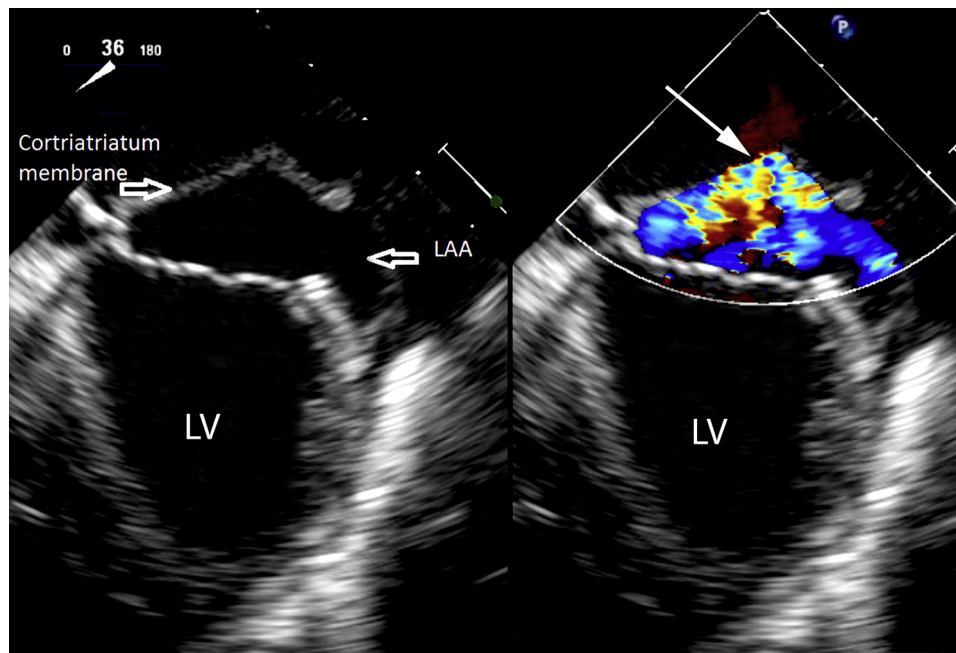
1. Measurement of LV size is recommended in the TG SAX views in children because the TG LAX view does not account for the lateral motion of the LV seen in many children.
2. LV systolic function is generally assessed qualitatively but can be quantified with linear shortening fraction and 2D/3D volumetric ejection fraction.
3. Assessment of RV size and function is generally assessed qualitatively but 3D volumetric programs do allow for quantitative assessment.

## Atria, Systemic and Pulmonary Veins

**Anatomy.** Determining the atrial situs (solitus, inversus, ambiguous) is essential in children and adults with CHD and can be obtained by visualization of the atrial appendages. The right atrial appendage is triangular and broad-based while the LAA is narrow-based and tubular (finger-like). The atrial septum and its components complement the identification of atrial situs and have been discussed in detail in the 2013 ASE/SCA Comprehensive TEE Guideline.<sup>16</sup>

Venous structures, particularly the suprahepatic portion of the IVC, the Eustachian valve, and the ostium of the CS, are markers of a morphologic RA and can be visualized in the ME 4-Ch view. The SVC can be seen as it enters the RA with the ME Bicaval view and the DTG Atr Sept view, where a sweep from right to left at 90° helps identify the presence of a left SVC (LSVC).

Determining drainage of the pulmonary veins into the LA can be accomplished with the ME right and left pulmonary veins views. Evaluation of the pulmonary veins by color flow and spectral



**Figure 7** Midesophageal 4-Ch view with transducer angle rotated forward to 36°, focused on the left atrium and cor triatriatum membrane. Note the location of the membrane lies above the left atrial appendage (LAA). The membrane divides the left atrium into proximal and distal portions. On the right hand side, color Doppler shows turbulent flow through the membrane (arrow) indicative of obstruction. LV, Left ventricle.

Doppler is required for evaluation of venous obstruction. The Doppler pattern of the pulmonary veins is triphasic with a forward S and D wave and a short reverse-flow A wave. In young children and infants the S wave of forward flow is dominant.<sup>152</sup> Mean gradients across pulmonary veins should be measured over 1 or 2 cardiac cycles, and stenosis should be recognized as loss of the phasic flow pattern. One must be aware that gradients can be deceiving, as flow can be redistributed to other lung segments drained by patent veins. The assessment of pulmonary venous Doppler patterns can help assess other conditions such as LA hypertension caused by mitral regurgitation (presence of a prominent A wave), and the signal can also help distinguish junctional versus sinus rhythm by associating the A wave with the ECG tracing (in sinus rhythm the A wave precedes the QRS while in a junctional rhythm it is dissociated).

**Role of TEE in Abnormalities of the Atria. Cor Triatriatum.**—Cor triatriatum involves the presence of a fibromuscular band that divides the atria into proximal and distal parts.<sup>153,154</sup> An important distinction from a supra-valvular mitral ring is the location of the LAA, which is always distal to the membrane in cor triatriatum sinister (Figure 7 and Video 38). The TEE assessment of this lesion begins in the ME 4-Ch view, with the probe slightly retroflexed to prevent compression of a possible hypertensive pulmonary venous chamber. The probe is then turned counterclockwise to identify the membrane and its insertion below the left pulmonary veins but above the LAA. Adding color Doppler interrogation helps identify the connection(s) of the proximal and distal chamber in both the ME 4- and 2-Ch views. Not infrequently, the communicating orifices are eccentric and need to be visualized by color Doppler at varying angles of interrogation to find the best alignment for Doppler assessment of the degree of stenosis and estimation of pulmonary venous pressure. A delineation of the pulmonary venous return needs to be complete, as partial forms of cor triatriatum may exist with only the right or left veins entering the proximal chamber. In addition, one must interrogate the atrial septum

to identify an ASD or a patent foramen ovale from the ME 4-Ch, ME Bicaval view and DTG Atr Sept views. Finally, there should be an evaluation of the mitral valve to exclude obstructive lesions or mitral regurgitation. After surgical resection of the membrane, TEE helps identify adequacy of the repair (residual membrane, residual atrial level shunting) and drainage of the pulmonary veins.<sup>155</sup>

**Juxtaposed Atrial Appendages.**—Juxtaposition of the atrial appendages is a rare anomaly (approximately 0.8% of CHD), frequently seen in association with other complex CHD. It is more common to have “left juxtaposition” in which both appendages are oriented side by side on the left, especially when associated with transposition of the great arteries, tricuspid atresia, and heterotaxy syndrome.<sup>156-158</sup> Recognizing juxtaposition of the atrial appendages is challenging, and confirmation requires identification of the anatomical features of the atrial appendages (previously described) with a series of sweeps from posterior to anterior in several planes. Imaging the atrial appendage crossing behind the great arteries is a first clue; however, suspicion for this anomaly arises with a lateral deviation of the mid-portion of the atrial septum and a frontal orientation of the antero-superior portion forming the floor and posterior wall of the junction of the right atrial appendage with the venous component of the atrial cavity.<sup>159</sup> The ME 4-Ch and ascending Ao SAX views can demonstrate the RAA behind the aorta and anterior to the LA. The use of color and pulsed-wave Doppler can help distinguish flow into the atrial appendage from an ASD. Although the diagnosis of juxtaposed atrial appendages may be an incidental finding, its recognition is important during interventions to guide catheter position or balloon catheter tips across the atrial septum and not into the RAA. In addition, thrombus has been noted in the juxtaposed RAA and LAA in patients with atrial fibrillation prior to cardioversion.<sup>160,161</sup>

**Role of TEE in Systemic Venous Anomalies. Left Superior Vena Cava to Coronary Sinus.**—Drainage of the LSVC into the CS

is a relatively frequent finding in the normal heart, and can be found in 3-10% of patients with CHD.<sup>162</sup> Recognition of an LSVC is important in the operating room for cannulation, and in the planning of complex repairs such as atrial baffles and the superior cavopulmonary connections (Glenn or Hemi-Fontan) discussed below, but its presence should be known prior to cardiac surgery.

Imaging the LSVC can be accomplished by identifying a dilated CS in the ME 4-Ch view with retroflexion and slight advancement of the probe, and also in the ME 2-Ch view. Once the dilated CS is identified, an LSVC can be imaged with a counterclockwise probe rotation in the ME to UE level and a transducer angle between 60-80°. The LSVC is located on the left of the descending Ao and anterior to the left PA, where it usually connects to the CS. Intravenous injection of agitated saline into the left arm can help identify this vein, as the saline fills the CS.

Failure to recognize the LSVC-to-CS connection can lead to misinterpretation of the dilated CS ostium for an ASD. Other conditions that can be associated with a dilated CS and not an LSVC should be considered, including anomalous pulmonary venous return, anomalous drainage of hepatic veins, or stenosis of the ostium of the CS.

**Left Superior Vena Cava to Left Atrium.**—The LSVC can drain directly into the dome of the LA in up to 8% of cases, rarely in isolation, and mostly associated with other congenital heart defects.<sup>163,164</sup> Identification of the LSVC by TEE can be challenging in this case, as a normal size CS does not raise suspicion. Direct visualization of the LSVC entering the roof of the LA while interrogating the pulmonary veins, or actively searching for this connection when identifying a small right-sided SVC, is what helps identify this anomalous drainage. The use of agitated-saline injection through the left arm can help identify connection of the LSVC with the LA.

**Interrupted Inferior Vena Cava.**—Interruption of the IVC is rare and is characterized by absence of the IVC below the hepatic veins.<sup>165</sup> The IVC connects to the azygous vein, which drains into the SVC. Because of the drainage into the SVC, this finding has important implications during surgery at the time of cannulation. Imaging by TEE starts at the TG IVC/Hep Veins view and will show the hepatic veins but not the IVC, even with forward rotation of the transducer angle to 90°. Following the azygous vein into the right or left SVC can be challenging and multiple sweeps by 2D and color Doppler imaging are required, as the azygous vein travels from a retrocardiac position anteriorly into the SVC, with the esophagus in its path. The use of agitated-saline injection from the leg can help identify this connection by entrance of saline bubbles into the SVC.

**Right Superior Vena Cava to Left Atrium.**—The right SVC drainage into the LA is rare and sometimes biatrial drainage is also possible.<sup>166,167</sup> Using the DTG Atr Sept view or the ME Bicaval view with color Doppler demonstrates flow into the LA. The use of agitated-saline injection from the right arm can help identify this drainage by entrance of bubbles into the LA.

**Role of TEE in Pulmonary Venous Anomalies.** *Partial Anomalous Pulmonary Venous Return (PAPVR).*—PAPVR is most commonly associated with an ASD, either sinus venosus (up to 85% and described below) or secundum type (10-15%), but can occur in isolation.<sup>168</sup> The most common type of PAPVR is the connection of right pulmonary veins to the SVC and RA.<sup>169</sup> The evaluation of anomalous right pulmonary veins into the SVC can start with the probe in the ME Rt Pulm Veins view. While withdrawing the probe in this plane, the SVC is circular, and a distortion of this vessel to a “tear drop” appearance suggests the anomalous entrance of the pulmonary vein. Once identified in

this view, forward rotation of the transducer angle to a ME Bicaval view (90-100°) will show the pulmonary veins entering the SVC, and allows an estimate of distance from the SVC/RA junction, which is helpful for surgical planning. Advancing the probe inferiorly in these same views can identify drainage of the veins into the RA or IVC. This maneuver can be applied to identify Scimitar syndrome, where some or all of the right-sided veins drain to the IVC. Partial anomalous connections of the left-sided veins is typically to a left vertical vein draining superiorly into the left innominate vein. This can be visualized with 2D and color Doppler imaging, using the UE Ao arch SAX view with leftward rotation.

**Total Anomalous Pulmonary Venous Return (TAPVR).**—The anomalous drainage of all pulmonary veins to the systemic circulation occurs in 2.2% of all children with CHD.<sup>170</sup> They can be classified in order of prevalence: supracardiac, infracardiac, cardiac, or mixed.

The use of TEE in TAPVR can be limited because the location of the pulmonary venous confluence is subject to compression by the probe, which may cause hemodynamic compromise.<sup>85</sup> Insertion of the probe after sternotomy has been reported to be a safer alternative.<sup>86</sup>

When a TEE probe can be placed without causing hemodynamic compromise, it is most helpful to visualize the anomalous venous return of the supracardiac variant by starting in the ME 4-Ch view toward the left and identifying the confluence. Each individual pulmonary vein can be seen draining into the confluence by rotating the probe clockwise from left to right. The right veins are imaged by rotating the transducer angle forward to 30-50°, and the left veins will be seen best at 90-110° or closer to the descending Ao.

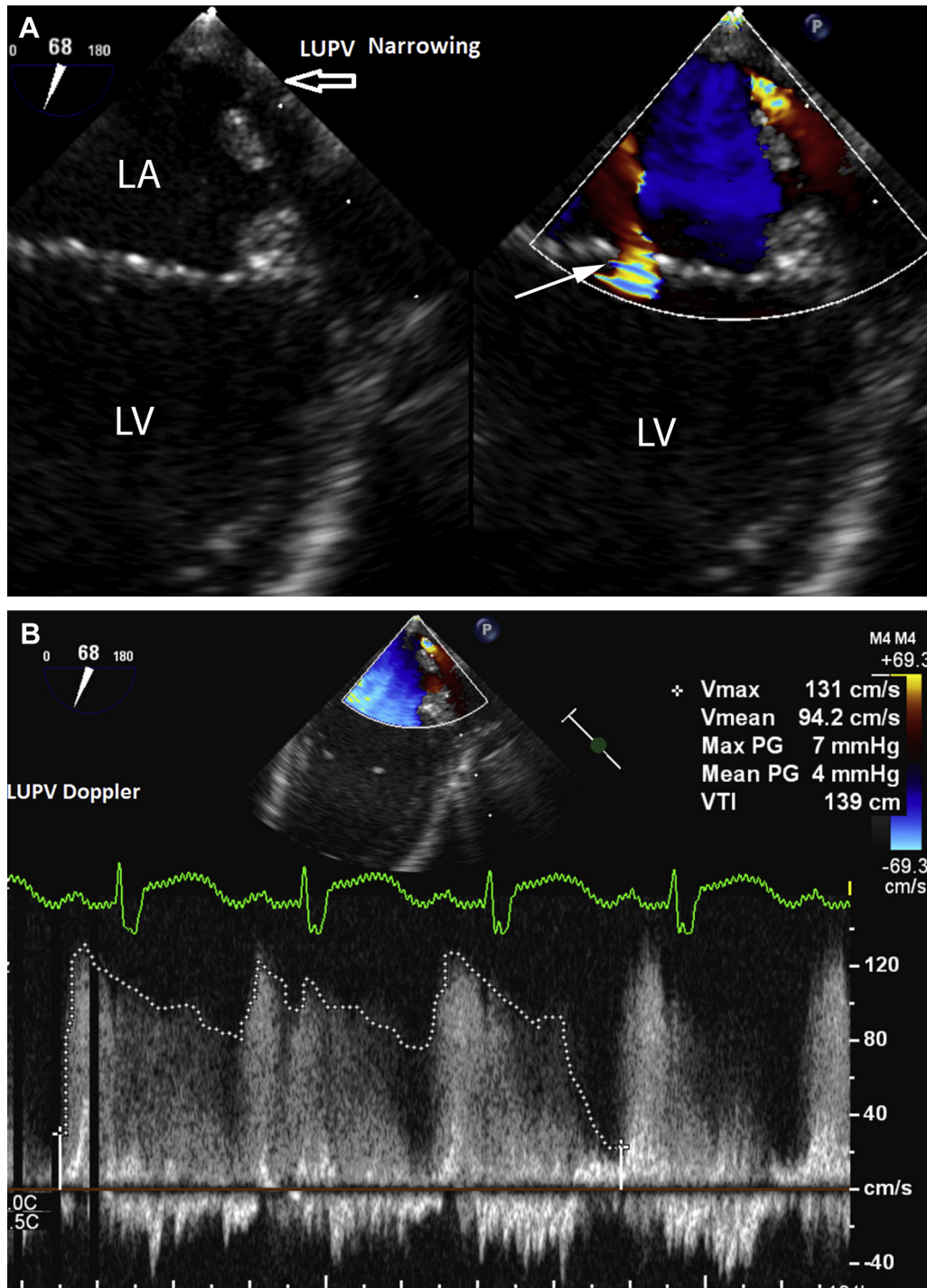
The infradiaphragmatic variants are difficult to assess by TEE, however, there is often high-velocity return into the portal system with dilated hepatic veins. The evaluation of TAPVR to the CS requires long sweeps, advancement and withdrawal of the probe, and/or change in imaging planes to follow the venous confluence to the CS. Prominent color flow seen returning into the CS and RA can be helpful. The evaluation of mixed veins employs all of the techniques noted above.

Evaluation of the pulmonary venous confluence anastomosis to the LA and any individual pulmonary vein stenosis is essential in a patient after repair of TAPVR (Figure 8 and Video 39). The presence of turbulent flow at the anastomotic site may suggest intrinsic stenosis or torsion of the confluence, and while spectral Doppler interrogation will determine the degree of obstruction, return to bypass may be indicated and should be discussed with the surgeon.

## Key Points

1. Determination of atrial situs can be performed by identification of the atrial appendages and key systemic venous structures. While the ME views are most commonly used, *all* TEE positions and views should be employed.
2. TEE can identify unusual systemic venous anomalies such as left SVC to coronary sinus or left atrium, interrupted hepatic portion of the IVC, and atrial anomalies such as juxtaposed atrial appendages and cor triatriatum.
3. TEE provides excellent visualization of normal left and right pulmonary venous return and enables accurate pulmonary venous Doppler assessment, which can be utilized in the evaluation of stenosis within individual veins or the pulmonary venous confluence.
4. TEE can also be used to evaluate partial and total anomalous pulmonary venous return. However with the latter, care must be taken because hemodynamic compromise has been described with TEE probe insertion/manipulation.





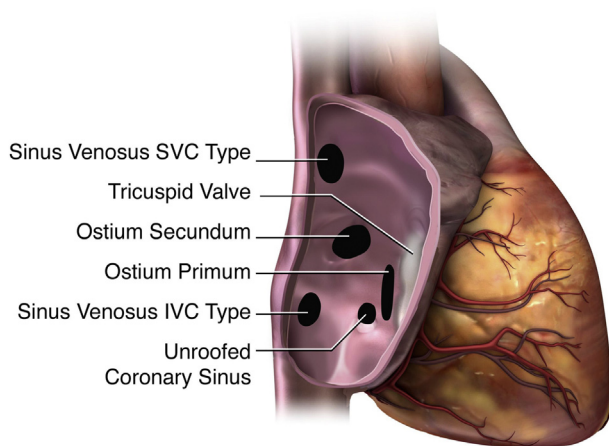
**Figure 8** Modified midesophageal LAA view shows: **(A)** Narrowed orifice of the left upper pulmonary vein with corresponding color Doppler mapping indicating flow turbulence. Mild mitral regurgitation is also seen (arrow). **(B)** Some loss of phasic flow in the left upper pulmonary vein with a mean gradient of 4 mm Hg consistent with mild stenosis. LA, Left atrium; LV, left ventricle; LUPV, left upper pulmonary vein.

### Septal Defects

Atrial and ventricular septal defects are common types of CHD that can occur as isolated defects or in combination with other cardiac anomalies.<sup>167,171-179</sup> Atrial septal defects undergo both surgical and catheter-based closure, often with TEE guidance, so an understanding

of the septal anatomy, as well as type and location of the defects is important and outlined in detail in a previous ASE guideline<sup>22</sup> (Figure 9).

*Ostium secundum* ASDs are often amenable to catheter device closure provided the surrounding rims are adequate and the defect



**Figure 9** Subtypes of atrial septal communications when viewed from the right atrium (RA). Patent foramen ovale (PFO) is not illustrated. SVC, Superior vena cava; IVC, inferior vena cava. Reprinted with permission from Silvestry et al.<sup>22</sup>

is not too large. Secundum ASDs are seen well from the ME 4-Ch, ME AoV SAX, ME RV In-Out, ME Bicaval and DTG Atr Sept views.

The echocardiographer must define a number of features and parameters, including the ASD dimensions and number, size, and location of orifices. If closure is being performed in the catheterization lab, one must measure the length of the aortic, superior, inferior, posterior, and crux rims. An important factor in choosing ASD closure device size is the stop-flow occlusive balloon waist diameter. TEE is also used to perform live monitoring of device deployment, configuration, and stability. Once the device is fully deployed and released one must assess for residual shunting as well as for blood flow obstruction and device impingement on surrounding anatomic structures including the aortic root, roof of the LA, AV valves, right pulmonary veins, caval veins, and the CS. Lastly, assessment for complications such as pericardial effusion, thrombus, and device embolization is necessary.

*Ostium primum* ASDs are located at the apical margin of the atrial septum immediately adjacent to the AV valves. This type of ASD is within the spectrum of AVSD and is almost always associated with a cleft mitral valve. Ostium primum ASD is best seen from the ME 4-Ch view. After primum ASD repair, the mitral valve should be assessed for residual cleft, stenosis, and regurgitation in the ME 4-Ch, Mitral, 2-Ch, and LAX views. Further interrogation of the mitral valve cleft should include the TG Basal SAX view. LVOT obstruction should also be assessed in the DTG 5-Ch view where spectral Doppler can rule out residual obstruction.

*Sinus venosus* ASD may be one of two types: superior or inferior. The superior form involves the uppermost portion of the atrial septum and extends superiorly. It is associated with the SVC overriding the defect and almost always has anomalous connections of some or all of the right pulmonary veins to the SVC near the cavoatrial junction. The inferior type sinus venosus ASD is associated with the IVC overriding the defect and is less commonly associated with anomalous pulmonary venous connection. Sinus venosus ASDs are best seen from the ME Bicaval and DTG Atr Sept views. After a sinus venosus repair, it is important to assess for pulmonary venous stenosis or baffle obstruction. This is best imaged with ME Rt Pulm Veins and Bicaval views and including the UE for a superior sinus venosus defect, or using the ME RV In-Out and ME Bicaval

views and extending to the lower esophagus for an inferior sinus venosus defect.

*Coronary sinus* ASD is a rare anomaly in which partial or complete unroofing of the CS into the LA typically results in shunting from the LA to the CS and into the RA.<sup>180</sup> It is almost always associated with an LSVC connecting to the CS (see above).

**Role of TEE in ASD Repair.** Preoperative TEE during surgical repair of an ASD can confirm the size and location of the ASD, evaluate for additional associated cardiac lesions, including partial anomalous pulmonary venous return, assess ventricular size and function, and estimate PA pressures. Postoperative TEE focuses on residual atrial level shunting, assessment of the vena cavae, presence of residual AV valve regurgitation, and ventricular function.

**Use of 3D TEE in ASD Imaging.** Imaging of atrial septal defects using 3D TEE is very useful during interventional-catheter treatment and prior to surgery. For ASD imaging, the wide-angle ME RA and LA *en face* views are very effective, as is the DTG Atr Sept live 3D narrow-sector view. These renderings accurately and rapidly demonstrate the important features of an ASD. Biplane TEE with and without color Doppler flow mapping is time-efficient because it provides 2 simultaneous views. Secundum atrial septal defect *en face* views are demonstrated with device closure of a secundum ASD using 3D TEE guidance (Video 40).

**Ventricular Septal Anatomy.** The ventricular septum has inlet, trabecular, and outlet portions. The right side has a septal band to which the moderator band attaches. It extends from the apex toward the base and bifurcates into two limbs that form a “Y” or “U” shape. A VSD can occur in any of these locations (Figure 10). In addition, there may be multiple VSDs in the same patient, malalignment relative to the septal band of muscular septum, and association with other types of congenital cardiac anomalies.

**Ventricular Septal Defects.** We will focus on 5 types: perimembranous, muscular, inlet, malaligned, and outlet.

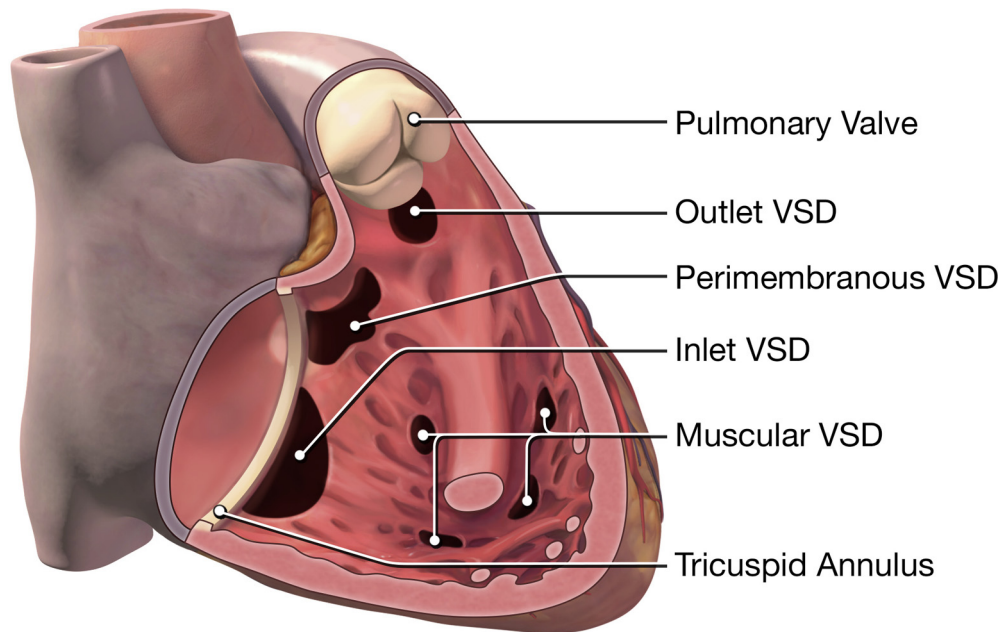
**Perimembranous.**—Defects in this region are common and may be isolated or associated with any other type of CHD. Perimembranous VSDs are best seen in the ME 4-Ch, 5-Ch, AoV SAX, and RV In-Out views.

**Muscular.**—Multiple defects and associated other cardiac anomalies are fairly common. These defects may be amenable to catheter device closure if clinically necessary. Muscular VSDs are usually best seen in the ME 4-Ch, ME 5-Ch, and TG Basal SAX views.

**Inlet.**—Associated with coplanar AV valves and atrioventricular septal defect (AVSD) lesions, inlet VSDs are best seen in the ME 4-Ch view.

**Malaligned.**—This type of VSD is present in tetralogy of Fallot (TOF), double-outlet right ventricle (DORV,) and interrupted aortic arch complex. Malaligned VSDs are best seen in the ME 4-Ch, 5-Ch, LAX, AoV SAX, and RV In-Out, as well as the DTG 5-Ch and RVOT views.

**Outlet.**—This type of VSD is also called a supracristal VSD and can be seen alone or in lesions such as truncus arteriosus, for example. It can be associated with aortic cusp prolapse. Outlet VSDs can be displayed with the ME 4-Ch, 5-Ch, AoV SAX, LAX, and RV In-Out, DTG 5-Ch and RVOT views.



**Figure 10** Subtypes of ventricular septal defects (VSDs) when viewed from the right ventricle (RV). Malalignment ventricular septal defect is not illustrated but is caused by anterior or posterior deviation of the infundibular or conal septum and is typically present in tetralogy of Fallot, double outlet right ventricle, or interrupted aortic arch complex.

**Role of TEE in VSD Repair.** Preoperatively, the focus is on confirmation of the anatomic findings including type, number, size, shunt direction, and assessment of adjacent structures. Postoperative assessment addresses residual septal defects or patch integrity, PA pressures, ventricular function, and device configuration in interventional cases. Assessment for a residual VSD should always occur in more than one view and the decision to return to bypass should take into account several factors, including associated aortic regurgitation, outflow tract obstruction, and hemodynamic significance. Most residual VSDs  $\leq 2$  mm will spontaneously resolve with time.<sup>181</sup> Residual VSDs  $\leq 3$  mm are typically not hemodynamically significant and some will spontaneously resolve. Residual VSDs measuring 3 to 4 mm require careful analysis including measurement of Qp:Qs by echocardiographic or blood oxygen saturation analysis to better determine need of return to bypass. A Qp:Qs of  $> 1.5:1$  or a residual VSD  $\geq 4$  mm should have an additional attempt(s) at closure in most cases.<sup>182,183</sup>

**Use of 3D TEE in VSD Imaging.** Imaging of VSDs is effective from the ME 4-Ch view using live 3D, biplane echo, and full-volume 3D with cropping. The *en face* views from RV and LV aspects, along with the ME 4-Ch view best demonstrate the anatomic features. Live 3D color flow Doppler mapping is used to assess residual shunts. Biplane TEE has color flow Doppler mapping frame rates that are significantly higher than for live 3D color flow Doppler, thereby overcoming the limited temporal resolution of the latter modality in some cases. Perimembranous VSD *en face* views are demonstrated in [Video 41](#). The use of live 3D TEE guidance of VSD device closure can be useful and is illustrated in [Figure 11](#) (closure of muscular VSD).

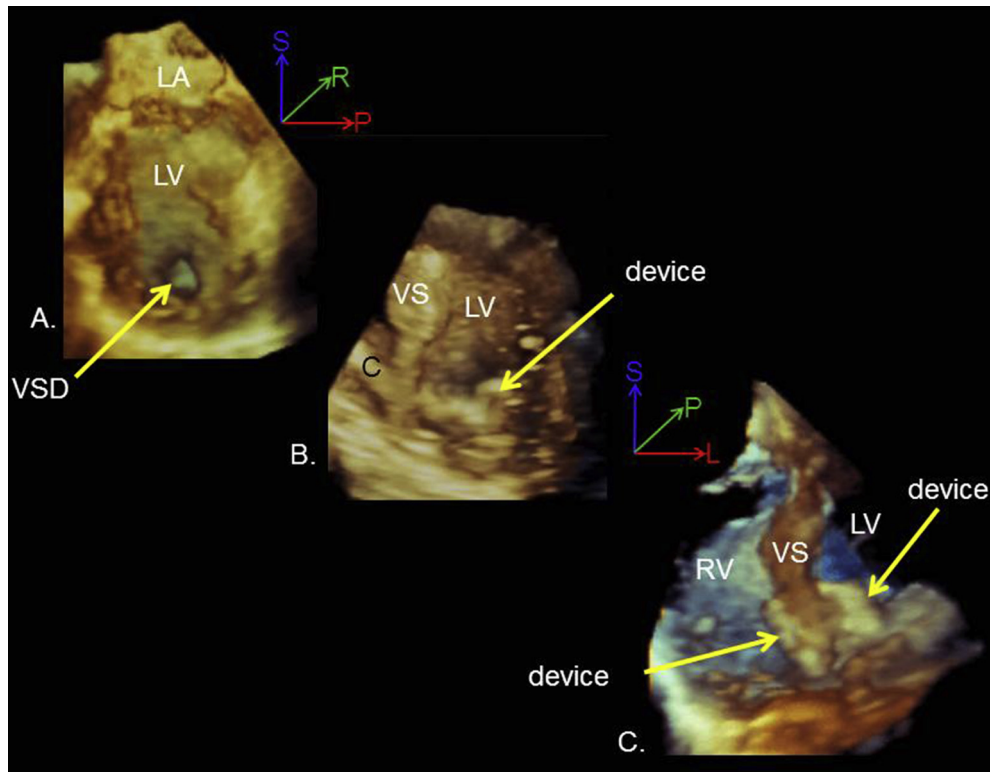
### Atrioventricular Septal Defects

**Anatomy.** Atrioventricular septal defect, also called AV canal defect, results from incomplete development of the endocardial cushions,

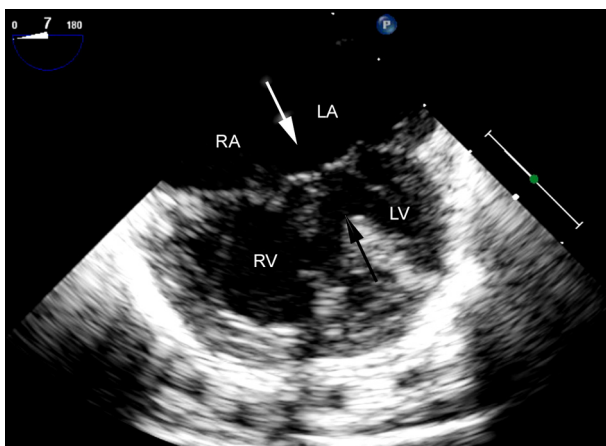
leading to defects in atrial and ventricular septa as well as the AV valves.<sup>184</sup> There can be morphologic variability at many levels, therefore this lesion comprises an anatomic spectrum that can range from partial to complete forms. The variability spectrum includes the following: a) size or extent of deficiency in the primum atrial septum; b) size or extent of deficiency in the ventricular septum, here called the “ventricular component;” c) degree of commonality or anatomical separation of the left- and right-sided AV valves; d) AV valve morphology and function; and e) degree of commitment of the AV valves to the ventricles.

The primum ASD, which is present in almost all AVSDs, is best outlined when the atrial septum is perpendicular to the transducer and can be accomplished from the ME 4-Ch view with slight clockwise rotation. Additional defects in the secundum septum can be identified here as well. The ventricular component is best viewed from the ME 4-Ch view in systole, during which time assessment of the valve relationship to the septum can be obtained ([Figure 12](#) and [Video 42](#)). In addition, commitment of the AV orifice to the underlying ventricles can also be defined. Given that the common AV valve junction is shared between both ventricles, the aorta is unwedged and positioned more anterosuperiorly instead of between the normal mitral and tricuspid valves.

Complete AVSD can occur in isolation or associated with other more complex congenital heart lesions such as disorders of laterality (heterotaxy/isomerism). Partial AVSD, where there is a defect in the primum atrial septum but no discernible ventricular component, will have a lack of AV valve offset and a cleft in the anterior leaflet of the left AV valve, which can be visualized in the TG Basal SAX view. The ME LAX and DTG 5-Ch views are used to demonstrate the LVOT and confirm the separation between the left AV valve inlet and the aortic outlet. Accessory tissue from the superior bridging leaflet may cause LVOT obstruction. Backward rotation of the probe from the ME LAX view can show the inlet muscular septum and presence/extent of any



**Figure 11** Transesophageal three-dimensional (3D) echocardiography live narrow sector views during catheter device closure of a muscular ventricular septal defect (VSD). **(A)** The left sided *en face* view of the apical muscular VSD (arrow). **(B)** The frontal view of the device (arrow) with the left side deployed in the left ventricle (LV) and the device still attached to the catheter **(C)** delivery system. **(C)** The device in its final position with the discs of the device (arrows) on opposite sides of the ventricular septum. L, Left; LA, left atrium; P, posterior; R, right; RV, right ventricle; S, superior; VS, ventricular septum.



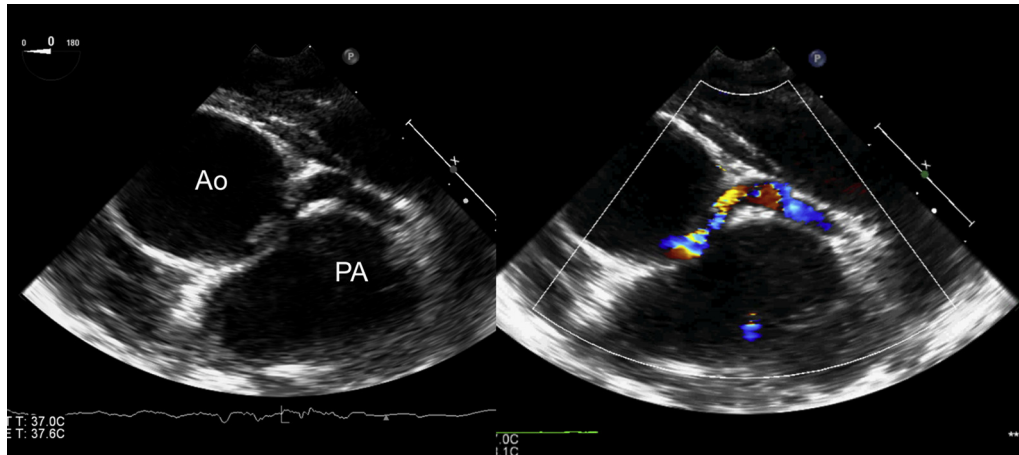
**Figure 12** Midesophageal 4-Ch view of a complete atrioventricular septal defect including primum atrial septal defect (white arrow), inlet ventricular septal defect (black arrow), and common atrioventricular valve. RA, Right atrium; LA, left atrium; RV, right ventricle; LV, left ventricle.

ventricular component to the septal defect. The AV valves can be seen using the TG Basal SAX view, and the site of AV valve regurgitation shown with color Doppler.

**Role of TEE in AVSD Repair.** Transthoracic echocardiography will demonstrate most of the relevant preoperative diagnostic data in AVSD with few exceptions.<sup>185</sup> TEE is indicated preoperatively in essentially all patients with AVSD, but particularly in the older infant/child in whom surgical decision-making might require delineation of the degree and mechanism of AV valve regurgitation, mechanism of outflow tract obstruction, and or suitability for biventricular correction. TEE can also add value in the clarification of pulmonary and systemic venous drainage, particularly in heterotaxy.

Intraoperative and immediate postoperative TEE can detect clinically significant residual findings, thereby prompting a return to cardiopulmonary bypass in both the native valve repair and in older children and adults being considered for reintervention to improve AV valve function or to close residual septal defects following prior AVSD repair.<sup>11,186,187</sup>

**Use of 3D TEE in AVSD Imaging.** A multi-beat full-volume 3D acquisition from a ME 4-Ch view can provide a complete view of the AV junction from both atrial and ventricular aspects, allowing clear appreciation of the anatomical relationships and fine details of both the bridging and mural leaflets. Novel *en face* views of the atrial and ventricular septa obtained by cropping away the ventricular free walls will show the curved crest of the IVS and size and shape of any septal defects (Video 43). 3D TEE with color flow Doppler provides further spatial information and the precise site(s) of AV valve regurgitation, which enhances surgical planning for the repair.



**Figure 13** Midesophageal AoV SAX view in a patient with anomalous origin of the left coronary artery from the right sinus of Valsalva. Note the slit like orifice as the left coronary artery arises from the right sinus. The color Doppler clip demonstrates the interarterial course between the aorta and pulmonary artery. *Ao*, Aorta; *PA*, pulmonary artery.

## Key Points

1. Atrial septal defect (ASD) subtypes include secundum, primum, sinus venosus, and coronary sinus defects (Figure 9).
2. Ventricular septal defect (VSD) subtypes include perimembranous, inlet, muscular, outlet, and malalignment (the last is associated with conotruncal defects) (Figure 10).
3. TEE plays an important role in monitoring of ASD and VSD closures in the catheterization laboratory.
4. TEE is important for postoperative assessment of VSD closure, especially for determination of significant residual VSDs, outflow tract obstruction, and aortic regurgitation, as well as whether return to bypass is indicated.
5. TEE is indicated preoperatively in essentially all patients with AVSD, but particularly in the older infant/child in whom surgical decision-making might require delineation of the degree and mechanism of AV valve regurgitation, mechanism of outflow tract obstruction, and or suitability for biventricular correction.
6. 3D TEE is useful for assessment of ASD and VSD morphology, and for monitoring of ASD/VSD closure in the catheterization laboratory. 3D TEE can also facilitate preoperative assessment of atrioventricular septal defects.

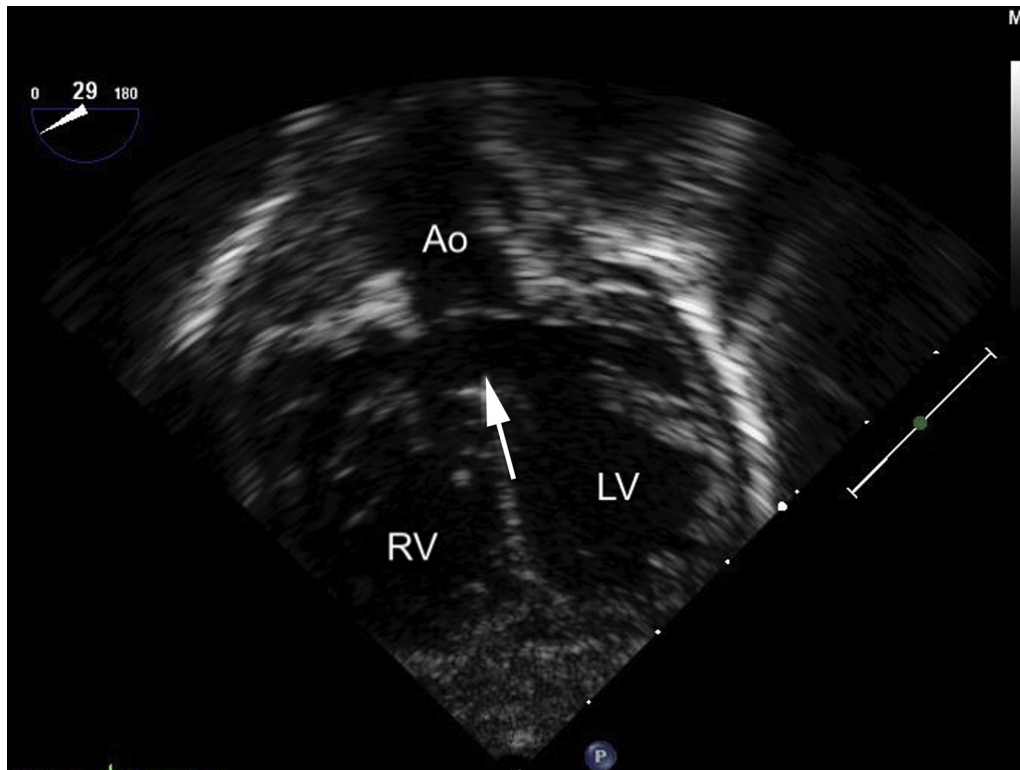
## Coronary Anomalies

**Anatomy.** Complete evaluation of the CAs for preoperative confirmation of suspected anomalies should include multiple planes to visualize the coronary connections to the great artery as well as the course and size of the arteries as they pass in the AV groove.<sup>188-190</sup> Color flow Doppler assessment should be performed to document connections since 2D imaging can at times be deceptive. The imaging of CA origins is performed primarily using the ME AoV SAX and RV In-Out views. These two views provide excellent imaging of all aortic cusps and can show the connections to the aorta. Anteflexion of the probe to move the imaging plane slightly superiorly may be necessary to properly demonstrate the origins, as they can arise above the aortic valve sinuses. Forward rotation of the transducer angle to between 0-20°, along with rotation of the probe toward the patient's right, dem-

onstrates the right CA course in the anterior AV groove. The left CA courses inferiorly in the anterior left AV groove. Starting from the ME AoV SAX view, the probe is advanced slightly to move the plane inferiorly, using a transducer angle of 30-40°. Rotation of the probe to the patient's left demonstrates the left AV groove and the bifurcation of the left main CA into the left anterior descending and circumflex CAs.

**Role of TEE in Anomalous Origin of the Coronary Artery.**  
**Anomalous Origin of the Coronary Artery from the Aortic Root.**—Anomalous origin of the CA from the opposite sinus of Valsalva is associated with an abnormal slit-like origin, an intramural course, and may include a course between the great arteries. TEE can be very helpful in the diagnosis of anomalous origin from the inappropriate sinus.<sup>189,191,192</sup> (Figure 13 and Video 44) The demonstration of anomalous origin from the aorta requires careful interrogation with both 2D imaging and color Doppler. Because the anomalous artery frequently has an intramural segment, 2D imaging can give the appearance of a normal origin from the appropriate sinus. In this setting, careful color flow Doppler interrogation of the aortic wall is important in demonstrating abnormal flow in the intramural segment.<sup>193</sup> Color Doppler shows an abnormal narrow region of flow that appears within the wall of the aorta. When the right CA arises from the left sinus, demonstration of the course requires forward rotation of the transducer angle from the ME AoV SAX view to 30-50°. In addition, the ME LAX view can show a circular cross-section of the right CA immediately anterior to the aorta. To image the left CA arising from the right sinus of Valsalva, the transducer angle is either kept the same or rotated backward to 0-25° and the transducer is rotated to the patient's left.

**Coronary Imaging in the Setting of Anomalous Origin of the Left or Right Coronary Artery from the Pulmonary Artery (ALCAPA and ARCAPA).**—As is the case in anomalous origin from the aorta, systematic and detailed evaluation of the coronary origins by 2D imaging, supplemented by documentation of flow using color Doppler, is critical to making an accurate diagnosis of anomalous CA from the PA.<sup>194,195</sup> Starting from the ME AoV SAX view, anteflexion of the probe brings the imaging plane superior to the PA and can directly show the anomalous connection. In some cases the artery arises laterally and may require rotation of the transducer to the patient's left to visualize the lateral wall. In addition, other important hallmarks of these defects



**Figure 14** Deep transgastric 5-Ch view of double outlet right ventricle (DORV) with subaortic ventricular septal defect (“tetralogy type” DORV). The aorta overrides the ventricular septal defect (*arrow*) to receive blood from the RV and LV. Ao, Aorta; RV, right ventricle; LV, left ventricle.

(particularly ALCAPA) should be evaluated, including segmental wall motion abnormalities, ventricular dysfunction, mitral regurgitation, and echogenic and fibrotic papillary muscles.

### Key Points

1. Imaging of the coronary artery origins is primarily done in the ME SAX views.
2. The demonstration of anomalous origin of a coronary artery from the opposite sinus of Valsalva requires careful interrogation with both 2D imaging and color Doppler.
3. In ALCAPA and ARCAPA, the anomalous origin of the coronary artery from the pulmonary artery can be visualized using the ME views.
4. Segmental wall motion abnormalities, ventricular dysfunction and mitral regurgitation should be assessed.

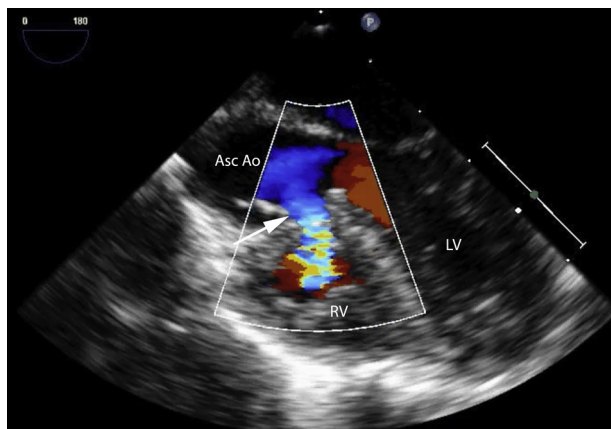
### Conotruncal Defects

**Anatomy.** Conotruncal defects are a group of CHDs characterized anatomically by abnormal ventriculo-arterial connections including TOF, DORV, truncus arteriosus, d-TGA, and l-TGA, which can occur in isolation or in association with heterotaxy and Hooped hearts. Delineating the anatomic features is important for accurate diagnosis, pre-operative planning, and post-operative evaluation; in particular the ventriculo-arterial alignment, the anatomy of the conus, and the VSD. The ventriculo-arterial alignment can be normal (TOF), or abnormal such as in TGA, DORV, and double-outlet left ventricle (rare, not discussed here). The great arteries can be positioned anteroposteriorly or

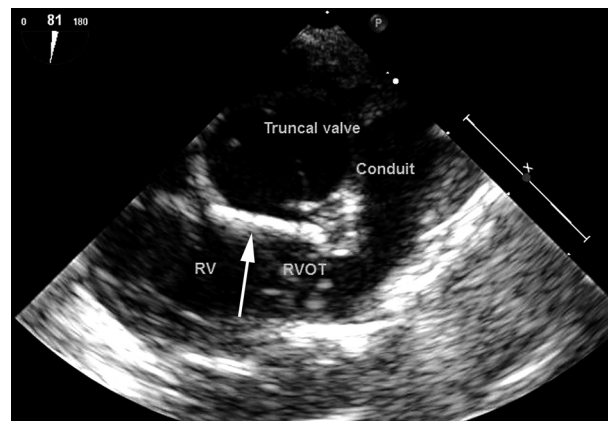
mediolaterally. The fibrous continuity between a great artery and an AV valve is important along with the anatomy of the conal septum, which should be described regarding 1) location: sub-pulmonary (normal), as in TOF, sub-aortic conus, as in TGA, and bilateral conus, as in types of DORV; 2) position: the conal septum can be anterior or posteriorly malaligned; and 3) size: the conus can be hypoplastic or absent. Associated VSDs can be subaortic (“tetralogy type” DORV, [Figure 14](#) and [Video 45](#)), subpulmonary (as in the Taussig-Bing type of DORV), remote (usually the canal or inlet type, but can be muscular), or doubly committed (absence or hypoplasia of the conal septum).

TEE allows evaluation of outflow tract patency/obstruction, residual VSDs, residual atrial level communications, AV or semilunar valve insufficiency, and ventricular function. An important consideration in conotruncal defects in general is the presence of a residual intramural VSD (communication located anterior to the VSD patch between the great artery and right ventricular trabeculations). These defects are distinct from the more common peri-patch defects and their identification is important, as they tend to increase in size over time and are associated with worse post-operative outcomes.<sup>196,197</sup> Each type of defect will be reviewed in detail with the focus being on post-operative factors.

**Tetralogy of Fallot.**—In the current era, most patients with tetralogy of Fallot are operated upon in infancy and therefore the pre-operative assessment is usually achieved with TTE. However, TEE can be complementary if there are remaining questions, such as the presence of additional VSDs, and is useful postoperatively to assess residual lesions.<sup>198,199</sup> Starting with the ME 4-Ch view, the probe is withdrawn to a ME 5-Ch view to profile the VSD patch, which is then interrogated with color Doppler for residual shunting and direction of flow ([Figure 15](#)). Further withdrawal of the probe with rightward rotation



**Figure 15** Midesophageal 5-Ch view with color Doppler in a patient with tetralogy of Fallot shows a large residual VSD (arrow) with left to right shunting into the right ventricle (RV). Asc Ao, Ascending aorta; LV, left ventricle.



**Figure 16** Modified midesophageal RV In-Out view around 90° in a patient after truncus arteriosus repair. The ventricular septal defect patch is seen (arrow) as well as the right ventricle (RV) to pulmonary artery conduit. RVOT, Right ventricular outflow tract.

will display the IAS at 0°–30° to assess for residual ASDs. The ME RV In-Out view can evaluate for residual RVOT obstruction and can also be used to obtain a TR peak velocity for estimation of RV systolic pressure. Residual RVOT obstruction can also be assessed in the DTG RVOT view, with the transducer angle at 50°–90°. It is important to remember that a hypercontractile state can exist following surgery so if the obstruction is dynamic, rather than fixed, it does not warrant surgical revision.<sup>200</sup>

**Double Outlet Right Ventricle.**—Preoperative TEE can help determine the location and size of the VSDs, relationship of the great vessels to each other and to the VSD, restriction at the level of the VSDs, anatomy of AV valves (e.g., straddling), and coronary anomalies to help in the determination of optimal surgical strategy. The ME 5-Ch view with probe ante flexion profiles the great vessels arising from the RV. The ME AoV LAX view allows for profiling the LVOT and potential pathway to the aorta. In a physiologic two-ventricle repair, a VSD patch is placed to baffle the LV outflow to the Ao and care must be taken to evaluate this area as significant obstruction from subaortic conus or the VSD patch is possible. In patients with DORV and TGA (Taussig-Bing anatomy), the VSD patch is placed to baffle the LV outflow to the PA and is followed by the arterial switch operation. The DTG 5-Ch and RVOT views provide visualization of the great arteries and their relationship to the VSD in all conotruncal defects.

**Truncus Arteriosus Communis (Referred to as Truncus Arteriosus).**—The pre-operative assessment of truncus arteriosus is mostly achieved with TTE, however, TEE can provide additional information with respect to the anatomy and function of the truncal valve, additional VSDs, and origin of the branch PAs in addition to a complete evaluation for residual lesions post-operatively. Withdrawing the probe from a near TG position through the ME position with the transducer angle at 0° profiles the VSD patch, which is then interrogated with color Doppler for residual shunting and direction of flow. The ME RV In-Out view is useful to demonstrate a peri-patch residual leak. In addition, the RV-to-PA conduit is best seen in this view with a counterclockwise turn of the probe toward the left side of the patient (Figure 16). Rotation of the probe to the ME ascending Ao LAX view and withdrawal to the UE Ao arch SAX view will demonstrate the most distal portion of the conduit as it is connected to the branch pulmonary arteries. Backward rotation to 0°–10°, using the UE PA view, provides good visualization of the right PA but the left PA can be difficult to visu-

alize in some patients and may require forward rotation to 90° with a turn to the left. The LV-to-truncal-valve pathway can be seen well in the ME AoV LAX or 5-Ch views, which, along with the ME AoV SAX view will allow assessment of truncal stenosis and regurgitation.<sup>201</sup> When available, the DTG views (5-Ch and RVOT) can provide visualization of the LVOT and proximal RV-to-PA conduit, as well as an excellent angle for spectral Doppler assessment. The ME Asc Ao SAX and UE PA views are the best to demonstrate the PAs.

**d-TGA with Arterial Switch.**—In d-TGA with an intact ventricular septum, preoperative TEE may not be needed if the coronary arteries are well defined by TTE, but this varies by institution.<sup>202</sup> Post-operative TEE should assure patent right and left ventricular outflow tracts after transection and “switching” of the great arteries, determine regional and global systolic ventricular function after transfer of the coronary arteries, and provide assessment of residual intracardiac shunts. The ME 4-Ch view provides a global assessment of ventricular performance. The TG Basal and Mid Pap SAX views allow determination of regional wall motion abnormalities consistent with coronary obstruction, which may result from transfer to the neo-aorta.<sup>203</sup> Attempts at coronary imaging is often helpful to determine if there is adequate flow or narrowing seen by 2D to explain ventricular dysfunction. The supravalvular regions are evaluated as the probe is withdrawn to the UE PA view (as well as the branch PAs, which are anterior and straddling the ascending Ao) and rotated in the ME plane to the ME AoV LAX view. Importantly, the function of the neo-aortic and -pulmonic valves should be determined, because valve distortion can occur with the procedure. With the color flow Doppler scale reduced, coronary blood flow in diastole can also be seen in some cases.

**d-TGA with Rastelli.**—In cases of d-TGA with posterior malalignment VSD and LV outflow tract stenosis (subpulmonary/PV stenosis), other surgical options may be considered, including the Rastelli operation (intracardiac tunnel baffling the LV to the rightward aorta) with RV-to-PA conduit placement. Postoperative TEE should include surveillance for a residual VSD, assurance of an unobstructed pathway from the LV to the aorta, and assessment of function of the RV-to-PA conduit in a fashion similar to that described in truncus arteriosus, DORV, and tetralogy of Fallot.

**d-TGA with Atrial Switch (Senning or Mustard Procedure).**—A complete scan of the atrial switch pathway can begin in the TG

IVC/Hep Veins view with demonstration of the inferior limb of the systemic venous baffle directing IVC blood flow to the subpulmonic LV (Video 46).<sup>204</sup> As the probe is gradually withdrawn to the ME 4-Ch view, the pulmonary venous pathway is now demonstrated as it connects to the systemic RV (Figure 17 and Video 47). Further probe withdrawal into the upper esophagus (30-45° plane) exposes the superior limb of the systemic venous atrium. The ME Bicaval view (90° plane) provides visualization of both the inferior and superior limbs of the systemic venous baffle. With counterclockwise probe rotation, the pulmonary venous pathway can also be seen in the ME Bicaval view. Doppler interrogation of continuous turbulent flow allows for estimation of pressure gradients across a pathway obstruction. The DTG Atr Sept view provides excellent angles of insonation for venous return, particularly for the superior systemic venous pathway. A dilated SVC/IVC or presence of significant venous collaterals should provide a clue for downstream obstruction in the systemic venous pathway. Color Doppler should be employed to assess location and size of baffle leaks in conjunction with an agitated-saline study. Simultaneous biplane imaging further enhances the assessment of the atrial pathways with the orthogonal view. Finally, assessment of intracardiac thrombus is often indicated after stroke or in the setting of tachyarrhythmias before cardioversion. In the normal heart, thrombus is typically assessed in the LAA as previously discussed; however, the LAA is part of the systemic venous pathway in the atrial switch patient. Therefore, thrombus should also be excluded in the pulmonary venous pathway.

**Congenitally Corrected TGA (also known as l-TGA).**—Pre-operative and post-operative assessments require an evaluation similar to what was discussed for the other conotruncal lesions. In particular, the preoperative assessment involves evaluation of the systemic AV valve, since there is commonly an Ebstein-like malformation of the left-sided TV. Post-operative assessment, when the repair entails an anatomic repair or “double switch” operation, evaluates all aspects of the atrial and arterial switches discussed earlier.

**Use of 3D TEE in Conotruncal Defects.** Views that demonstrate the VSD, outflow tracts, and semilunar valves can be analyzed individually and sequentially using focused narrow-sector live 3D. For example, 3D Video 48 shows a patient with Taussig-Bing double outlet right ventricle who underwent an arterial switch operation and VSD closure. In addition, obtaining a 3D full-volume acquisition from the ME 4-Ch or DTG 5-Ch view followed by cropping on cart or off-line is very useful. Focused imaging of an intra-atrial baffle obstruction or leak can be effectively performed with narrow-sector live 3D and biplane echo with color flow Doppler mapping. Imaging of the entire baffle requires 3D full-volume acquisition and cropping.<sup>205-207</sup>

## Key Points

1. Conotruncal defects include TOF, DORV, truncus arteriosus, d-TGA and l-TGA.
2. Anatomic assessment should include great artery positioning (anteroposterior, mediolateral), as well as conal septum location (sub-pulmonary, subaortic or bilateral), position (anterior or posterior), and size (hypoplastic or absent). Associated VSDs can be classified as subaortic, subpulmonary, remote or doubly committed.
3. For all conotruncal defects, TEE allows for pre- and post-operative evaluation of outflow tract patency/obstruction, residual VSDs (including intramural VSDs), residual atrial level communications, AV or semilunar valve insufficiency, and ventric-

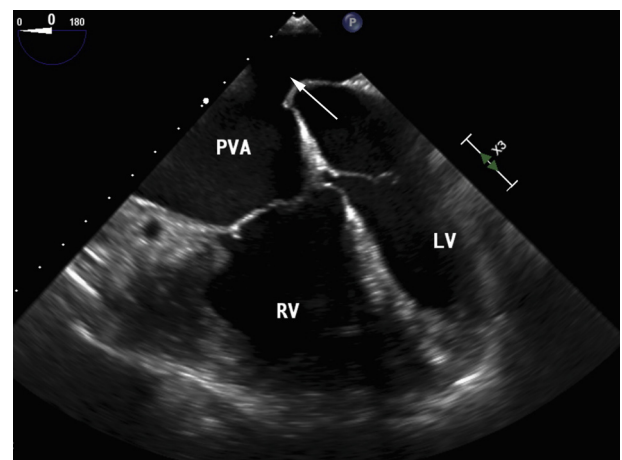
ular function. A combination of ME, TG, and DTG views should be used for evaluation.

4. 3D TEE can be used to provide further elucidation of the VSD/outflow tract anatomy and semilunar valve morphology/function. Where applicable, intra-atrial baffle obstructions or leaks can also be evaluated by narrow sector live 3D, biplane echo, or full volume acquisition.

## Complex Single Ventricle

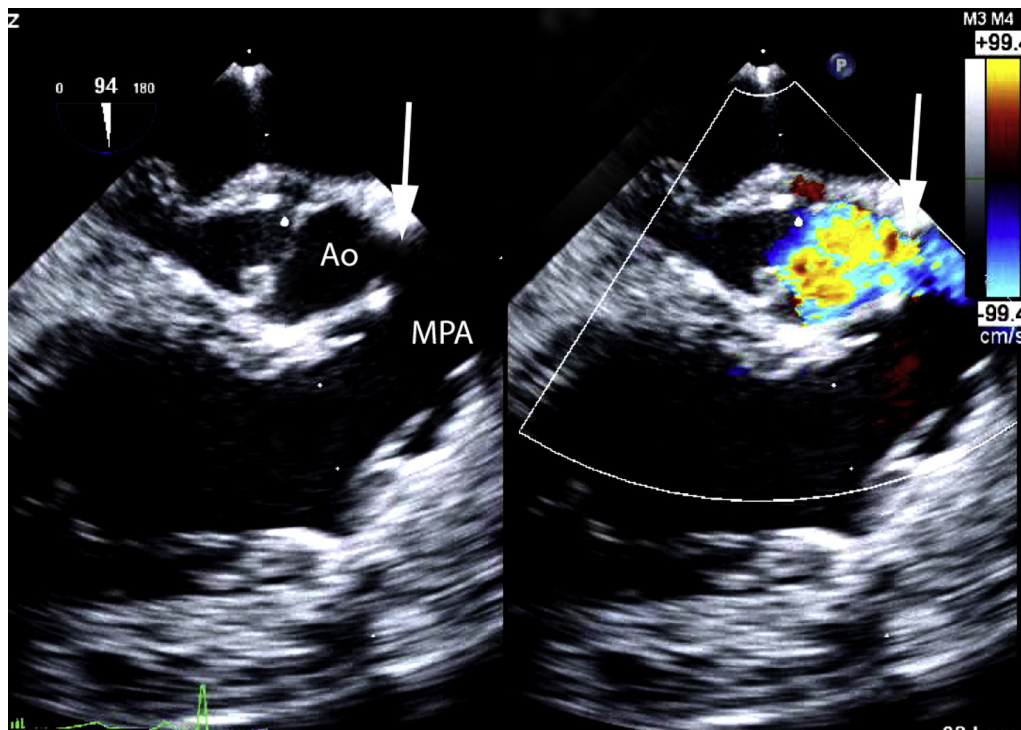
**Anatomy.** Single ventricles encompass a number of different cardiac morphologies where either the subpulmonary ventricle or the subsystemic ventricle is poorly developed, have a deficient or absent inlet, or a stenotic or absent outlet. Irrespective of the underlying morphology, the aim of surgical and/or catheter intervention is to connect the remaining functional ventricle with an outlet to the systemic circulation and allow the pulmonary circulation to receive blood passively from the head and body via cavo-pulmonary connections (SVC and IVC drain directly into the pulmonary arteries).

**Role of TEE in Initial Palliation for Single Ventricles.** The role of routine TEE in the complex single ventricle will depend primarily on preoperative status and surgical stage. Initial palliation (stage 1) requires either a new source of pulmonary blood flow from a modified Blalock-Taussig shunt, central shunt, or Sano shunt, or by limiting pulmonary blood flow through a PA band. Visualization and assessment of the shunt and branch PAs is often difficult, but can be achieved using the UE Ao arch LAX, Ao arch SAX, and PA views. The PA band is best viewed with the DTG RVOT or UE PA views, given their alignment for spectral Doppler assessment. In patients with obstruction to the native Ao (like hypoplastic left heart syndrome, Video 49), stage 1 also requires construction of a neo-aorta with a Damus-Kaye-Stansel (DKS) procedure. The DKS procedure is an anastomosis between the native MPA and ascending Ao, which allows systemic outflow from the native Ao or native MPA to be delivered to the brain and body. When this procedure is coupled with an arch reconstruction it is called the Norwood procedure. The DKS anastomosis is best viewed in the ME AoV LAX and ME Asc Ao LAX views and



**Figure 17** Midesophageal 4-Ch view of D-transposition of the great arteries after atrial switch repair (Mustard or Senning operation). The pathway (arrow) to the pulmonary venous atrium (PVA) is demonstrated to the systemic right ventricle (RV). LV, left ventricle.



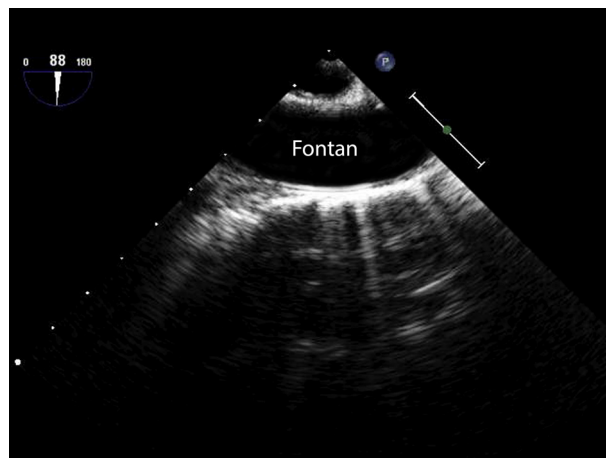


**Figure 18** Midesophageal AoV LAX view with backwards rotation of the transducer angle to 90-120° and slight probe withdrawal demonstrating a Damus-Kaye-Stansel anastomosis (arrow) between the ascending aorta (Ao) and main pulmonary artery (MPA).

lies just above the semilunar valves (Figure 18 and Video 50). The neo-aorta is best visualized with the ME AoV LAX view. Additional Ao arch and descending Ao views include the ME Asc Ao LAX, the UE Ao arch LAX (with clockwise or counterclockwise probe rotation to visualize the aortic arch), and Desc Ao SAX and LAX.

**Role of TEE in Glenn Assessment.** Stage 2 reconstruction, the superior cavopulmonary anastomosis or Glenn procedure, involves an anastomosis between the SVC and the right PA, left PA, or both. Visualization of the Glenn anastomosis is often difficult with TEE but it does offer the ability to assess for any narrowing or turbulence at the anastomotic site to the PA. The best views for the Glenn connection are in the mid to upper esophagus (ME Asc Ao LAX, UE Ao arch SAX) with clockwise or counterclockwise rotation of the probe, depending upon if it is a right- or left-sided Glenn. Additionally, thrombus in the cavopulmonary connection can also be ruled out with TEE (early or late) in the setting of suspected or persistent oxygen desaturation.

**Role of TEE in Fontan Assessment.** Stage 3 reconstruction, the Fontan operation, directs IVC flow to the pulmonary circulation using an intracardiac lateral tunnel or an extracardiac conduit, although there are still some atrio-pulmonary connections in the ACHD population.<sup>208,209</sup> The initial assessment of the Fontan cavopulmonary connection utilizes the ME 4-Ch view. From this position, the probe is advanced to the TG position, until the IVC is identified within the liver. The probe is then withdrawn until the Fontan is visualized in cross section. Changing the transducer angle to 90° in this position (TG IVC/Hep Veins view) will allow for visualization of the baffle longitudinally and as the probe is withdrawn to the ME Bicaval view, more of the Fontan pathway is seen (Figure 19). The addition of color and spectral Doppler can evaluate a Fontan fenestration or residual right-to-left shunting and, if needed, agitated saline injected into the systemic



**Figure 19** Midesophageal Bicaval view (transducer angle around 90°) in a patient after lateral tunnel or extracardiac Fontan. The length of the Fontan tunnel is shown here.

venous circulation from below the diaphragm can be helpful. Importantly, positive pressure ventilation for TEE under general anesthesia may impede venous return to the heart, and caution should be exercised in this patient group. Interventional device closure or creation of a Fontan fenestration can be guided largely or even exclusively using 2D and 3D TEE. Finally, all views that profile intracardiac structures can be used for assessment of thrombus, including, but not limited to the ME 4-Ch, LAA, and RV In-Out views.<sup>210-212</sup>

**Single Ventricle Function.** Quantification of functional single ventricles remains difficult. Function may differ between the morphologic left and right single ventricles.<sup>213</sup> There are important alterations in

loading conditions that affect systolic function before and after Glenn and Fontan palliation. Superior cavopulmonary anastomosis results in a significant reduction in preload in the single ventricle. Ventricular function may acutely fall and then normalize over a period of months, with ventricular remodeling.<sup>214</sup> The Fontan operation results in further reduction in preload and subsequent decrease in ventricular function, however, subsequent ventricular remodeling and normalization of ventricular size and function vary with age at Fontan and magnitude of pre-Fontan volume overload.<sup>215</sup> Qualitative assessment in multiple orthogonal planes is recommended in the ME 4-Ch, TG Mid Pap SAX, or TG LAX views. There is poor correlation between echocardiographic geometric assessment of single ventricular function (modified biplane Simpson's method) and MRI-derived EF.<sup>216</sup> Non-geometric indices may offer the best method for quantifying ventricular function in an objective and reproducible manner.

**Use of 3D TEE in Single Ventricle.** In the single-ventricle patient, the use of 3D TEE is almost entirely performed after the Fontan procedure, given the needed body size of >30 kg to allow probe insertion. Interventional catheterization procedure guidance, atrial and Fontan thrombus analysis, and assessment of AV valve function are frequently required. The Fontan, if not too large, can be imaged using a narrow-sector live 3D longitudinal view which allows analysis in a rapid fashion, free of stitch artifact. In those patients with atrio-pulmonary type connections, a full-volume 3D acquisition with cropping provides the best option. More recently, fusion imaging of 3D TEE and angiography allows simultaneous use of both modalities at a lower total radiation dose.<sup>217</sup>

## Key Points

1. The role of TEE in the complex single ventricle will depend upon the underlying anatomy and also the stage of surgical palliation: (1) Damus-Kaye-Stansel (DKS) or Norwood procedure with modified Blalock-Taussig shunt or Sano shunt; (2) superior cavopulmonary (Glenn) procedure; (3) total cavopulmonary (Fontan) operation.
2. The DKS anastomosis is best viewed in the ME AoV LAX and ME Asc Ao LAX views and lies just above the semilunar valves. Visualization and assessment of the shunt and branch PAs is often difficult, but can be achieved using the UE Ao arch LAX, Ao arch SAX, and PA views.
3. Visualization of the Glenn anastomosis is often difficult with TEE but it does offer the ability to assess for any narrowing or turbulence at the anastomotic site to the PA. The best views are in the ME Asc Ao LAX and UE Ao arch SAX.
4. TEE in the Fontan patient allows for assessment of thrombus, residual Fontan fenestration, AV valve function and ventricular function. It is important to assess the Fontan pathway in both ME 4-Ch view and ME Bicaual view so that the entire conduit is visualized from IVC to PA.
5. Interventional device closure or creation of a Fontan fenestration is guided with both 2D and 3D TEE. 3D TEE can also be used to assess atrial and Fontan conduit thrombus and AV valve function.

## Future Developments

The past several years have brought significant advances in both hardware and software technology that have directly impacted TEE in children. The development of 3D TEE transducers by most of the major

vendors has facilitated evaluation of older children and ACHD patients. Likewise, the development of automated or semi-automated assessment of 3D function, wall motion, and ventricular strain have not only enhanced the ability to care for patients but also have increased our understanding of cardiac mechanics in normal and disease states. Limitations remain, however, and include: suboptimal 3D color flow analysis, lack of a 3D TEE probe for pediatric patients, and lack of a high-quality TEE probe for the smallest neonates on all platforms.

**Probe Development.** The limitations above represent design challenges that push against the physics of ultrasound probe development. The current micro-multiplane probe contains 32 elements, as opposed to 64 in the standard pediatric TEE probe.<sup>19</sup> This places limits on the imaging quality of the probe. A very small multiplane TEE probe capable of passage through the esophagus of smaller neonates needs to balance a transducer size with the need for excellent image quality. Although advances in computer technology have miniaturized the electronics and computers, some of these miniaturizations cannot translate directly to imaging. Image resolution is dependent not only upon element number and transducer frequency, but also upon aperture size, which is proportional to element size.<sup>218</sup> Therefore, miniaturization of probe size ultimately places limits on either element number or size, which limits resolution, or on other aspects, such as the ability to manipulate the array plane. On the other hand, a 3D TEE probe for pediatric patients may be possible. Three-dimensional arrays, albeit somewhat limited ones, have been developed that fit into an intracardiac echocardiography catheter.<sup>219,220</sup> Clearly this array cannot be manipulated and exists in only the longitudinal (90°) plane; however, it does raise the possibility for a 3D array that can be placed into an endoscope of reasonable size for the infant, if not neonatal patient.

**Three-Dimensional Printing/Virtual Reality.** The development of 3D printers promises to impact the TEE community significantly. MRI- and CT-based algorithms have been shown to be useful in the surgical planning of an array of CHD.<sup>221-223</sup> 3D echocardiography has been shown to be feasible for printing accurate models but as the spatial and temporal resolution of 3D TEE improves and printing speed and cost decreases, the potential exists for printing to become a standard component of the preoperative evaluation.<sup>224-226</sup>

Virtual reality (VR) applications in medicine are rapidly expanding into the field of CHD. VR is being used to create virtual 3D models for education, and has been used for surgical planning.<sup>227-229</sup> The ability of TEE to create accurate 3D datasets opens the possibility of building not only VR databases for education, but potentially to build 3D models quickly for planning and diagnosis in the operating room.

**Software Automation/Flow Measurement/Image Analysis.** Automated image analysis has the potential to not only shorten scan time but also to improve accuracy and enhance the analysis of the echocardiogram. Three-dimensional EF by echocardiography has been shown to be superior to standard methods but by definition requires a 3D probe.<sup>230</sup> Vendors have begun to provide automated measurement capabilities and automated EF and strain. However, the 3D dataset contains a large amount of flow data that has not been used and can be localized to specific areas of the heart. This information has the potential to allow echocardiography to provide flow information currently only available by MRI such as simultaneous chamber volumes, valvular flow and regurgitant fraction, regional flow measurement, and shunt fractions. Additionally, this dataset has the ability to provide automated global and regional strain, as well as advanced information such as LV torsion. As vendors increase

**Table 7** Recommended TEE imaging views in selected CHD diagnostic scenarios

	Primary lesion and corresponding views	Common associated lesions and corresponding views (where appropriate)
Atrial septal defect	<ul style="list-style-type: none"> <li>Location, size, number, morphology, and suitability for device closure: ME 4-Ch (View 1), ME AoV SAX (View 12), ME RV In-Out (View 13), ME Bicaval (View 15), DTG Atr Sept (View 23)</li> </ul>	<ul style="list-style-type: none"> <li>Partial anomalous pulmonary venous return: ME Rt and Lt Pulm veins (Views 9 and 10), ME Bicaval (View 15), DTG Atr Sept (View 23)</li> <li>May require extending to UE and LE to evaluate superior and inferior sinus venosus defect</li> <li>LSVC to CS: ME 4-Ch with retroflexion (View 1), ME 2-Ch (View 4), ME Bicaval (View 15) and UE Ao Arch SAX (View 25), both with leftward rotation of TEE probe</li> </ul>
Ventricular septal defect	<ul style="list-style-type: none"> <li>Location, size, number: ME 4-Ch (View 1), ME 5-Ch (View 2), ME LAX (View 5), ME AoV LAX (View 6), ME Ao SAX (View 12), ME RV In-Out (View 13), DTG 5-Ch (View 21), DTG RVOT (View 22), TG Basal SAX (View 17), TG Mid Pap SAX (View 18), TG Apical SAX (View 19)</li> </ul>	<ul style="list-style-type: none"> <li>AoV prolapse: ME AoV LAX (View 6), ME Ao SAX (View 12)</li> <li>Double chamber right ventricle: ME AoV SAX (View 12), ME RV In-Out (View 13), DTG RVOT (View 22)</li> </ul>
Atrioventricular septal defect	<ul style="list-style-type: none"> <li>Primum ASD and inlet VSD: ME 4-Ch (View 1), TG Basal SAX (View 17), TG Mid Pap SAX (View 18)</li> <li>Common Atrioventricular Valve: ME 4-Ch (View 1), ME LAX (View 5), TG Basal SAX (View 17), TG LAX (View 20), DTG 5-Ch (View 21), DTG RVOT (View 22)</li> </ul>	<ul style="list-style-type: none"> <li>Cleft mitral valve: ME 4-Ch (View 1), ME Mitral (View 3), ME 2-Ch (View 4), ME LAX (View 5), TG Basal SAX (View 17)</li> <li>Subaortic obstruction: ME 5-Ch (View 2), ME LAX (View 5), ME AoV LAX (View 6), DTG 5-Ch (View 21), DTG RVOT (View 22)</li> </ul>
Ebstein's anomaly	<ul style="list-style-type: none"> <li>Morphology of leaflets, and suitability for repair (mobility of anterior leaflet, choral attachments to RVOT, number of regurgitant jets): ME 4-Ch (View 1), ME RV In-Out (View 13), ME Mod Bicaval TV (View 14), TG Basal SAX (View 17) with rightward probe rotation, DTG RVOT (View 22)</li> </ul>	<ul style="list-style-type: none"> <li>ASD: see above</li> <li>Noncompaction of LV: ME 4-Ch (View 1), ME 2-Ch (View 4), TG Apical SAX (View 19), TG LAX (View 20)</li> </ul>
Conotruncal defects (TOF, DORV, truncus arteriosus, D-TGA)	<ul style="list-style-type: none"> <li>Great artery position including conal septal location (subpulmonary, subaortic or bilateral), position (anterior or posterior) and size (hypoplastic or absent): ME 5-Ch (View 2), ME AoV LAX (View 6), ME RV In-Out (View 13), DTG 5-Ch (View 21), DTG RVOT (View 22)</li> <li>Location and size of VSD (subaortic, subpulmonary, doubly committed, remote): ME 5-Ch (View 2), ME AoV LAX (View 6), ME Ao SAX (View 12), ME RV In-Out (View 13), DTG 5-Ch (View 21), DTG RVOT (View 22), TG Basal SAX (View 17), TG Mid Pap SAX (View 18), TG Apical SAX (View 19)</li> </ul>	<ul style="list-style-type: none"> <li>RV size and function: ME 4-Ch (View 1), ME AoV SAX (View 12), ME RV In-Out (View 13), TG Basal SAX (View 17), TG Mid Pap SAX (View 18), TG Apical SAX (View 19), DTG RVOT (View 22)</li> <li>AV valve abnormalities (stenosis, regurgitation, straddling/overriding): ME 4-Ch and ME 5-Ch (Views 1 and 2), ME Mitral (View 3), ME 2-Ch (View 4), ME LAX (View 5), ME RV In-Out (View 13), ME Modified Bicaval TV (View 14), TG Basal SAX (View 17), TG Mid Pap SAX (View 18), DTG 5-Ch (View 21), DTG RVOT (View 22)</li> </ul>
TOF (postoperative)	<ul style="list-style-type: none"> <li>Residual VSD: ME 5-Ch (View 2), ME AoV LAX (View 6), ME Ao SAX (View 12), ME RV In-Out (View 13), DTG 5-Ch (View 21), DTG RVOT (View 22)</li> <li>RVOT obstruction: ME RV In-Out (View 13), DTG RVOT (View 22), UE Ao Arch SAX (View 25) with leftward rotation of TEE probe</li> <li>Pulmonary regurgitation: ME Ao SAX (View 12), ME RV In-Out (View 13), UE Ao Arch SAX (View 25) with leftward rotation of TEE probe, UE PA (View 26), DTG RVOT (View 22)</li> </ul>	
DORV (postoperative)	<ul style="list-style-type: none"> <li>Residual VSD: see above</li> <li>LV to aorta pathway: ME 5-Ch (View 2), ME AoV LAX (View 6), DTG 5-Ch (View 21), DTG RVOT (View 22)</li> </ul>	

(Continued)

Table 7 (Continued)

	Primary lesion and corresponding views	Common associated lesions and corresponding views (where appropriate)
Truncus arteriosus (postoperative)	<ul style="list-style-type: none"> <li>Residual VSD: see above</li> <li>Anatomy and function of truncal valve: ME AoV LAX (View 6), ME Ao SAX (View 12), DTG 5-Ch (View 21)</li> <li>Location, size and function of RV to PA conduit: ME RV In-Out (View 13), DTG 5-Ch (View 21), DTG RVOT (View 22)</li> <li>PA size and residual PA stenosis: ME Asc Ao LAX (View 7) and SAX (View 8), UE Ao Arch SAX (View 25), UE PA (View 26).</li> <li>LV to aorta pathway: ME 5-Ch (View 2), ME AoV LAX (View 6), DTG 5-Ch (View 21)</li> </ul>	
d-TGA/arterial switch procedure	<ul style="list-style-type: none"> <li>Right and left ventricular outflow tract: ME 5-Ch (View 2), ME LAX (View 5), ME AoV LAX (View 6), ME RV In-Out (View 13), DTG 5-Ch (View 21), DTG RVOT (View 22)</li> <li>Supravalvular region: UE Ao Arch LAX (View 24) and SAX (View 25), UE PA (View 26)</li> <li>Anatomy and function of neo-aortic valve: ME AoV LAX (View 6), ME AoV SAX (View 12), DTG 5-Ch (View 21)</li> <li>Coronary reimplantation: ME AoV SAX (View 12)</li> </ul>	<ul style="list-style-type: none"> <li>LV size and function: ME 4-Ch (View 1), ME 2-Ch (View 4), ME LAX (View 5), TG Basal SAX (View 17), TG Mid Pap SAX (View 18), TG Apical SAX (View 19), TG LAX (View 20), DTG 5-Ch (View 21)</li> </ul>
d-TGA/Rastelli	<ul style="list-style-type: none"> <li>Residual VSD: see above</li> <li>Location, size and function of RV to PA conduit: ME LAX (View 5), ME RV In-Out (View 13), DTG RVOT (View 22)</li> <li>LV to aorta pathway: ME 5-Ch (View 2), ME LAX (View 5), ME Ao LAX (View 6), DTG 5-Ch (View 21), DTG RVOT (View 22)</li> </ul>	
d-TGA/atrial switch procedure	<ul style="list-style-type: none"> <li>Pulmonary venous baffle: ME 4-Ch (View 1)</li> <li>Superior and inferior limb of systemic venous baffle: ME Bicaval (View 15), ME Mod Bicaval TV (View 14), TG IVC/Hep Veins (View 16), DTG Atr Sept (View 23), UE Ao Arch SAX (View 25), UE PA (View 26)</li> <li>May require gradual sweeps in order to scan the superior and inferior limbs of systemic venous baffle including clockwise/counterclockwise probe rotation</li> </ul>	<ul style="list-style-type: none"> <li>Systemic RV size and function: ME 4-Ch (View 1), ME AoV SAX (View 12), ME RV In-Out (View 13), TG Basal SAX (View 17), TG Mid Pap SAX (View 18), TG Apical SAX (View 19), DTG RVOT (View 22)</li> <li>Systemic AV valve regurgitation: ME 4-Ch (View 1), ME RV In-Out (View 13), ME Mod Bicaval TV (View 14)</li> <li>Subpulmonary LV size and function: ME 4-Ch (View 1), ME 2-Ch (View 4), ME Mitral (View 3), ME LAX (View 5), TG Basal SAX (View 17), TG Mid Pap SAX (View 18), TG Apical SAX (View 19), TG LAX (View 20), DTG 5-Ch (View 21)</li> </ul>
I-TGA	<ul style="list-style-type: none"> <li>Systemic RV size and function: ME 4-Ch (View 1), ME 2-Ch (View 4), ME Mitral (View 3), ME LAX (View 5), TG Basal SAX (View 17), TG Mid Pap SAX (View 18), TG Apical SAX (View 19), TG LAX (View 20), DTG 5-Ch (View 21)</li> <li>Systemic AV valve regurgitation: ME 4-Ch (View 1), ME Mitral (View 3), ME LAX (View 5)</li> <li>Subpulmonic LV size and function: ME 4-Ch (View 1), ME AoV SAX (View 12), ME RV In-Out (View 13), TG Basal SAX (View 17), TG Mid Pap SAX (View 18), TG Apical SAX (View 19), DTG RVOT (View 22)</li> </ul>	<ul style="list-style-type: none"> <li>Physiologic repair (VSD closure and/or LV to PA conduit): see VSD and conduit views above</li> <li>Anatomic repair (Atrial switch repair and arterial switch repair or Rastelli): See D-TGA arterial switch repair and D-TGA Rastelli views</li> </ul>

(Continued)

**Table 7** (Continued)

	Primary lesion and corresponding views	Common associated lesions and corresponding views (where appropriate)
<b>Single Ventricle</b>		
• Stage 1	<ul style="list-style-type: none"> <li>• Assessment of size and function of modified Blalock-Taussig shunt, central shunt or Sano Shunt: UE Ao Arch LAX (View 24) and SAX (View 25), UE PA (View 26)</li> <li>• Assessment of PA band: DTG RVOT (View 22), UE PA (View 26)</li> <li>• Assessment of Damus-Kaye-Stansel (DKS) procedure: ME AoV LAX (View 6), ME Asc Ao LAX (View 7) and SAX (View 8), UE Ao Arch SAX (View 25), UE PA (View 26)</li> <li>• Assessment of Norwood and aortic arch: ME AoV LAX (View 6), ME Asc Ao LAX (View 7) and SAX (View 8), UE Ao arch LAX (View 24) and SAX (View 25), Desc Ao SAX (View 27) and LAX (View 28)</li> </ul>	
• Stage 2 (Glenn)	<ul style="list-style-type: none"> <li>• ME Asc Ao LAX (View 7) and SAX (View 8), UE Ao arch SAX (View 25)</li> <li>• May require clockwise or counterclockwise rotation of the probe</li> </ul>	
• Stage 3 (Fontan)	<ul style="list-style-type: none"> <li>• Atriopulmonary Connection: ME 4-Ch (View 1), ME RV In-Out (View 13), ME Asc Ao SAX (View 8), TG IVC/Hep Veins (View 16)</li> <li>• Lateral tunnel/extracardiac connection: ME 4-Ch (View 1), ME Asc Ao SAX (View 8), ME Mod Bicaval TV (View 14), TG IVC/Hep Veins (View 16), DTG Atr Sept (View 23)</li> <li>• Pulmonary artery flow: ME Asc Ao SAX (View 8), UE Ao Arch SAX (View 25)</li> </ul>	<ul style="list-style-type: none"> <li>• Right pulmonary vein compression by dilated right atrium of atriopulmonary connection: ME Rt Pulm Veins (View 9)</li> <li>• Right atrial clot in atriopulmonary connection: ME 4-Ch (View 1), ME Mod Bicaval TV (View 14), DTG Atr Sept (View 23)</li> <li>• Lateral tunnel and extracardiac patency, clot, and fenestration: ME 4-Ch (View 1), ME 2-Ch (View 4), ME Bicaval (View 15), TG IVC/Hep (View 16), DTG Atr Sept (View 23)</li> </ul>

ASD, Atrial septal defect; *ALCAPA*, anomalous origin of the left main coronary artery from the pulmonary artery; AV, atrioventricular; CS, coronary sinus; *d-TGA*, complete transposition of the great arteries; *DORV*, double outlet right ventricle; *DTG*, deep transgastric; *l-TGA*, congenitally corrected transposition of the great arteries; *LSVC*, Left superior vena cava; *LV*, left ventricle; *RV*, right ventricle; *TG*, transgastric; *TOF*, tetralogy of Fallot; *TV*, tricuspid valve; *VSD*, ventricular septal defect.  
Modified from Hahn *et al.*<sup>16</sup>

utilization of the dataset, ultrasound systems can take over tasks such as measurement and flow assessment, allowing clinicians to focus on the anatomy and physiology to obtain advanced diagnostic information.

## CONCLUSIONS

Transesophageal echocardiography in children and patients with CHD is clearly a unique and distinct discipline. The aim of this document was to provide the reader with an in-depth review of what is required to perform this procedure, as well as a comprehensive protocol for image acquisition. Given the tremendous amount of anatomic variability in CHD, these guidelines are meant to serve as a starting point from which additional customization may be needed to obtain information crucial for clinical decision-making in each patient. We have attempted to encapsulate much of CHD in summary Table 7 for ease of use. The continued incorporation of new and advanced technologies designed to shorten acquisition time, improve accuracy, and enhance analysis will further benefit patient care and reinforce the vital role of this imaging modality in a variety of clinical settings.

## SUPPLEMENTARY DATA

Supplementary data related to this article can be found at <https://doi.org/10.1016/j.echo.2018.08.016>.

## REFERENCES

1. Cyran SE, Kimball TR, Meyer RA, Bailey WW, Lowe E, Balisteri WF, et al. Efficacy of intraoperative transesophageal echocardiography in children with congenital heart disease. *Am J Cardiol* 1989;63:594-8.
2. Fyfe DA, Kline CH, Sade RM, Greene CA, Gillette PC. The utility of transesophageal echocardiography during and after Fontan operations in small children. *Am Heart J* 1991;122:1403-15.
3. Weintraub R, Shiota T, Elkadi T, Golebiovski P, Zhang J, Rothman A, et al. Transesophageal echocardiography in infants and children with congenital heart disease. *Circulation* 1992;86:711-22.
4. Acar P, Abadir S, Aggoun Y. Transcatheter closure of perimembranous ventricular septal defects with Amplatzer occluder assessed by real-time three-dimensional echocardiography. *Eur J Echocardiogr* 2007;8:110-5.
5. Gan C, An Q, Lin K, Tang H, Lui RC, Tao K, et al. Periventricular device closure of ventricular septal defects: six months results in 30 young children. *Ann Thorac Surg* 2008;86:142-6.

6. Kim HK, Kim WH, Hwang SW, Lee JY, Song JY, Kim SJ, et al. Predictive value of intraoperative transesophageal echocardiography in complete atrioventricular septal defect. *Ann Thorac Surg* 2005;80:56-9.
7. Kutty S, Delaney JW, Latson LA, Danford DA. Can we talk? Reflections on effective communication between imager and interventionalist in congenital heart disease. *J Am Soc Echocardiogr* 2013;26:813-27.
8. Mathewson JW, Bichell D, Rothman A, Ing FF. Absent posteroinferior and anterosuperior atrial septal defect rims: factors affecting nonsurgical closure of large secundum defects using the Amplatzer occluder. *J Am Soc Echocardiogr* 2004;17:62-9.
9. Miller-Hance WC, Silverman NH. Transesophageal echocardiography (TEE) in congenital heart disease with focus on the adult. *Cardiol Clin* 2000;18:861-92.
10. Motta P, Miller-Hance WC. Transesophageal echocardiography in tetralogy of Fallot. *Semin Cardiothorac Vasc Anesth* 2012;16:70-87.
11. Randolph GR, Hagler DJ, Connolly HM, Dearani JA, Puga FJ, Danielson GK, et al. Intraoperative transesophageal echocardiography during surgery for congenital heart defects. *J Thorac Cardiovasc Surg* 2002;124:1176-82.
12. Simpson J, Lopez L, Acar P, Friedberg MK, Khoo NS, Ko HH, et al. Three-dimensional echocardiography in congenital heart disease: an expert consensus document from the European Association of Cardiovascular Imaging and the American Society of Echocardiography. *J Am Soc Echocardiogr* 2017;30:1-27.
13. Smallhorn JF. Intraoperative transesophageal echocardiography in congenital heart disease. *Echocardiography* 2002;19:709-23.
14. Wong PC, Miller-Hance WC, editors. *Transesophageal Echocardiography for Congenital Heart Disease*. London: Springer-Verlag; 2014.
15. Levin DN, Taras J, Taylor K. The cost effectiveness of transesophageal echocardiography for pediatric cardiac surgery: a systematic review. *Pediatr Anaesth* 2016;26:682-93.
16. Hahn RT, Abraham T, Adams MS, Bruce CJ, Glas KE, Lang RM, et al. Guidelines for performing a comprehensive transesophageal echocardiographic examination: recommendations from the American Society of Echocardiography and the Society of Cardiovascular Anesthesiologists. *J Am Soc Echocardiogr* 2013;26:921-64.
17. Scohy TV, Matte G, van Neer PL, van der Steen AF, McGhie J, Bogers A, et al. A new transesophageal probe for newborns. *Ultrasound Med Biol* 2009;35:1686-9.
18. Scohy TV, Gommers D, Jan ten Harkel AD, Deryck Y, McGhie J, Bogers AJ. Intraoperative evaluation of micromultiplane transesophageal echocardiographic probe in surgery for congenital heart disease. *Eur J Echocardiogr* 2007;8:241-6.
19. Zyblewski SC, Shirali GS, Forbus GA, Hsia TY, Bradley SM, Atz AM, et al. Initial experience with a miniaturized multiplane transesophageal probe in small infants undergoing cardiac operations. *Ann Thorac Surg* 2010;89:1990-4.
20. Toole BJ, Slesnick TC, Kreeger J, Border WL, Ehrlich AC, Ferguson ME, et al. The miniaturized multiplane micro-transesophageal echocardiographic probe: a comparative evaluation of its accuracy and image quality. *J Am Soc Echocardiogr* 2015;28:802-7.
21. Pushparajah K, Miller OI, Rawlins D, Barlow A, Nugent K, Simpson JM. Clinical application of a micro multiplane transoesophageal probe in congenital cardiac disease. *Cardiol Young* 2012;22:170-7.
22. Silvestry FE, Cohen MS, Armsby LB, Burkule NJ, Fleishman CE, Hijazi ZM, et al. Guidelines for the echocardiographic assessment of atrial septal defect and patent foramen ovale: from the American Society of Echocardiography and Society for Cardiac Angiography and Interventions. *J Am Soc Echocardiogr* 2015;28:910-58.
23. Cossor W, Cui VW, Roberson DA. Three-dimensional echocardiographic en face views of ventricular septal defects: feasibility, accuracy, imaging protocols and reference image Collection. *J Am Soc Echocardiogr* 2015;28:1020-9.
24. Baker GH, Shirali G, Ringewald JM, Hsia TY, Bandisode V. Usefulness of live three-dimensional transesophageal echocardiography in a congenital heart disease center. *Am J Cardiol* 2009;103:1025-8.
25. Weitzel N, Salcedo E, Puskas F, Nasrallah F, Fullerton D, Seres T. Using real time three-dimensional transesophageal echocardiography during Ross procedure in the operating room. *Echocardiography* 2009;26:1278-83.
26. Huang X, Shen J, Huang Y, Zheng Z, Fei H, Hou Y, et al. En face view of atrial septal defect by two-dimensional transthoracic echocardiography: comparison to real-time three-dimensional transesophageal echocardiography. *J Am Soc Echocardiogr* 2010;23:714-21.
27. Simpson JM, Miller O. Three-dimensional echocardiography in congenital heart disease. *Arch Cardiovasc Dis* 2011;104:45-56.
28. Brantley HP, Nekkanti R, Anderson CA, Kypson AP. Three-dimensional echocardiographic features of unicuspid aortic valve stenosis correlate with surgical findings. *Echocardiography* 2012;29:E204-7.
29. Simpson J, Miller O, Bell A, Bellsham-Revell H, McGhie J, Meijboom F. Image orientation for three-dimensional echocardiography of congenital heart disease. *Int J Cardiovasc Imaging* 2012;28:743-53.
30. Vettukattil JJ. Three dimensional echocardiography in congenital heart disease. *Heart* 2012;98:79-88.
31. Ayres NA, Miller-Hance W, Fyfe DA, Stevenson JG, Sahn DJ, Young LT, et al. Indications and guidelines for performance of transesophageal echocardiography in the patient with pediatric acquired or congenital heart disease: report from the task force of the Pediatric Council of the American Society of Echocardiography. *J Am Soc Echocardiogr* 2005;18:91-8.
32. Fyfe DA, Ritter SB, Snider AR, Silverman NH, Stevenson JG, Sorensen G, et al. Guidelines for transesophageal echocardiography in children. *J Am Soc Echocardiogr* 1992;5:640-4.
33. Bai A, Steinberg M, Showler A, Bury L, Bhatia R, Tomlinson G, et al. Diagnostic accuracy of transthoracic echocardiography for infective endocarditis findings using transesophageal echocardiography as the reference standard: a meta-analysis. *J Am Soc Echocardiogr* 2017;30:639-46.e8.
34. Mart CR. Three-dimensional echocardiographic evaluation of the Fontan conduit for thrombus. *Echocardiography* 2012;29:363-8.
35. Saric M, Armour AC, Arnaout MS, Chaudhry FA, Grimm RA, Kronzon I, et al. Guidelines for the use of echocardiography in the evaluation of a cardiac source of embolism. *J Am Soc Echocardiogr* 2016;29:1-42.
36. Bouch D, Allsager C, Moore N. Peri-operative trans-oesophageal echocardiography and nitric oxide during general anaesthesia in a patient with Eisenmenger's syndrome. *Anaesthesia* 2006;61:996-1000.
37. Stumper O, Witsenburg M, Sutherland GR, Cromme-Dijkhuis A, Godman MJ, Hess J. Transesophageal echocardiographic monitoring of interventional cardiac catheterization in children. *J Am Coll Cardiol* 1991;18:1506-14.
38. Tumbarello R, Sanna A, Cardu G, Bande A, Napoleone A, Bini RM. Usefulness of transesophageal echocardiography in the pediatric catheterization laboratory. *Am J Cardiol* 1993;71:1321-5.
39. Van Der Velde ME, Perry SB. Transesophageal echocardiography during interventional catheterization in congenital heart disease. *Echocardiography* 1997;14:513-28.
40. Bhaya M, Mutluer F, Mahan E, Mahan L, Hsiung M, Yin W, et al. Live/Real time three-dimensional transesophageal echocardiography in percutaneous closure of atrial septal defects. *Echocardiography* 2013;30:345-53.
41. Faletta FF, Pedrazzini G, Pasotti E, Muzzarelli S, Dequarti MC, Murzilli R, et al. 3D TEE during catheter-based interventions. *JACC Cardiovasc Imaging* 2014;7:292-308.
42. Price MJ, Smith MR, Rubenson DS. Utility of on-line three-dimensional transesophageal echocardiography during percutaneous atrial septal defect closure. *Catheter Cardiovasc Interv* 2010;75:570-7.
43. Rigby M. Transoesophageal echocardiography during interventional cardiac catheterisation in congenital heart disease. *Heart* 2001;86(Suppl 2):II23-9.
44. van der Velde M, Perry S, Sanders S. Transesophageal echocardiography with color Doppler during interventional catheterization. *Echocardiography* 1991;8:721-30.
45. Feltes T, Friedman R. Transesophageal echocardiographic detection of atrial thrombi in patients with nonfibrillation atrial tachyarrhythmias and congenital heart disease. *J Am Coll Cardiol* 1994;24:1365-70.
46. Sachdeva R, Frazier EA, Jaquiss RD, Imamura M, Swearingen CJ, Vyas HV. Echocardiographic evaluation of ventricular assist devices in pediatric patients. *J Am Soc Echocardiogr* 2013;26:41-9.

47. Horenstein M, Karpawich P, Epstein M, Singh T. Transthoracic echocardiography for precardiography screening during atrial flutter/fibrillation in young patients. *Clin Cardiol* 2004;27:413-6.
48. Yousef N, Philips M, Shetty I, Cui VW, Zimmerman F, Roberson DA. Transesophageal echocardiography of intracardiac thrombus in congenital heart disease and atrial flutter: the importance of thorough examination of the Fontan. *Pediatr Cardiol* 2014;35:1099-107.
49. Catena E, Mele D. Role of intraoperative transesophageal echocardiography in patients undergoing noncardiac surgery. *J Cardiovasc Med (Hagerstown)* 2008;9:993-1003.
50. Neira V, Gardin L, Ryan G, Jarvis J, Roy D, Splinter W. A transesophageal echocardiography examination clarifies the cause of cardiovascular collapse during scoliosis surgery in a child. *Can J Anaesth* 2011;58:451-5.
51. Ho A, Chen C, Yang M, Chu J, Lin P. Usefulness of intraoperative transesophageal echocardiography in the assessment of surgical repair of pediatric ventricular septal defects with video-assisted endoscopic techniques in children. *Chang Gung Med J* 2004;27:646-53.
52. Ho A, Tan P, Yang M, Yang C, Chu J, Lin P, et al. The use of multiplane transesophageal echocardiography to evaluate residual patent ductus arteriosus during video-assisted thoracoscopy in adults. *Surg Endosc* 1999;13:975-9.
53. Lavioie J, Burrows F, Gentles T, Sanders S, Burke R, Javorski J. Transoesophageal echocardiography detects residual ductal flow during video-assisted thoracoscopic patent ductus arteriosus interruption. *Can J Anaesth* 1994;41:310-3.
54. Sardari F, Schlunt M, Applegate R, Gundry S. The use of transesophageal echocardiography to guide sternal division for cardiac operations via mini-sternotomy. *J Card Surg* 1997;12:67-70.
55. Marcus B, Wong P, Wells W, Lindesmith G, Starnes V. Transesophageal echocardiography in the postoperative child with an open sternum. *Ann Thorac Surg* 1994;58:235-6.
56. Scott PJ, Blackburn ME, Wharton GA, Wilson N, Dickinson DF, Gibbs JL. Transoesophageal echocardiography in neonates, infants and children: applicability and diagnostic value in everyday practice of a cardiothoracic unit. *Br Heart J* 1992;68:488-92.
57. Scheinin S, Radovancevic B, Ott D, Nihill M, Cabalka A, Frazier O. Post-cardiotomy LVAD support and transesophageal echocardiography in a child. *Ann Thorac Surg* 1993;55:529-31.
58. Russell I, Rouine-Rapp K, Stratmann G, Miller-Hance W. Congenital heart disease in the adult: a review with internet-accessible transesophageal echocardiographic images. *Anesth Analg* 2006;102:694-723.
59. Bezold L, Pignatelli R, Altman C, Feltes T, Gajarski R, Vick G, et al. Intraoperative transesophageal echocardiography in congenital heart surgery. The Texas Children's Hospital experience. *Tex Heart Inst J* 1996;23:108-15.
60. Srivastava S, Printz BF, Geva T, Shirali GS, Weinberg PM, Wong PC, et al. Task force 2: pediatric cardiology fellowship training in noninvasive cardiac imaging: endorsed by the American Society of Echocardiography and the Society of Pediatric Echocardiography. *J Am Soc Echocardiogr* 2015;28:1009-19.
61. Stevenson J. Incidence of complications in pediatric transesophageal echocardiography: experience in 1650 cases. *J Am Soc Echocardiogr* 1999;12:527-32.
62. Stevenson J, Sorensen G. Proper probe size for pediatric transesophageal echocardiography. *Am J Cardiol* 1993;72:491-2.
63. Quinones M, Douglas P, Foster E, Gorcsan J, Lewis J, Pearlman A, et al. ACC/AHA clinical competence statement on echocardiography: a report of the American College of Cardiology/American Heart Association/American College of Physicians-American Society of Internal Medicine Task Force on clinical competence. *J Am Soc Echocardiogr* 2003;16:379-402.
64. Srivastava S, Printz BF, Geva T, Shirali GS, Weinberg PM, Wong PC, et al. Task force 2: pediatric cardiology fellowship training in noninvasive cardiac imaging. *J Am Coll Cardiol* 2015;66:687-98.
65. Daniel W, Erbel R, Kasper W, Visser C, Engberding R, Sutherland G, et al. Safety of transesophageal echocardiography. A multicenter survey of 10,419 examinations. *Circulation* 1991;83:817-21.
66. Hilberath J, Oakes D, Sherman S, Bulwer B, D'Ambra M, Eltzhig H. Safety of transesophageal echocardiography. *J Am Soc Echocardiogr* 2010;23:1115-27. quiz 220-1.
67. Kallmeyer I, Collard C, Fox J, Body S, Sherman S. The safety of intraoperative transesophageal echocardiography: a case series of 7200 cardiac surgical patients. *Anesth Analg* 2001;92:1126-30.
68. Piercy M, McNicol L, Dinh D, Story D, Smith J. Major complications related to the use of transesophageal echocardiography in cardiac surgery. *J Cardiothorac Vasc Anesth* 2009;23:62-5.
69. Bettex D, Prêtre R, Jenni R, Schmid E. Cost-effectiveness of routine intraoperative transesophageal echocardiography in pediatric cardiac surgery: a 10-year experience. *Anesth Analg* 2005;100:1271-5. table of contents.
70. Bensky A, O'Brien J, Hammon J. Transesophageal echo probe compression of an aberrant right subclavian artery. *J Am Soc Echocardiogr* 1995;8:964-6.
71. Gilbert T, Panico F, McGill W, Martin G, Halley D, Sell J. Bronchial obstruction by transesophageal echocardiography probe in a pediatric cardiac patient. *Anesth Analg* 1992;74:156-8.
72. Lunn RJ, Oliver WC, Hagler DJ, Danielson GK. Aortic compression by transesophageal echocardiographic probe in infants and children undergoing cardiac surgery. *Anesthesiology* 1992;77:587-90.
73. Muhiudeen I, Silverman N. Intraoperative transesophageal echocardiography using high resolution imaging in infants and children with congenital heart disease. *Echocardiography* 1993;10:599-608.
74. Preisman S, Yusim Y, Mishali D, Perel A. Compression of the pulmonary artery during transesophageal echocardiography in a pediatric cardiac patient. *Anesth Analg* 2003;96:85-7. table of contents.
75. Andropoulos D, Ayres N, Stayer S, Bent S, Campos C, Fraser C. The effect of transesophageal echocardiography on ventilation in small infants undergoing cardiac surgery. *Anesth Analg* 2000;90:47-9.
76. Casta A, Brown D, Yuki K. Induction of supraventricular tachycardia during transesophageal echocardiography: an unusual complication. *J Cardiothorac Vasc Anesth* 2008;22:592-3.
77. Liu J, Hartnick C, Rutter M, Hartley B, Myer C. Subglottic stenosis associated with transesophageal echocardiography. *Int J Pediatr Otorhinolaryngol* 2000;55:47-9.
78. Muhiudeen-Russell I, Miller-Hance W, Silverman N. Unrecognized esophageal perforation in a neonate during transesophageal echocardiography. *J Am Soc Echocardiogr* 2001;14:747-9.
79. Hogue C, Lappas G, Creswell L, Ferguson T, Sample M, Pugh D, et al. Swallowing dysfunction after cardiac operations. Associated adverse outcomes and risk factors including intraoperative transesophageal echocardiography. *J Thorac Cardiovasc Surg* 1995;110:517-22.
80. Skoretz S, Yau T, Ivanov J, Granton J, Martino R. Dysphagia and associated risk factors following extubation in cardiovascular surgical patients. *Dysphagia* 2014;29:647-54.
81. Kohr L, Dargan M, Hague A, Nelson S, Duffy E, Backer C, et al. The incidence of dysphagia in pediatric patients after open heart procedures with transesophageal echocardiography. *Ann Thorac Surg* 2003;76:1450-6.
82. Michel J, Hofbeck M, Schineis C, Kumpf M, Heimberg E, Magunia H, et al. Severe upper airway obstruction after intraoperative transesophageal echocardiography in pediatric cardiac surgery: a retrospective analysis. *Pediatr Crit Care Med* 2017;18:924-30.
83. Kamata M, Hakim M, Tumin D, Krishna S, Naguib A, Tobias J. The effect of transesophageal echocardiography probe placement on intracuff pressure of an endotracheal tube in infants and children. *J Cardiothorac Vasc Anesth* 2017;31:543-8.
84. Greene M, Alexander J, Knauf D, Talbert J, Langham M, Kays D, et al. Endoscopic evaluation of the esophagus in infants and children immediately following intraoperative use of transesophageal echocardiography. *Chest* 1999;116:1247-50.
85. Frommelt PC, Stuth EA. Transesophageal echocardiographic in total anomalous pulmonary venous drainage: hypotension caused by compression of the pulmonary venous confluence during probe passage. *J Am Soc Echocardiogr* 1994;7:652-4.
86. Chang YY, Chang CI, Wang MJ, Lin SM, Chen YS, Tsai SK, et al. The safe use of intraoperative transesophageal echocardiography in the

- management of total anomalous pulmonary venous connection in newborns and infants: a case series. *Paediatr Anaesth* 2005;15:939-43.
87. Mart C, Parrish M, Rosen K, Dettorre M, Ceneviva G, Lucking S, et al. Safety and efficacy of sedation with propofol for transoesophageal echocardiography in children in an outpatient setting. *Cardiol Young* 2006;16:152-6.
  88. Yuki K, Casta A, Uezono S. Anesthetic management of noncardiac surgery for patients with single ventricle physiology. *J Anesth* 2011;25:247-56.
  89. Muhiudeen I, Roberson D, Silverman N, Haas G, Turley K, Cahalan M. Intraoperative echocardiography in infants and children with congenital cardiac shunt lesions: transesophageal versus epicardial echocardiography. *J Am Coll Cardiol* 1990;16:1687-95.
  90. Bansal R, Shakudo M, Shah P, Shah P. Biplane transesophageal echocardiography: technique, image orientation, and preliminary experience in 131 patients. *J Am Soc Echocardiogr* 1990;3:348-66.
  91. Bengur A, Li J, Herlong J, Jagers J, Sanders S, Ungerleider R. Intraoperative transesophageal echocardiography in congenital heart disease. *Semin Thorac Cardiovasc Surg* 1998;10:255-64.
  92. Gentles TL, Rosenfeld HM, Sanders SP, Laussen PC, Burke RP, van der Velde ME. Pediatric biplane transesophageal echocardiography: preliminary experience. *Am Heart J* 1994;128(6 Pt 1):1225-33.
  93. O'Leary PW, Hagler DJ, Seward JB, Tajik AJ, Schaff HV, Puga FJ, et al. Biplane intraoperative transesophageal echocardiography in congenital heart disease. *Mayo Clin Proc* 1995;70:317-26.
  94. Omoto R, Kyo S, Matsumura M, Adachi H, Shah P, Maruyama M. Recent advances in transesophageal echocardiography: development of biplane and pediatric transesophageal probes. *Am J Cardiac Imaging* 1990;4:207-14.
  95. Roelandt JR, Thomson IR, Vletter WB, Brommersma P, Bom N, Linker DT. Multiplane transesophageal echocardiography: latest evolution in an imaging revolution. *J Am Soc Echocardiogr* 1992;5:361-7.
  96. Seward J. Biplane and multiplane transesophageal echocardiography: evaluation of congenital heart disease. *Am J Card Imaging* 1995;9:129-36.
  97. Seward JB, Khandheria BK, Freeman WK, Oh JK, Enriquez-Sarano M, Miller FA, et al. Multiplane transesophageal echocardiography: image orientation, examination technique, anatomic correlations, and clinical applications. *Mayo Clin Proc* 1993;68:523-51.
  98. Ungerleider R. Biplane and multiplane transesophageal echocardiography. *Am Heart J* 1999;138(4 Pt 1):612-3.
  99. Vegas A. Three-dimensional transesophageal echocardiography: principles and clinical applications. *Ann Card Anaesth* 2016;19(Supplement):S35-43.
  100. Vegas A, Meineri M. Core review: three-dimensional transesophageal echocardiography is a major advance for intraoperative clinical management of patients undergoing cardiac surgery: a core review. *Anesth Analg* 2010;110:1548-73.
  101. Mart C, Fehr D, Myers J, Rosen K. Intraoperative transesophageal echocardiography in a 1.4-kg infant with complex congenital heart disease. *Pediatr Cardiol* 2003;24:84-5.
  102. Bruce C, O'Leary P, Hagler D, Seward J, Cabalka A. Miniaturized transesophageal echocardiography in newborn infants. *J Am Soc Echocardiogr* 2002;15:791-7.
  103. Cannesson M, Hénaine R, Metton O, Védrinne C, Delanoy B, Di Filippo S, et al. Images in cardiovascular medicine. Intraoperative transesophageal echocardiography using a miniaturized transducer in a neonate undergoing Norwood procedure for hypoplastic left heart syndrome. *Circulation* 2008;117:702-3.
  104. Ferns S, Komarlu R, Van Bergen A, Multani K, Cui V, Roberson D. Transesophageal echocardiography in critically ill acute postoperative infants: comparison of AcuNav intracardiac echocardiographic and microTEE miniaturized transducers. *J Am Soc Echocardiogr* 2012;25:874-81.
  105. Mart C, Rosen K. Optimal head position during transesophageal echocardiographic probe insertion for pediatric patients weighing up to 10 kg. *Pediatr Cardiol* 2009;30:441-6.
  106. Wellen SL, Glatz AC, Gaynor JW, Montenegro LM, Cohen MS. Transesophageal echocardiography probe insertion failure in infants undergoing cardiac surgery. *Congenital heart disease* 2013;8:240-5.
  107. Rutala W, Weber D, Healthcare, Committee ICPA. , Healthcare Infection Control Practices Advisory Committee. Guideline for Disinfection and Sterilization in Healthcare Facilities. Centers for Disease Control and Prevention; 2008.
  108. Mitchell C. Council on cardiovascular sonography review of the recently released ASE statement on sonographer involvement in the performance of TEE. *J Am Soc Echocardiogr* 2018;31:A28-9.
  109. Acar P, Abadir S, Paranon S, Latcu G, Grosjean J, Dulac Y. Live 3D echocardiography with the pediatric matrix probe. *Echocardiography* 2007;24:750-5.
  110. Cui W, Gambetta K, Zimmerman F, Freter A, Sugeng L, Lang R, et al. Real-time three-dimensional echocardiographic assessment of left ventricular systolic dyssynchrony in healthy children. *J Am Soc Echocardiogr* 2010;23:1153-9.
  111. Flachskampf FA, Wouters PF, Edvardsen T, Evangelista A, Habib G, Hoffman P, et al. Recommendations for transesophageal echocardiography: EACVI update 2014. *Eur Heart J Cardiovasc Imaging* 2014;15:353-65.
  112. Lang RM, Badano LP, Tsang W, Adams DH, Agricola E, Buck T, et al. EAE/ASE recommendations for image acquisition and display using three-dimensional echocardiography. *J Am Soc Echocardiogr* 2012;25:3-46.
  113. Simpson J, Lopez L, Acar P, Friedberg M, Khoo N, Ko H, et al. Three-dimensional echocardiography in congenital heart disease: an expert consensus document from the European Association of Cardiovascular Imaging and the American Society of Echocardiography. *Eur Heart J Cardiovasc Imaging* 2016;17:1071-97.
  114. Simpson JM. Real-time three-dimensional echocardiography of congenital heart disease using a high frequency paediatric matrix transducer. *Eur J Echocardiogr* 2008;9:222-4.
  115. Sugeng L, Sherman SK, Salgo IS, Weinert L, Shook D, Raman J, et al. Live 3-dimensional transesophageal echocardiography initial experience using the fully-sampled matrix array probe. *J Am Coll Cardiol* 2008;52:446-9.
  116. Lopez L, Colan SD, Frommelt PC, Ensing GJ, Kendall K, Younoszai AK, et al. Recommendations for quantification methods during the performance of a pediatric echocardiogram: a report from the Pediatric Measurements Writing Group of the American Society of Echocardiography Pediatric and Congenital Heart Disease Council. *J Am Soc Echocardiogr* 2010;23:465-95. quiz 576-7.
  117. Omran AS, Woo A, David TE, Feindel CM, Rakowski H, Siu SC. Intraoperative transesophageal echocardiography accurately predicts mitral valve anatomy and suitability for repair. *J Am Soc Echocardiogr* 2002;15:950-7.
  118. Zoghbi WA, Adams D, Bonow RO, Enriquez-Sarano M, Foster E, Grayburn PA, et al. Recommendations for noninvasive evaluation of native valvular regurgitation: a report from the American Society of Echocardiography Developed in Collaboration with the Society for Cardiovascular Magnetic Resonance. *J Am Soc Echocardiogr* 2017;30:303-71.
  119. Stewart WJ, Currie PJ, Salcedo EE, Klein AL, Marwick T, Agler DA, et al. Evaluation of mitral leaflet motion by echocardiography and jet direction by Doppler color flow mapping to determine the mechanisms of mitral regurgitation. *J Am Coll Cardiol* 1992;20:1353-61.
  120. Madiago EJ, Punn R, Geeter N, Silverman NH. Routine intra-operative trans-oesophageal echocardiography yields better outcomes in surgical repair of CHD. *Cardiol Young* 2016;26:263-8.
  121. Rosenfeld HM, Gentles TL, Wernovsky G, Laussen PC, Jonas RA, Mayer JE Jr, et al. Utility of intraoperative transesophageal echocardiography in the assessment of residual cardiac defects. *Pediatr Cardiol* 1998;19:346-51.
  122. Banakal SC. Intraoperative transesophageal echocardiographic assessment of the mitral valve repair. *Ann Card Anaesth* 2010;13:79-84.
  123. Freeman WK, Schaff HV, Khandheria BK, Oh JK, Orszulak TA, Abel MD, et al. Intraoperative evaluation of mitral valve regurgitation and repair by transesophageal echocardiography: incidence and significance of systolic anterior motion. *J Am Coll Cardiol* 1992;20:599-609.



124. Wu YT, Chang AC, Chin AJ. Semiquantitative assessment of mitral regurgitation by Doppler color flow imaging in patients aged < 20 years. *Am J Cardiol* 1993;71:727-32.
125. Lang RM, Badano LP, Mor-Avi V, Afilalo J, Armstrong A, Ernande L, et al. Recommendations for cardiac chamber quantification by echocardiography in adults: an update from the American Society of Echocardiography and the European Association of Cardiovascular Imaging. *J Am Soc Echocardiogr* 2015;28:1-39.e14.
126. Lim DS, Dent JM, Gutgesell HP, Matherne GP, Kron IL. Transesophageal echocardiographic guidance for surgical repair of aortic insufficiency in congenital heart disease. *J Am Soc Echocardiogr* 2007;20:1080-5.
127. Stern KW, White MT, Verghese GR, Del Nido PJ, Geva T. Intraoperative echocardiography for congenital aortic valve repair: predictors of early reoperation. *Ann Thorac Surg* 2015;100:678-85.
128. le Polain de Waroux JB, Pouleur AC, Robert A, Pasquet A, Gerber BL, Noirhomme P, et al. Mechanisms of recurrent aortic regurgitation after aortic valve repair: predictive value of intraoperative transesophageal echocardiography. *JACC Cardiovasc Imaging* 2009;2:931-9.
129. Pethig K, Miltz A, Hagl C, Harringer W, Haverich A. Aortic valve reimplantation in ascending aortic aneurysm: risk factors for early valve failure. *Ann Thorac Surg* 2002;73:29-33.
130. Goldstein SA, Evangelista A, Abbara S, Arai A, Asch FM, Badano LP, et al. Multimodality imaging of diseases of the thoracic aorta in adults: from the American Society of Echocardiography and the European Association of Cardiovascular Imaging: endorsed by the Society of Cardiovascular Computed Tomography and Society for Cardiovascular Magnetic Resonance. *J Am Soc Echocardiogr* 2015;28:119-82.
131. MacKnight BM, Maldonado Y, Augoustides JG, Cardenas RA, Patel PA, Ghadimi K, et al. Advances in imaging for the management of acute aortic syndromes: focus on transesophageal echocardiography and type-A aortic dissection for the perioperative echocardiographer. *J Cardiothorac Vasc Anesth* 2016;30:1129-41.
132. Erbel R, Aboyans V, Boileau C, Bossone E, Bartolomeo RD, Eggebrecht H, et al. 2014 ESC Guidelines on the diagnosis and treatment of aortic diseases: document covering acute and chronic aortic diseases of the thoracic and abdominal aorta of the adult. The Task Force for the Diagnosis and Treatment of Aortic Diseases of the European Society of Cardiology (ESC). *Eur Heart J* 2014;35:2873-926.
133. Hiratzka LF, Bakris GL, Beckman JA, Bersin RM, Carr VF, Casey DE Jr, et al. 2010 ACCF/AHA/AATS/ACR/ASA/SCA/SCAI/SIR/STS/SVM guidelines for the diagnosis and management of patients with thoracic aortic disease: a report of the American College of Cardiology Foundation/American Heart Association Task Force on Practice Guidelines, American Association for Thoracic Surgery, American College of radiology, American Stroke Association, Society of Cardiovascular Anesthesiologists, Society for Cardiovascular Angiography and Interventions, Society of Interventional radiology, Society of Thoracic Surgeons, and Society for Vascular Medicine. *Circulation* 2010;121:e266-369.
134. Maslow AD, Schwartz C, Singh AK. Assessment of the tricuspid valve: a comparison of four transesophageal echocardiographic windows. *J Cardiothorac Vasc Anesth* 2004;18:719-24.
135. Lancellotti P, Moura L, Pierard LA, Agricola E, Popescu BA, Tribouilloy C, et al. European Association of Echocardiography recommendations for the assessment of valvular regurgitation. Part 2: mitral and tricuspid regurgitation (native valve disease). *Eur J Echocardiogr* 2010;11:307-32.
136. Puchalski MD, Askovich B, Sower CT, Williams RV, Minich LL, Tani LY. Pulmonary regurgitation: determining severity by echocardiography and magnetic resonance imaging. *Congenit Heart Dis* 2008;3:168-75.
137. Maciel BC, Simpson IA, Valdes-Cruz LM, Recusani F, Hoit B, Dalton N, et al. Color flow Doppler mapping studies of "physiologic" pulmonary and tricuspid regurgitation: evidence for true regurgitation as opposed to a valve closing volume. *J Am Soc Echocardiogr* 1991;4:589-97.
138. Stumper O, Kaulitz R, Elzenga NJ, Bom N, Roelandt JR, Hess J, et al. The value of transesophageal echocardiography in children with congenital heart disease. *J Am Soc Echocardiogr* 1991;4:164-76.
139. Stumper O, Kaulitz R, Sreeram N, Fraser AG, Hess J, Roelandt JR, et al. Intraoperative transesophageal versus epicardial ultrasound in surgery for congenital heart disease. *J Am Soc Echocardiogr* 1990;3:392-401.
140. Wolfe LT, Rossi A, Ritter SB. Transesophageal echocardiography in infants and children: use and importance in the cardiac intensive care unit. *J Am Soc Echocardiogr* 1993;6(3 Pt 1):286-9.
141. Colombo PC, Municino A, Brofferio A, Kholdarova L, Nanna M, Ilcercil A, et al. Cross-sectional multiplane transesophageal echocardiographic measurements: comparison with standard transthoracic values obtained in the same setting. *Echocardiography* 2002;19:383-90.
142. Hozumi T, Shakudo M, Shah PM. Quantitation of left ventricular volumes and ejection fraction by biplane transesophageal echocardiography. *Am J Cardiol* 1993;72:356-9.
143. Stoddard MF, Liddell NE, Vogel RL, Longaker RA, Dawkins PR. Comparison of cardiac dimensions by transesophageal and transthoracic echocardiography. *Am Heart J* 1992;124:675-8.
144. Regen DM, Graham TP, Wyse RK, Deanfield J, Franklin RC. Left-ventricular cavity dimensions in children with normal and dilated hearts. *Pediatr Cardiol* 1988;9:17-24.
145. Bailey JM, Shanewise JS, Kikura M, Sharma S. A comparison of transesophageal and transthoracic echocardiographic assessment of left ventricular function in pediatric patients with congenital heart disease. *J Cardiothorac Vasc Anesth* 1995;9:665-9.
146. O'Leary PW, Durongpisitkul K, Cordes TM, Bailey KR, Hagler DJ, Tajik J, et al. Diastolic ventricular function in children: a Doppler echocardiographic study establishing normal values and predictors of increased ventricular end-diastolic pressure. *Mayo Clin Proc* 1998;73:616-28.
147. Nagueh SF, Smiseth OA, Appleton CP, Byrd BF 3rd, Dokainish H, Edvardsen T, et al. Recommendations for the evaluation of left ventricular diastolic function by echocardiography: an update from the American Society of Echocardiography and the European Association of Cardiovascular Imaging. *J Am Soc Echocardiogr* 2016;29:277-314.
148. Swaminathan M, Nicoara A, Phillips-Bute BG, Aeschlimann N, Milano CA, Mackensen GB, et al. Utility of a simple algorithm to grade diastolic dysfunction and predict outcome after coronary artery bypass graft surgery. *Ann Thorac Surg* 2011;91:1844-50.
149. Kasper J, Bolliger D, Skarvan K, Buser P, Filipovic M, Seeberger MD. Additional cross-sectional transesophageal echocardiography views improve perioperative right heart assessment. *Anesthesiology* 2012;117:726-34.
150. Iino M, Shiraishi H, Ichihashi K, Hoshina M, Saitoh M, Hirakubo Y, et al. Volume measurement of the left ventricle in children using real-time three-dimensional echocardiography: comparison with ventriculography. *J Cardiol* 2007;49:221-9.
151. Riehle TJ, Mahle WT, Parks WJ, Sallee D 3rd, Fyfe DA. Real-time three-dimensional echocardiographic acquisition and quantification of left ventricular indices in children and young adults with congenital heart disease: comparison with magnetic resonance imaging. *J Am Soc Echocardiogr* 2008;21:78-83.
152. Ayabakan C, Ozkutlu S. Normal patterns of flow in the superior caval, hepatic and pulmonary veins as measured using Doppler echocardiography during childhood. *Cardiol Young* 2003;13:143-51.
153. Sidik HB, Park JM, Lee YJ, Kim JD, Kang WS, Kim SH, et al. Usefulness of intraoperative real-time three-dimensional transesophageal echocardiography in preprocedural evaluation of cor triatriatum -a case report. *Korean J Anesthesiol* 2013;65:565-8.
154. Krasemann Z, Scheld HH, Tjan TD, Krasemann T. Cor triatriatum: short review of the literature upon ten new cases. *Herz* 2007;32:506-10.
155. Shuler CO, Fyfe DA, Sade R, Crawford FA. Transesophageal echocardiographic evaluation of cor triatriatum in children. *Am Heart J* 1995;129:507-10.
156. Van Praagh S, O'Sullivan J, Brili S, Van Praagh R. Juxtaposition of the morphologically right atrial appendage in solitus and inversus atria: a study of 35 postmortem cases. *Am Heart J* 1996;132(2 Pt 1):382-90.
157. Van Praagh S, O'Sullivan J, Brili S, Van Praagh R. Juxtaposition of the morphologically left atrial appendage in solitus and inversus atria: a study of 18 postmortem cases. *Am Heart J* 1996;132(2 Pt 1):391-402.

158. Zhang YQ, Yu ZQ, Zhong SW, Wu LP, Chen GZ, Zhang ZF, et al. Echocardiographic assessment of juxtaposition of the right atrial appendage in children with congenital heart disease. *Echocardiography* 2010;27:878-84.
159. Stumper O, Rijlaarsdam M, Vargas-Barron J, Romero A, Hess J, Sutherland GR. The assessment of juxtaposed atrial appendages by transoesophageal echocardiography. *Int J Cardiol* 1990;29:365-71.
160. Viswanathan S, Vaidyanathan B, Kumar RK. Thrombus in a juxtaposed right atrial appendage. *Cardiol Young* 2007;17:574.
161. Bansal M, Kasliwal RR. Echocardiography for left atrial appendage structure and function. *Indian Heart J* 2012;64:469-75.
162. Bunker PC, Neufeld DA, Moore JC, Carter GA. Persistent left superior vena cava and associated structural and functional considerations. *Angiology* 1981;32:601-8.
163. Raghbi G, Ruttenberg HD, Anderson RC, Amplatz K, Adams P Jr, Edwards JE. Termination of left superior vena cava in left atrium, atrial septal defect, and absence of coronary sinus; a developmental complex. *Circulation* 1965;31:906-18.
164. Taybi H, Kurlander GJ, Lurie PR, Campbell JA. Anomalous systemic venous connection to the left atrium or to a pulmonary vein. *Am J Roentgenol Radium Ther Nucl Med* 1965;94:62-77.
165. Anderson RC, Adams P Jr, Burke B. Anomalous inferior vena cava with azygos continuation (infrahepatic interruption of the inferior vena cava). Report of 15 new cases. *J Pediatr* 1961;59:370-83.
166. Oppido G, Pace Napoleone C, Turci S, Giardini A, Formigari R, Angeli E, et al. Right superior vena cava draining in the left atrium: anatomical, embryological, and surgical considerations. *Ann Thorac Surg* 2006;81:2313-5.
167. Van Praagh S, Geva T, Lock JE, Nido PJ, Vance MS, Van Praagh R. Biatrial or left atrial drainage of the right superior vena cava: anatomic, morphogenetic, and surgical considerations—report of three new cases and literature review. *Pediatr Cardiol* 2003;24:350-63.
168. Wong ML, McCrindle BW, Mota C, Smallhorn JF. Echocardiographic evaluation of partial anomalous pulmonary venous drainage. *J Am Coll Cardiol* 1995;26:503-7.
169. Hiji T, Fukushige J, Hara T. Diagnosis and management of partial anomalous pulmonary venous connection. A review of 28 pediatric cases. *Cardiology* 1998;89:148-51.
170. Ferencz C, Rubin JD, McCarter RJ, Brenner JJ, Neill CA, Perry LW, et al. Congenital heart disease: prevalence at livebirth. The Baltimore-Washington Infant Study. *Am J Epidemiol* 1985;121:31-6.
171. Hoffman JJ, Kaplan S. The incidence of congenital heart disease. *J Am Coll Cardiol* 2002;39:1890-900.
172. al Zagal AM, Li J, Anderson RH, Lincoln C, Shore D, Rigby ML. Anatomical criteria for the diagnosis of sinus venosus defects. *Heart* 1997;78:298-304.
173. Anderson RH, Brown NA, Webb S. Development and structure of the atrial septum. *Heart* 2002;88:104-10.
174. Anderson RH, Wilcox BR. The surgical anatomy of ventricular septal defect. *J Card Surg* 1992;7:17-35.
175. Pascoe RD, Oh JK, Warnes CA, Danielson GK, Tajik AJ, Seward JB. Diagnosis of sinus venosus atrial septal defect with transesophageal echocardiography. *Circulation* 1996;94:1049-55.
176. Sunaga Y, Hayashi K, Okubo N, Taniichi Y, Sugiura T, Tsuda N, et al. Transesophageal echocardiographic diagnosis of coronary sinus type atrial septal defect. *Am Heart J* 1992;124:1657-9.
177. Tee SD, Shiota T, Weintraub R, Teien DE, Deng YB, Sahn DJ, et al. Evaluation of ventricular septal defect by transesophageal echocardiography: intraoperative assessment. *Am Heart J* 1994;127:585-92.
178. Van Praagh S, Carrera ME, Sanders SP, Mayer JE, Van Praagh R. Sinus venosus defects: unroofing of the right pulmonary veins—anatomic and echocardiographic findings and surgical treatment. *Am Heart J* 1994;128:365-79.
179. Silverman NH. *Pediatric echocardiography*. Baltimore: Williams & Wilkins; 1993. xii, 628.
180. Schmidt KG, Silverman NH. Cross-sectional and contrast echocardiography in the diagnosis of interatrial communications through the coronary sinus. *Int J Cardiol* 1987;16:193-9.
181. Dodge-Khatami A, Knirsch W, Tomaske M, Pretre R, Bettex D, Rousson V, et al. Spontaneous closure of small residual ventricular septal defects after surgical repair. *Ann Thorac Surg* 2007;83:902-5.
182. Yang SC, Novello R, Nicolson S, Steven J, Gaynor JW, Spray TL, et al. Evaluation of ventricular septal defect repair using intraoperative transesophageal echocardiography: frequency and significance of residual defects in infants and children. *Echocardiography* 2000;17:681-4.
183. Hanna BM, El-Hewala AA, Gruber PJ, Gaynor JW, Spray TL, Seliem MA. Predictive value of intraoperative diagnosis of residual ventricular septal defects by transesophageal echocardiography. *Ann Thorac Surg* 2010;89:1233-7.
184. Faletta FF, Nucifora G, Ho SY. Real-time 3-dimensional transesophageal echocardiography of the atrioventricular septal defect. *Circ Cardiovasc Imaging* 2011;4:e7-9.
185. Smallhorn JF. Cross-sectional echocardiographic assessment of atrioventricular septal defect: basic morphology and preoperative risk factors. *Echocardiography* 2001;18:415-32.
186. Kamra K, Russell I, Miller-Hance WC. Role of transesophageal echocardiography in the management of pediatric patients with congenital heart disease. *Paediatr Anaesth* 2011;21:479-93.
187. Lee HR, Montenegro LM, Nicolson SC, Gaynor JW, Spray TL, Rychik J. Usefulness of intraoperative transesophageal echocardiography in predicting the degree of mitral regurgitation secondary to atrioventricular defect in children. *Am J Cardiol* 1999;83:750-3.
188. Transesophageal echocardiographic diagnosis of anomalous left coronary artery from the right aortic sinus, (1993).
189. Anomalous origin and course of coronary arteries in adults: Identification and improved imaging utilizing transesophageal echocardiography, (1991).
190. Smolin MR, Gorman PD, Gaither NS, Wortham DC. Origin of the right coronary artery from the left main coronary artery identified by transesophageal echocardiography. *Am Heart J* 1992;123(4 Pt 1):1062-5.
191. Kaku B, Shimizu M, Kita Y, Yoshio H, Ino H, Takeda R. Detection of anomalous origin of the left coronary artery by transesophageal echocardiography and magnetic resonance imaging. *Jpn Heart J* 1994;35:383-8.
192. Anwar S, Brook M, Mavroudis C, Hobbs R, Lorber R. Anomalous origin of the left coronary artery from the noncoronary cusp: not a benign lesion. *Pediatr Cardiol* 2012;33:1187-9.
193. Frommelt PC, Berger S, Pelech AN, Bergstrom S, Williamson JG. Prospective identification of anomalous origin of left coronary artery from the right sinus of valsalva using transthoracic echocardiography: importance of color Doppler flow mapping. *Pediatr Cardiol* 2001;22:327-32.
194. Multiplane transesophageal echocardiography in diagnosis of anomalous origin of the left coronary artery from the pulmonary artery: a case report, (1998).
195. Kececioglu D, Kottthoff S, Konertz W, Scheld HH, Vogt J. Pulmonary artery origin of the left coronary artery: diagnosis by transesophageal echocardiography in infancy. *Eur Heart J* 1993;14:1006-7.
196. Patel JK, Glatz AC, Ghosh RM, Jones SM, Natarajan S, Ravishankar C, et al. Intramural ventricular septal defect is a distinct clinical entity associated with postoperative morbidity in children after repair of conotruncal anomalies. *Circulation* 2015;132:1387-94.
197. Patel JK, Glatz AC, Ghosh RM, Jones SM, Ravishankar C, Mascio C, et al. Accuracy of transesophageal echocardiography in the identification of postoperative intramural ventricular septal defects. *J Thorac Cardiovasc Surg* 2016;152:688-95.
198. Jijeh AM, Omran AS, Najm HK, Abu-Sulaiman RM. Role of intraoperative transesophageal echocardiography in pediatric cardiac surgery. *J Saudi Heart Assoc* 2016;28:89-94.
199. Joyce JJ, Hwang EY, Wiles HB, Kline CH, Bradley SM, Crawford FA Jr. Reliability of intraoperative transesophageal echocardiography during Tetralogy of Fallot repair. *Echocardiography* 2000;17:319-27.
200. Kaushal SK, Radhakrishnan S, Dagar KS, Iyer PU, Girotra S, Shrivastava S, et al. Significant intraoperative right ventricular outflow gradients after repair for tetralogy of Fallot: to revise or not to revise? *Ann Thorac Surg* 1999;68:1705-12. discussion 12-3.

201. Kalavrouziotis G, Purohit M, Ciotti G, Corno AF, Pozzi M. Truncus arteriosus communis: early and midterm results of early primary repair. *Ann Thorac Surg* 2006;82:2200-6.
202. Pasquini L, Sanders SP, Parness IA, Wernovsky G, Mayer JE Jr, Van der Velde ME, et al. Coronary echocardiography in 406 patients with d-loop transposition of the great arteries. *J Am Coll Cardiol* 1994;24:763-8.
203. Rouine-Rapp K, Ionescu P, Balea M, Foster E, Cahalan MK. Detection of intraoperative segmental wall-motion abnormalities by transesophageal echocardiography: the incremental value of additional cross sections in the transverse and longitudinal planes. *Anesth Analg* 1996;83:1141-8.
204. Kaulitz R, Stumper O, Fraser AG, Kreis A, Tuccillo B, Sutherland GR. The potential value of transesophageal evaluation of individual pulmonary venous flow after an atrial baffle procedure. *Int J Cardiol* 1990;28:299-307.
205. Cua CL, Kollins K, Roble S, Holzer RJ. Three-dimensional image of a baffle leak in a patient with a Mustard operation. *Echocardiography* 2014;31:E315-6.
206. Klein AJ, Kim MS, Salcedo E, Fagan T, Kay J. The missing leak: a case report of a baffle-leak closure using real-time 3D transesophageal guidance. *Eur J Echocardiogr* 2009;10:464-7.
207. Enar S, Singh P, Douglas C, Panwar SR, Manda J, Kesanolla SK, et al. Live/real time three-dimensional transthoracic echocardiographic assessment of transposition of the great arteries in the adult. *Echocardiography* 2009;26:1095-104.
208. de Leval MR, Kilner P, Gewillig M, Bull C. Total cavopulmonary connection: a logical alternative to atriopulmonary connection for complex Fontan operations. Experimental studies and early clinical experience. *J Thorac Cardiovasc Surg* 1988;96:682-95.
209. Marcelletti C, Corno A, Giannico S, Marino B. Inferior vena cavopulmonary artery extracardiac conduit. A new form of right heart bypass. *J Thorac Cardiovasc Surg* 1990;100:228-32.
210. Moodley S, Gandhi SK, Harris KC. Subtotal obstruction of a tube fenestrated fontan conduit. *Heart* 2014;100:522.
211. Hallbergson A, Mascio CE, Rome JJ. Transcatheter fontan takedown. *Catheter Cardiovasc Interv* 2015;86:849-54.
212. Atz AM, Zak V, Mahony L, Uzark K, Shrader P, Gallagher D, et al. Survival data and predictors of functional outcome an average of 15 years after the Fontan procedure: the pediatric heart network Fontan cohort. *Congenit Heart Dis* 2015;10:E30-42.
213. Berman NB, Kimball TR. Systemic ventricular size and performance before and after bidirectional cavopulmonary anastomosis. *J Pediatr* 1993;122:S63-7.
214. Colan SD. Systolic and diastolic function of the univentricular heart. *Prog Pediatr Cardiol* 2002;16:79-87.
215. Sluysmans T, Sanders SP, van der Velde M, Matitiau A, Parness IA, Spevak PJ, et al. Natural history and patterns of recovery of contractile function in single left ventricle after Fontan operation. *Circulation* 1992;86:1753-61.
216. Margossian R, Schwartz ML, Prakash A, Wruck L, Colan SD, Atz AM, et al. Comparison of echocardiographic and cardiac magnetic resonance imaging measurements of functional single ventricular volumes, mass, and ejection fraction (from the Pediatric Heart Network Fontan Cross-Sectional Study). *Am J Cardiol* 2009;104:419-28.
217. Jone PN, Ross MM, Bracken JA, Mulvahill MJ, Di Maria MV, Fagan TE. Feasibility and safety of using a fused echocardiography/fluoroscopy imaging system in patients with congenital heart disease. *J Am Soc Echocardiogr* 2016;29:513-21.
218. Szabo TL, ebrary Inc. Diagnostic ultrasound imaging: inside out. Available at: <http://site.ebrary.com/lib/yale/Doc?id=10815316>.
219. Knackstedt C, Franke A, Mischke K, Zarse M, Gramley F, Schimpf T, et al. Semi-automated 3-dimensional intracardiac echocardiography: development and initial clinical experience of a new system to guide ablation procedures. *Heart Rhythm* 2006;3:1453-9.
220. Silvestry FE, Kadakia MB, Willhide J, Herrmann HC. Initial experience with a novel real-time three-dimensional intracardiac ultrasound system to guide percutaneous cardiac structural interventions: a phase I feasibility study of volume intracardiac echocardiography in the assessment of patients with structural heart disease undergoing percutaneous transcatheter therapy. *J Am Soc Echocardiogr* 2014;27:978-83.
221. Use of a Three Dimensional Printed Cardiac Model to Assess Suitability for Biventricular Repair, (2016).
222. Clinical Application and Multidisciplinary Assessment of Three Dimensional Printing in Double Outlet Right Ventricle With Remote Ventricular Septal Defect, (2016).
223. Three-dimensional printed prototypes refine the anatomy of post-modified Norwood-1 complex aortic arch obstruction and allow presurgical simulation of the repair, (2016).
224. Integration of Computed Tomography and Three-Dimensional Echocardiography for Hybrid Three-Dimensional Printing in Congenital Heart Disease, (2016).
225. Ultrasound-Derived Three-Dimensional Printing in Congenital Heart Disease, (2014).
226. Olivieri LJ, Krieger A, Loke YH, Nath DS, Kim PC, Sable CA. Three-dimensional printing of intracardiac defects from three-dimensional echocardiographic images: feasibility and relative accuracy. *J Am Soc Echocardiogr* 2015;28:392-7.
227. Axelrod D. The Stanford Virtual Heart – revolutionizing education on congenital heart defects [Internet]. Available at: <http://www.stanfordchildrens.org/en/innovation/virtual-reality/stanford-virtual-heart>; 2017.
228. Digitale E. Virtual reality imaging gives surgeons a better view of patient anatomy. Available at: <https://med.stanford.edu/news/all-news/2017/02/virtual-reality-imaging-gives-surgeons-a-better-view-of-anatomy.html>. 2017.
229. Cohen E. Google Carboard saves baby's life. Available at: <http://www.cnn.com/2016/01/07/health/google-cardboard-baby-saved/>; 2016.
230. Thavendiranathan P, Grant AD, Negishi T, Plana JC, Popovic ZB, Marwick TH. Reproducibility of echocardiographic techniques for sequential assessment of left ventricular ejection fraction and volumes: application to patients undergoing cancer chemotherapy. *J Am Coll Cardiol* 2013;61:77-84.